

STUDIES TOWARD THE ENANTIOSELECTIVE SYNTHESIS OF THE GELSEMIUM
ALKALOIDS

by

CHRISTOPHER MATTHEW HARRINGTON

(Under the Direction of Eric Ferreira)

ABSTRACT

Developments in catalysis using late transition metals, such as gold and platinum, have provided an abundance of transformations that are useful to the organic chemist. The unique alkynophilic properties of these metal catalysts is a consequence of relativistic effects, which allows these metals to function in reactions as more than just a Lewis acid. Herein, we sought to discover new modes of reactive nucleophilic partners for α,β -unsaturated platinum carbenes, in particular, nucleophiles which also contained a heteroatom. In addition, we were interested in converting our previous racemic synthesis of gelsenicine into an enantioselective synthesis by utilizing a chirality transfer approach. Two generations of substrates were created in order to see if such a strategy would prove successful.

INDEX WORDS: alkyne activation, platinum carbene, chirality transfer

STUDIES TOWARD THE ENANTIOSELECTIVE SYNTHESIS OF THE GELSEMIUM
ALKALOIDS

by

CHRISTOPHER MATTHEW HARRINGTON

BS, University of Georgia, 2013

A Thesis Submitted to the Graduate Faculty of The University of Georgia in Partial Fulfillment
of the Requirements for the Degree

MASTER OF SCIENCE

ATHENS, GEORGIA

2019

© 2019

Christopher Matthew Harrington

All Rights Reserved

STUDIES TOWARD THE ENANTIOSELECTIVE SYNTHESIS OF THE GELSEMIUM
ALKALOIDS

by

CHRISTOPHER MATTHEW HARRINGTON

Major Professor:	Eric Ferreira
Committee:	Vladimir Popik
	Robert Phillips

Electronic Version Approved:

Suzanne Barbour
Dean of the Graduate School
The University of Georgia
August 2019

TABLE OF CONTENTS

	Page
LIST OF TABLES	vi
LIST OF FIGURES	vii
LIST OF SCHEMES.....	viii
 CHAPTER	
1 Alkyne Activation Chemistry of Gold and Platinum Complexes.....	1
1.1 Introduction.....	1
1.2 General Reactivity of Au / Pt – Alkyne Complexes	1
1.3 Relativistic Effects	4
1.4 Gold and Platinum Alkyne Activation in Total Synthesis.....	6
1.5 Conclusion	10
CHAPTER ONE NOTES AND REFERENCES	11
2 Trapping of α,β -Unsaturated Platinum Carbenes with Nitrogen-Containing Nucleophiles	13
2.1 Trapping of α,β -Unsaturated Platinum Carbenes	13
2.2 The Search for New Nucleophiles to Add Into α,β -Unsaturated Platinum Carbenes.....	18
2.3 Conclusion	22
CHAPTER TWO NOTES AND REFERENCES.....	23

3	Enantioselective Synthesis of the Gelsemium Alkaloids.....	24
3.1	Overview	24
3.2	<i>Gelsemium</i> Alkaloids	24
3.3	Gelsedine-Type Alkaloids	25
3.4	Syntheses of the Gelsedine-Type Alkaloids	26
3.5	Strategies Toward an Enantioselective Synthesis of Gelsenicine.....	39
3.6	Conclusions	51
3.7	Experimental	52
	CHAPTER THREE NOTES AND REFERENCES	133

LIST OF TABLES

	Page
Table 3.5.1.: Effects of protecting group on observed chirality transfer	46
Table 3.5.2.: Results of cycloisomerizations of diastereomer 3-115A	50
Table 3.5.3.: Results of cycloisomerizations of diastereomer 3-115B	51

LIST OF FIGURES

	Page
Figure 1.2.1.: The “pull” and “push” reactivity in alkyne activation catalysis.....	3
Figure 1.2.2.: Acetylenic Schmidt Reaction by Toste and coworkers.....	4
Figure 1.3.1.: Molecular orbital energies for Au, Hg, and Pt prior to and after considering relativistic effects	6
Figure 2.2.1.: Nucleophile testing with homopropargyl alcohol substrate 2-27	20
Figure 2.2.2.: Nucleophile testing with aniline substrate 2-40	22
Figure 3.2.1.: The six types of <i>Gelsemium</i> alkaloids.....	25
Figure 3.5.1.: Strategies to make oxabicyclic core of gelsenicine enantioselectively	41
Figure 3.5.3.: Preliminary results of the reductive radical decarboxylation of compound 3-98 ...	43
Figure 3.5.7.: Use of acetonides as a cleavable chiral auxiliary with α -branching	48

LIST OF SCHEMES

	Page
Scheme 1.4.1.: Synthesis of (+)-schisanwilsonene.....	8
Scheme 1.4.2.: Platinum-catalyzed cycloisomerization step of the formal synthesis of 7-methoxymitosene	10
Scheme 2.1.1.: Generation of an α,β -unsaturated platinum carbene	13
Scheme 2.1.2: Proposed mechanism of Iwasawa's [3+2] cycloaddition of platinum carbenes and vinyl ethers.....	14
Scheme 2.1.3.: Hashmi's [3+3] cycloaddition with unsaturated platinum carbenes and nitrones	15
Scheme 2.1.4.: Kim and coworkers synthesis of vinylphenanthrenes via a platinum carbene.....	16
Scheme 2.1.5.: Ferreira's trapping of unsaturated platinum carbenes using pendant nucleophiles to generate a net bisheterocyclization	17
Scheme 2.1.6.: Other nucleophiles that can react with unsaturated platinum carbenes	18
Scheme 3.4.1.: Hiemstra's construction of the spiroindole core	27
Scheme 3.4.2.: Assembly of the oxabicycle core and pyrrolidine ring of <i>ent</i> -gelsedine.....	28
Scheme 3.4.3.: Fukuyama's synthesis of (–)-gelsemoxonine.....	29
Scheme 3.4.4.: Carreira's synthesis of gelsemoxonine: formation of dialdehyde intermediate 3-40	30
Scheme 3.4.5.: Final steps of Carreira's synthesis of gelsemoxonine	31
Scheme 3.4.6.: Ferreira's generation of the oxabicycle core of gelsenicine.....	32
Scheme 3.4.7.: Final steps of Ferreira's total synthesis of gelsenicine.....	33

Scheme 3.4.8.: Fukuyama's divergent syntheses of the gelsedine-type alkaloids.....	34
Scheme 3.4.9.: Zhao's racemic synthesis of gelsedilam.....	36
Scheme 3.4.10.: Synthesis of Ma's common intermediate.....	37
Scheme 3.4.11.: Synthesis of (–)-gelsedilam from 3-80	38
Scheme 3.4.12.: Ma's syntheses of (–)-gelsenicine, (–)-gelsedine, and (–)-gelsemoxonine.....	39
Scheme 3.5.2.: Synthesis of reductive decarboxylation substrate 3-98	42
Scheme 3.5.4.: Synthesis of first generation substrates for chirality transfer.....	44
Scheme 3.5.8. : Synthesis of second generation substrates	49

CHAPTER 1

ALKYNE ACTIVATION CHEMISTRY OF GOLD AND PLATINUM COMPLEXES

1.1 Introduction

The Lewis acidity of late transition metals offers distinctive reactivity that can enable new pathways to forming carbon-carbon and carbon-heteroatom bonds. The goal of this chapter is to provide an overall understanding of concepts like π -acidity and alkynophilicity and why these chemical properties of late transition metals allow gold and platinum to function in diverse transformations with alkynes. The examples highlighted are not meant to be comprehensive, but to showcase the selectivity, efficiency, and novel reactivity of these metal complexes.

1.2 General Reactivity of Au / Pt – Alkyne Complexes

A π acid is described as a Lewis acid that binds to a carbon-carbon multiple bond and partially removes some of the electron density from the π -bond. When this occurs, a partial positive charge develops on the carbon-carbon bond, making both carbons prone to nucleophilic attack. This is similar to how classical Lewis acids, like TiCl_4 or BF_3 , activate carbonyls to make the carbonyl π -system a better electrophile.¹ In regards to Hard-Soft Acid Base (HSAB) theory, metals such as titanium and boron tend to be harder in character and therefore not suitable to alkyne activation. π bonds are considered soft and therefore, softer Lewis acids that tend to be polarizable (Au^{I} and Pt^{II}) make the desired interactions necessary for alkyne activation.

While other electrophiles can act as π -acids, there are special properties that enable gold and platinum to have catalytically useful reactivity. Reactions to alkynes catalyzed by a Brønsted acid (H^+) tend to require harsh conditions and form carbocation intermediates, which can lead to numerous undesired side products.² Using a softer Lewis acid like Au^+ alleviates the need for harsh reaction conditions by having high affinity for π bonds as well as a kinetically labile gold carbon bond.³ One of the first applications of gold alkyne activation was the addition of methanol across an alkyne.⁴ Since then, numerous examples including various carbon, nitrogen, and oxygen nucleophiles have been explored.⁵

1.2.1 Pull-Push Reactivity

One of the key characteristics of gold and platinum alkyne activation is the “Pull-Push” reactivity of activated alkynes. As seen in Figure 1.2.1, “pull” refers to the activation of the alkyne by the metal, rendering it electrophilic in character. After attack of the nucleophile, electrons from the metal can donate into the metal-carbon bond and stabilize any adjacent positive charges (“push”). The formed gold carbenoid can either function as a carbene, if the reaction conditions allow it, or just simply act as an electrophile. The data that is available does not point to either an explicit metal carbene or metal-bound carbocation as an intermediate; therefore it is reasonable to assume that these two descriptions of the intermediate are extremes of a more generic picture.^{6,7} It is important to note that the latter two forms of reactivity can only occur once the initial alkyne activation is completed.

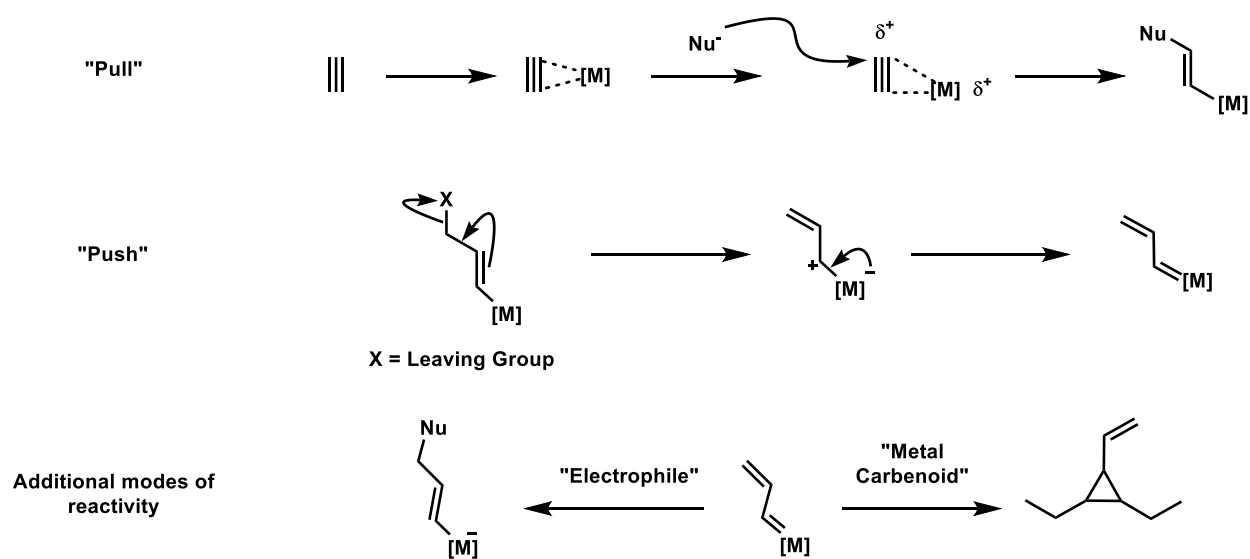


Figure 1.2.1. The "Pull" and "Push" reactivity in alkyne activation catalysis.

A classic example of these forms of reactivity are highlighted in the Au(I)-catalyzed acetylenic Schmidt reaction by Toste and coworkers in 2005 (See Figure 1.2.2).⁸ The alkyne activation with gold allows for the 5-*endo*-dig cyclization from the internal nitrogen of the azide ("pull"). Electrons from gold push into the gold-carbon bond, forming the gold carbenoid and releasing molecular nitrogen ("push"). The resulting gold carbenoid is then quenched by a 1,2-alkyl shift, forming tertiary carbocation **1-4**. Deauration and aromatization of the pyrrole ring leads to final product **1-5**.

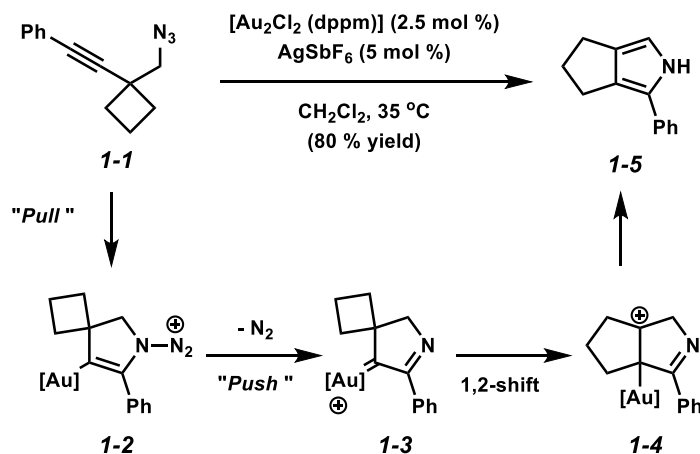


Figure 1.2.2 Acetylenic Schmidt Reaction by Toste and Coworkers.⁸

1.3 Relativistic Effects

The “push-pull” reactivity of gold and platinum can ultimately be further described by relativistic effects.⁹ Therefore, an initial understanding of how these relativistic effects operate in the metal centers of interest is necessary. One consequence of special relativity is that an object’s mass increases toward infinity as the object’s velocity approaches the speed of light. In heavier elements, the average velocity of the electrons is higher than that of lighter elements. This increase in radial velocity therefore increases the mass of the electrons. The Bohr radius of an electron orbiting a nucleus is inversely proportional to the mass of the electron, and so, the Bohr radius of the electrons decrease. This contraction also provides other characteristics to the relativistic effects (Figure 1.3.1). As the 6s electrons contract, electrons in *d* and *f* orbitals now experience a shielding effect from the 6s electrons, and therefore experience a weaker attraction to the nucleus.

For the elements gold, platinum, and mercury, these relativistic effects translate into their unique alkynophilic properties. For example, following the contraction of the 6s electrons, the lowest unoccupied molecular orbitals (LUMO) also lower in energy, making the metals very

effective “soft” Lewis acids. In return, these metals are now capable of complexing with softer nucleophiles, like alkenes and alkynes.

This explanation for the soft Lewis acidity still does not tell the full picture of why metal-alkyne complexes react preferentially over the analogous metal-alkene complex. Even looking at the binding of Au^+ -ethylene versus Au^+ -ethyne shows that there is a greater stabilization ($\sim 10 \text{ kcal mol}^{-1}$) for the Au^+ -ethylene complex over Au^+ -ethyne.¹⁰ So then, why does the nucleophile prefer to attack the activated alkyne over the alkene when metals are not necessarily showing preferential activation of an alkyne over an alkene? The answer lies in the relative energy levels of the LUMO of ethylene versus ethyne. Alkynes, in general, have lower highest occupied molecular orbitals and LUMOs compared to their alkene analogues. This difference in energy makes the resulting metal complex also have a lower LUMO, and therefore be more susceptible towards nucleophilic attack. Thus, the combination of relativistic effects on late transition metals in combination with the lower energy molecular orbitals of alkynes accounts for the observed alkynophilicity.

The relativistic effects also help explain how gold, platinum and mercury are able to stabilize adjacent positive charges on carbon atoms. The additional shielding of the $5d$ orbitals by the $6s$ electrons destabilizes the HOMO, increasing its relative energy to allow sufficient overlap with the empty LUMO of the adjacent carbon. This overlap of orbitals could be the origin of the metal stabilized cationic intermediates observed with gold, platinum, and mercury. What still remains uncertain, however, is whether the carbenoid-like reactivity is a result of the formation of a metal carbene, or just metal stabilization of a carbocation. Because of this carbenoid-like reactivity, the gold, platinum, or mercury in these alkyne activation processes behave differently than just as a Lewis acid.

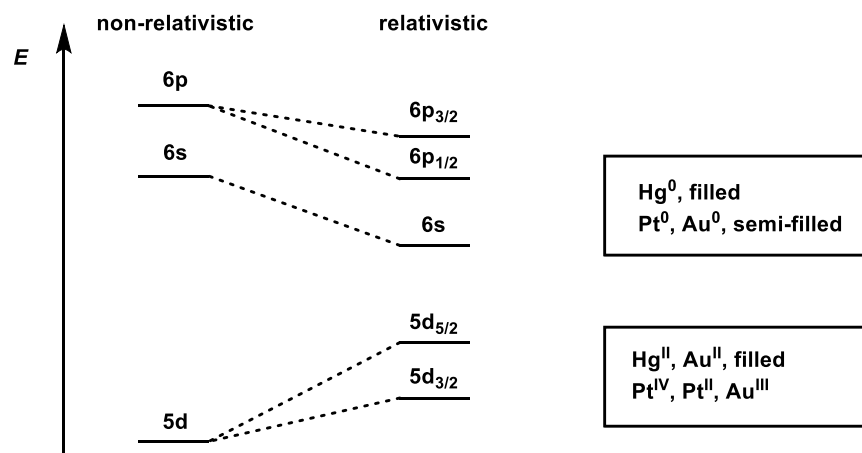


Figure 1.3.1 Molecular Orbital Energies for Au, Hg, and Pt prior to and after Considering Relativistic Effects.

1.4 Gold and Platinum Alkyne Activation in Total Synthesis

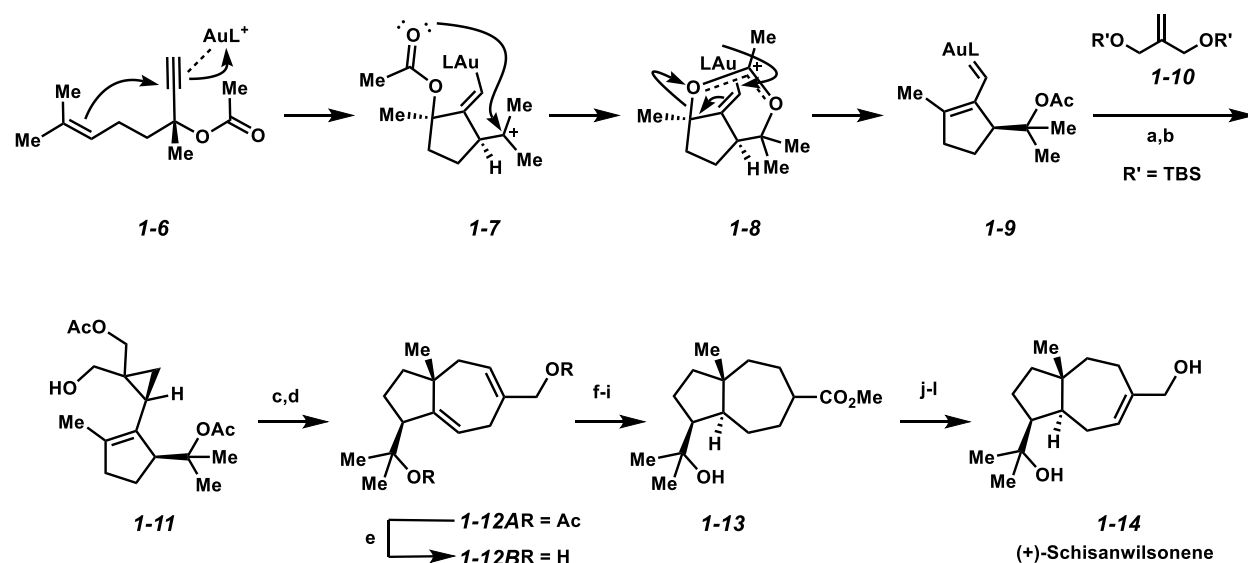
The relativistic effects shown in the previous section highlight why these heavy metal catalysts have reactivity beyond functioning as Lewis acids. Because of this, researchers have sought to use the push, pull and carbenoid type reactivities to take relatively simple substrates and quickly add molecular complexity in one step. These types of transformations are therefore very powerful tools in the synthesis of complex natural products. Gold tends to be the metal of choice for these transformations; however, there are cases where platinum has been utilized as well. In this section, a brief example of a synthesis utilizing gold and platinum catalysis will be shown in order to show just some of the many types of transformations these catalysts can do, while also not being fully comprehensive.

1.4.1 Synthesis of (+)-Schisanwilsonene

In 2013, Echavarren and coworkers disclosed the first enantioselective total synthesis of (+)-schisanwilsonene,¹¹ a carotane type sesquiterpenoid that was isolated from *Schisandra*

wilsoniana, a plant used in Chinese folk medicine to treat hepatitis.¹² The key steps of this synthesis include a stereoselective gold catalyzed tandem cyclization / 1,5-migration / intermolecular cyclopropanation (Figure 1.4.1). Propargylic acetate **1-6** is activated at the alkyne by gold. After cyclization, attack from the carbonyl oxygen releases the strain in the cyclopropane ring, forming intermediate **1-7**. Electrons from gold push into the gold-carbon bond, alleviating the positive charge from oxygen (**1-8**). Cyclopropanation of the gold carbenoid with alkene **1-10** leads to intermediate **1-11**. Interestingly, this transformation did not show any gold(I)-catalyzed 1,2- or 1,3-migrations, which are prone to happen in similar propargyl acetate systems.

Deprotection, followed by singular acetate protection, DMP oxidation and Wittig olefination, sets up the divinylcyclopropane, which undergoes a [3,3] sigmatropic rearrangement to form **1-12**. The synthesis was finished by removal of the acetate groups, followed by hydrogenation with Raney nickel to form the desired trans ring fusion. Oxidation of the primary alcohol followed by esterification led to **1-13**. Selenylation of the potassium enolate, subsequent elimination of the selenoxide, and reduction of the ester led to the finished natural product (+)-schisanwilsonene (**1-14**).



Scheme 1.4.1. Synthesis of (+)-Schisanwilsonene. Reagents and conditions: a) a) TBAF, THF, 23 °C (81%); b) Ac₂O, pyridine, DMAP, CH₂Cl₂, 0 °C (70%, 3:1); c) DMP, NaHCO₃, CH₂Cl₂, 23 °C; d) Ph₃PCH₃Br, *n*-BuLi, THF, -20 to 23 °C (83%, 2 steps); e) LiAlH₄, THF, 0 to 23 °C (90%); f) Raney-Ni, H₂ (80 atm), acetone, 63 °C, 60 h (83%); g) TEMPO, PhI(OAc)₂, CH₂Cl₂/H₂O (2:1), 23 °C (55%); h) NaClO₂, 2-methyl-2-butene, NaH₂PO₄, *t*-BuOH/H₂O (5:1), 23 °C; i) TMSCHN₂, toluene/MeOH (1:2), 0 °C (74%, 2 steps); j) KHMDS, PhSeCl, THF, -78 to 0 °C (93%); k) H₂O₂, CH₂Cl₂, 23 °C (73%); l) DIBAL, THF, -78 to 23 °C (78%). DIBAL=diisobutylaluminum hydride, DMAP=4-(*N,N*-dimethylamino)pyridine, DMP=Dess–Martin periodinane, HMDS=hexamethyldisilazide, TBAF=*tert*-butylammonium fluoride, TEMPO=2,2,6,6-tetramethylpiperidin-1-oxyl, THF= tetrahydrofuran, TMS=trimethylsilyl.

1.4.2 Synthesis of 7-Methoxymitosene

The mitomycins are a family of natural products that possess potent antibiotic and antitumor activities. Mitomycin C, for example is already in clinical use, and its mode of action is to crosslink DNA after activation *in vivo*. Removal of methanol forms the more stable

aziridinomitosenes which have similar activities against tumor cells compared to mitomycin C.¹³ One of the more important derivatives of this family, 7-methoxymitosene, has been shown to have bioactivity against Gram positive bacteria.¹⁴

In 2012, Zhang and coworkers completed a formal synthesis 7-Methoxymitosene¹⁵ using a PtCl₂-mediated cycloisomerization of β -lactam **1-15** (Figure 1.4.2). Starting from this substrate, the desired dihydropyrrolo[1,2-*a*]indolone moiety of the natural product could be quickly assembled. Activation of the alkyne by platinum leads to nucleophilic attack by the lactam nitrogen (**1-15**). Opening of the lactam by donation of electrons into the carbonyl forms acylium intermediate **1-16**, which can be attacked by the alkene. Donation of electrons from platinum helps stabilize the resulting carbocation. A hydride shift occurs (**1-18**), creating a tertiary carbocation that can be stabilized by the neighboring nitrogen. Loss of platinum allows for the carbocation to be quenched (**1-19**). A Wolff-Kishner reduction, followed by a Vilsmeier-Haack reaction led to formylated product **1-22**. Oxidation of the *p*-dimethoxybenzene to the *p*-benzoquinone was achieved with NaNO₂. Lastly, reduction of the aldehyde led to alcohol **1-23**, which has been used previously as the precursor to 7-Methoxymitosene (**1-24**).¹⁶

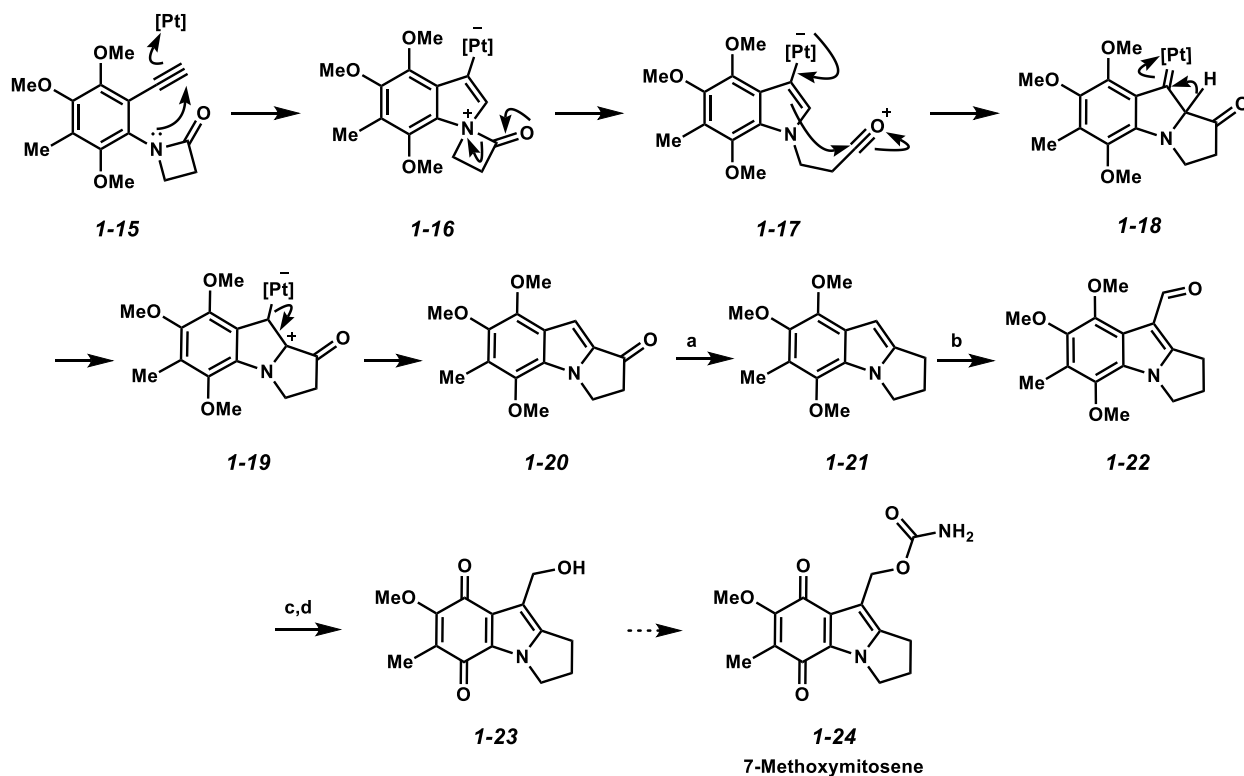


Figure 1.4.2. Platinum-Catalyzed Cycloisomerization Step of the Formal Synthesis of 7-Methoxymitosene. Reagents and conditions: a) N_2H_4 , K_2CO_3 , Diethylene glycol (74%); b) POCl_3 , DMF (77%); c) NaNO_2 , HCl ; d) NaBH_4 , then O_2 (68% over 2 steps).

1.5 Conclusion

Alkyne activation chemistry has enabled the discoveries of new tools for synthetic organic chemists to quickly introduce molecular complexity during a synthesis. The examples shown above highlight only a fraction of the transformations possible with this chemistry. The physical properties of late transition metal centers, such as gold and platinum, allow for the observed reactivity. Because of the capability to form several bonds at once, alkyne activation has been utilized in key steps of natural product syntheses, as well as in the development of new reactions.

In Chapters Two and Three, strides towards the discovery of new reactivity of platinum-activated alkynes and enantioselective cycloisomerizations of gold-activated 1,6-enynes will be discussed.

Chapter 1 References

-
- ¹ Shambayati, S.; Crowe W. E.; Schreiber S. L. *Angew. Chem. Int. Ed. Engl.* **1990**, *29*, 256–272.
- ² Hoffmann R. *Angew. Chem. Int. Ed. Engl.* **1982**, *21*, 711–724.
- ³ Fürstner, A.; Davies, P. W. *Angew. Chem. Int. Ed.* **2007**, *46*, 3410 – 3449.
- ⁴ Teles, J. H.; Schulz, M. (BASFAG), WO-A1 9721648, **1997** [*Chem. Abstr.* **1997**, *127*, 121499].
- ⁵ a) For several examples, see ref. 3; b) Dorel, R.; Echavarren, A. M. *Chem. Rev.* **2015**, *115*, 9028–9072.
- ⁶ a) Nieto-Oberhuber, C.; Muñoz, M. P.; Buñuel, E.; Nevado, C.; Echavarren, A. M. *Angew. Chem. Int. Ed.* **2004**, *43*, 2402–2406; b) Méndez, M.; Muñoz, M. P.; Nevado, C.; Cárdenas, D. J.; Echavarren, A. M. *J. Am. Chem. Soc.* **2001**, *123*, 10511–10520; c) Faza, O. N.; López, C. S.; Álvarez, R.; de Lera, A. R. *J. Am. Chem. Soc.* **2006**, *128*, 2434–2437; d) Nieto-Oberhuber, C.; López, S.; Jiménez-Núñez, E.; Echavarren, A. M. *Chem. Eur. J.* **2006**, *12*, 5916–5923.
- ⁷ a) Méndez, M.; Mamane, V.; Fürstner, A. *Chemtracts* **2003**, *16*, 397–425; b) Fürstner, A.; Stelzer, F.; Szillat, H. *J. Am. Chem. Soc.* **2001**, *123*, 11863–11869; c) Fürstner, A.; Szillat, H.; Stelzer, F. *J. Am. Chem. Soc.* **2000**, *122*, 6785–6786; d) Fürstner, A.; Szillat, H.; Gabor, B.; Mynott, R. *J. Am. Chem. Soc.* **1998**, *120*, 8305–8314.
- ⁸ Gorin, D. J.; Davis, N. R.; Toste, F. D. *J. Am. Chem. Soc.* **2005**, *127*, 11260–11261.

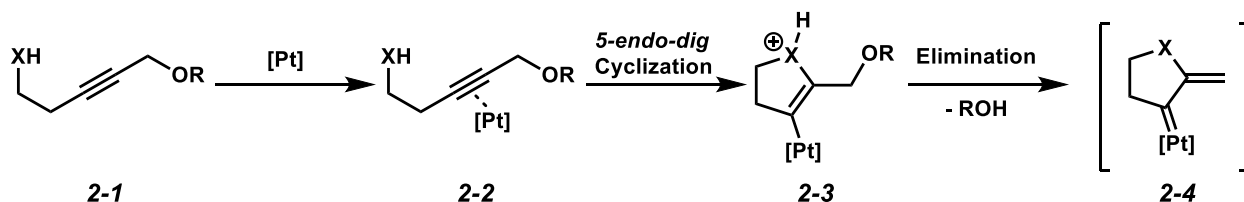
-
- ⁹ a) Gorin, D. J.; Toste, F. D. *Nature* **2007**, *446*, 395–403; (b) Leyva-Pérez, A.; Corma, A. *Angew. Chem. Int. Ed.* **2012**, *51*, 614–635; (c) Pitzer, K. S. *Acc. Chem. Res.* **1979**, *12*, 271–276; (d) Pyykko, P.; Desclaux, J. P. *Acc. Chem. Res.* **1979**, *12*, 276–281.
- ¹⁰ (a) Hertwig, R. H.; Koch, W.; Schröder, D.; Schwarz, H.; Hrušák, J.; Schwerdtfeger, P. *J. Phys. Chem.* **1996**, *100*, 12253–12260; (b) Nechaev, M. S.; Rayon, V. M.; Frenking, G. *J. Phys. Chem. A* **2004**, *108*, 3134–3142.
- ¹¹ Gaydou, M.; Miller, R. E.; Delpont, N.; Ceccon, J.; Echavarren, A. M. *Angew. Chem. Int. Ed.* **2013**, *52*, 6396–6399.
- ¹² Ma, W.-H.; Huang, H.; Zhou, P.; Chen, D.-F. *J. Nat. Prod.* **2009**, *72*, 676–678.
- ¹³ (a) Orlemans, E. O. M.; Verboom, W.; Scheltinga, M. W.; Reinhoudt, D. N.; Lelieveld, P.; Fiebig, H. H.; Winterhalter, B. R.; Double, J. A.; Bibby, M. C. *J. Med. Chem.* **1989**, *32*, 1612–1620. (b) Iyengar, B. S.; Remers, W. A.; Bradner, W. T. *J. Med. Chem.* **1986**, *29*, 1864–1868. (c) Iyengar, B. S.; Dorr, R. T.; Remers, W. A. *J. Med. Chem.* **1991**, *34*, 1947–1951.
- ¹⁴ Allen, G. R.; Poletto, J. F.; Weiss, M. J. *J. Am. Chem. Soc.* **1964**, *86*, 3877–3878.
- ¹⁵ Liu, L.; Wang, Y.; Zhang, L. *Org. Lett.* **2012**, *14*, 3736–3739.
- ¹⁶ a) Coates, R. M.; MacManus, P. A. *J. Org. Chem.* **1982**, *47*, 4822–4824. b) Wender, P. A.; Cooper, C. B. *Tetrahedron Lett.* **1987**, *28*, 6125–6128.

CHAPTER 2

TRAPPING OF α,β -UNSATURATED PLATINUM CARBENES WITH NITROGEN-CONTAINING NUCLEOPHILES

2.1 Trapping of α,β -Unsaturated Platinum Carbenes

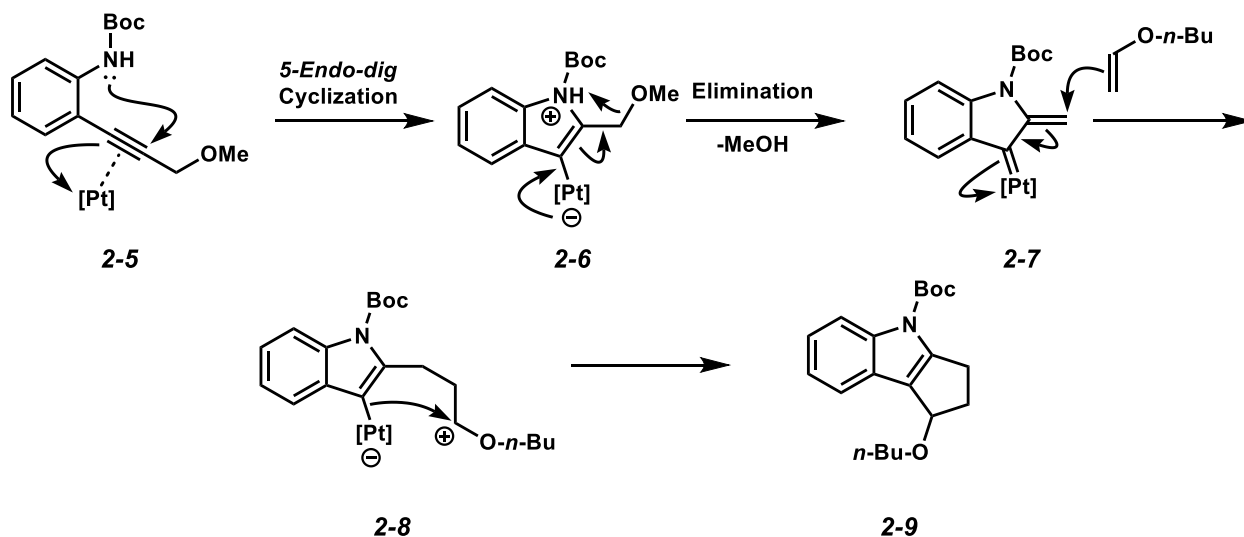
For the past several years, α,β -unsaturated platinum carbenes have been utilized in numerous transformations, ranging from cycloaddition reactions¹ to 1,2-migrations² to interception by nucleophiles.³ The key intermediate is formed from alkyne activation by the platinum catalyst (Scheme 2.1.1). By designing substrates with a leaving group beta to the metal-carbon bond, the platinum can donate electrons into the metal-carbon bond to form the carbene while displacing the leaving group, generating the α,β -unsaturated platinum carbenes (**2-4**). These carbenes are electrophilic at the beta position and at the carbon bound to the metal. It is important to note that while it is convenient to describe this intermediate as a platinum carbene, there have not been any studies to date that have confirmed its existence. Several of examples of the utility of these α,β -unsaturated platinum carbene intermediates will be discussed below.



Scheme 2.1.1. Generation of an α,β -unsaturated platinum carbene.

2.1.1 Cycloadditions with Platinum Carbenes

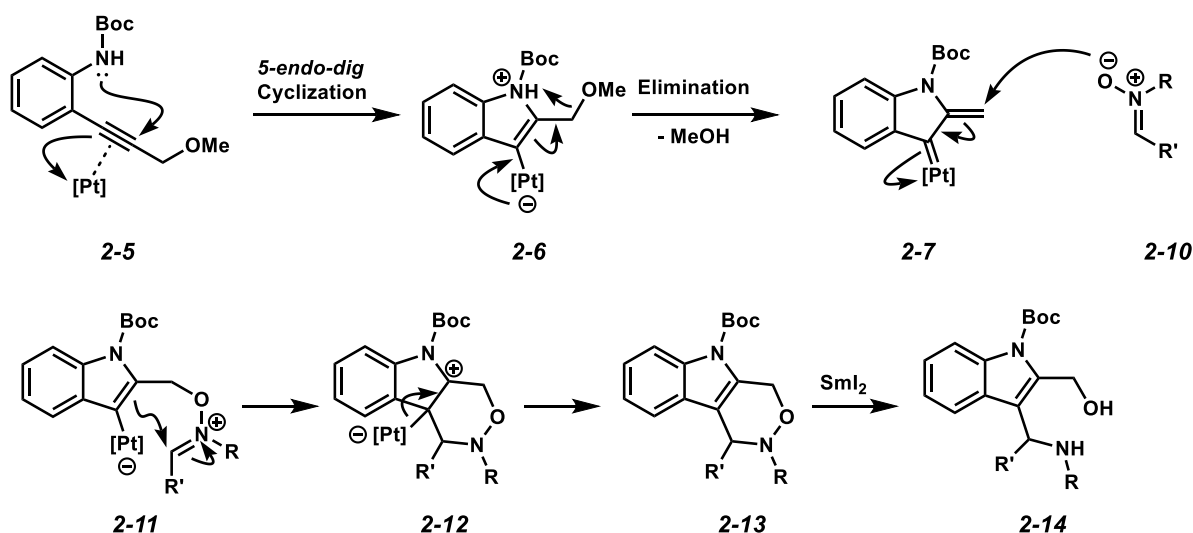
In 2010, Iwasawa and coworkers developed a [3+2] cycloaddition reaction between α,β -unsaturated platinum carbenes and vinyl ethers (Scheme 2.1.2).^{1a} This was the first example of using an unsaturated carbene complex generated catalytically to undergo [3+2] cycloadditions. By using various phenols or protected aniline substrates, various tricyclic benzofurans or indoles could be formed. After generating the α,β -unsaturated carbene (**2-7**), attack from an electron rich vinyl ether onto the α,β -unsaturated carbene forms intermediate **2-8**, with a carbocation stabilized by the adjacent oxygen. A demetallation event occurs, causing the electrons of the platinum-carbon bond to attack the stabilized carbocation, forming the tricyclic product **2-9**.



Scheme 2.1.2. Proposed mechanism of Iwasawa's [3+2] cycloaddition of platinum carbenes and vinyl ethers.^{1a}

Since Iwasawa's report, there have been other studies¹ that have utilized these intermediates as partners in [2+3], [3+3], and [4+3] cycloadditions. In 2013, Hashmi and

coworkers developed a protocol to trap α,β -unsaturated platinum carbenes with nitrones (Scheme 2.1.3).^{1d} After the generation of the α,β -unsaturated platinum carbene (**2-7**), nucleophilic attack of the nitrone oxygen (**2-10**) on the α,β -unsaturated platinum carbene, followed by attack of the alkene on the iminium (**2-11**) leads to [3+3] cycloaddition product **2-12**. A demetallation event occurs next, forming the indole and alleviating all charges in the molecule. A variety of substituents on the propargyl ether substrates were tolerated, with electron donating groups tending to outperform the electron withdrawing substituents. The resulting products can undergo ring opening at the N-O bond with SmI_2 to form the corresponding 1,4 amino alcohol (**2-14**).

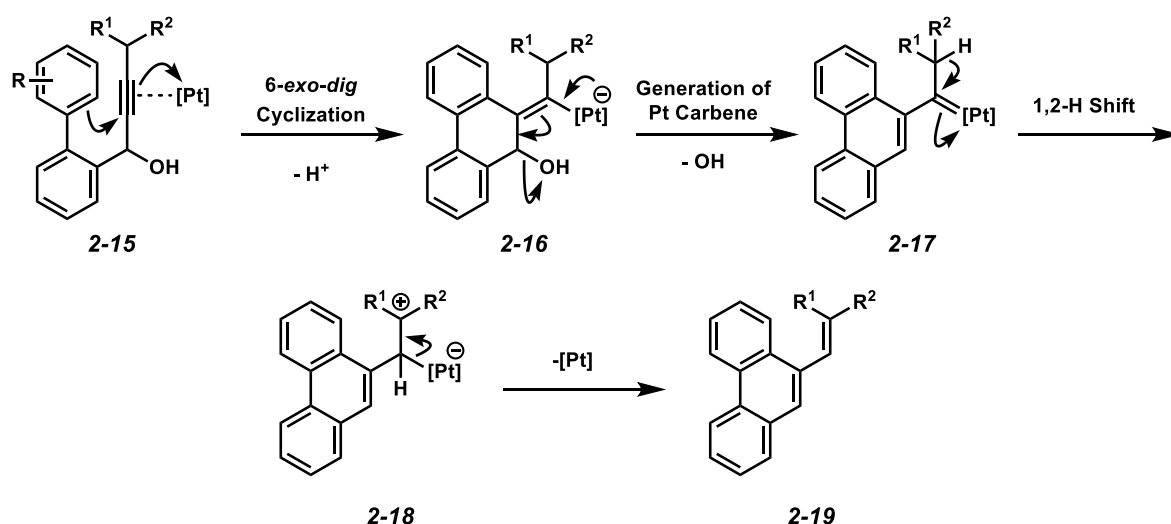


Scheme 2.1.3. Hashmi's [3+3] Cycloaddition with Unsaturated Platinum Carbenes and Nitrones.^{1d}

2.1.2 1,2-Shift Trapping of Platinum Carbenes

Generated platinum carbenes are electrophilic, and thus under the right conditions can be quenched by an electron rich sigma bond. In 2014, Kim and coworkers were able to utilize this reactivity to form a variety of substituted vinyl phenanthrenes (Scheme 2.1.4).^{2c} After activation of the alkyne by platinum, pi electrons from the electron rich arene attack the alkyne (**2-15**). The

pushing of electrons from the platinum form the platinum carbene and release the leaving group (-OH) (**2-16**). A 1,2-hydride shift occurs, forming intermediate **2-18** with a stabilized carbocation. The resulting demetallation forms the desired product and releases the platinum back into the reaction mixture. An important thing to note is that electron neutral arenes (R=H) were unsuccessful in this reaction, meaning it was necessary to have electron donating groups in the ring that were attacking the activated alkyne.

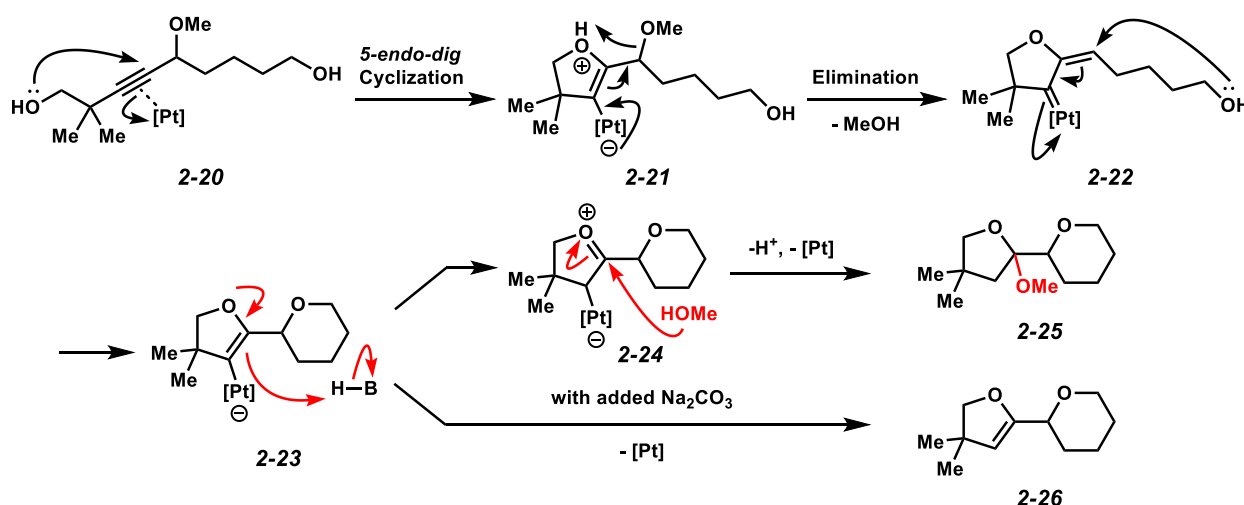


Scheme 2.1.4. Kim and coworkers synthesis of vinylphenanthrenes via a platinum carbene.^{2c}

2.1.3 Bisheterocyclizations of Platinum Carbenes

Bisheterocycles are commonly found motifs in biologically important molecules. These two rings are typically formed one at a time;⁴ however, being able to form both at the same time could be more efficient. In 2013, Ferreira showed that this could be done with α,β -unsaturated platinum carbenes by taking propargyl ether substrates with two heteroatoms at each terminus of the molecule and using a platinum catalyst to achieve the transformation (Scheme 2.1.5).^{3a} The typical reactivity of alkynes with two heteroatom nucleophiles is geminal additions; however,

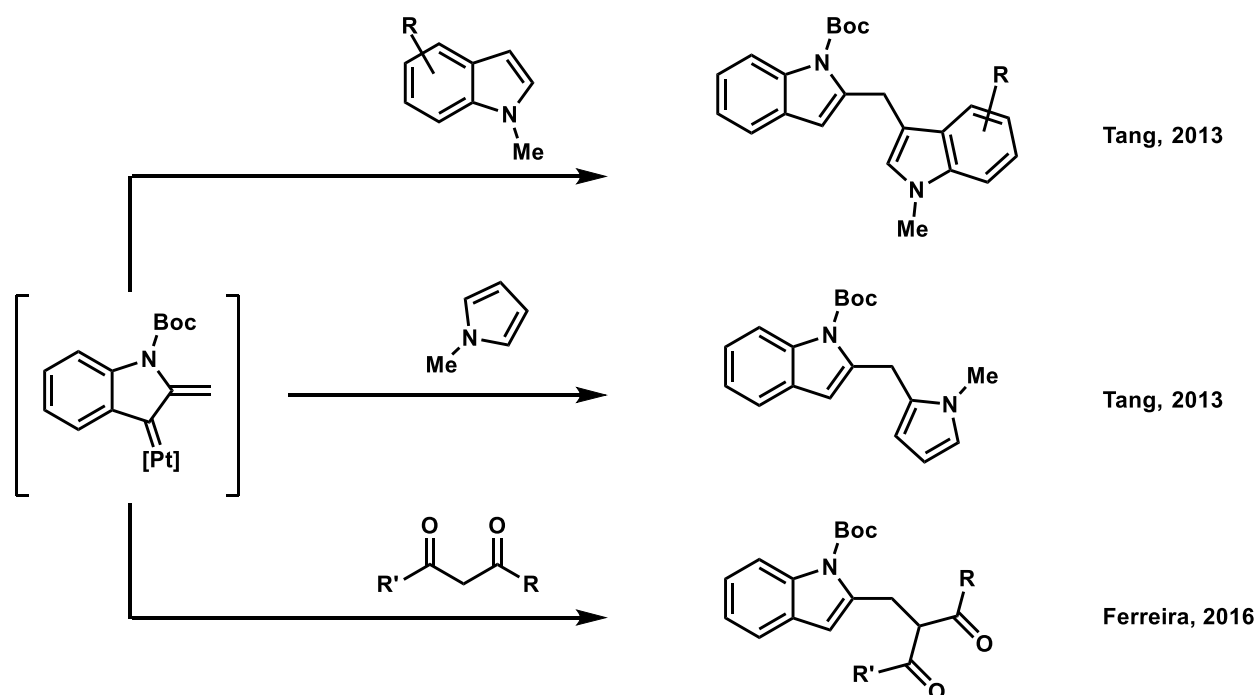
initial reaction conditions showed that the platinum carbene was indeed getting attacked by the second heteroatom. Unfortunately, the formed enol ether was getting attacked by methanol under the reaction conditions, leading to acetal **2-25**. By adding an inorganic base to the reaction conditions, this acetal formation was able to be suppressed, with the desired dihydrofuran being the only observed product (**2-26**). The substrate scope showed that various ring sizes could be formed, in addition to different nucleophiles (N,O).



Scheme 2.1.5. Ferreira's trapping of unsaturated platinum carbenes using pendant nucleophiles to generate a net bisheterocyclization.^{3a}

2.1.4 Additional Nucleophiles used with Carbenes

Outside of the cycloaddition reactions and the intramolecular example presented above, there have been a few other nucleophiles that have shown reactivity towards α,β -unsaturated platinum carbenes. These nucleophiles tend to be carbon based, such as electron rich *N*-methylindoles, *N*-methylpyrrole, and 1,3-dicarbonyl compounds. Scheme 2.1.6 shows the diverse products that can be formed from nucleophilic additions into α,β -unsaturated platinum carbenes.



Scheme 2.1.6. Other nucleophiles that can react with unsaturated platinum carbenes.^{3b-c}

2.2 The Search for New Nucleophiles to Add Into α,β -Unsaturated Platinum Carbenes

With the above examples constituting a sample of the reactivity of the α,β -unsaturated platinum carbene moiety, we sought to find other reaction partners for this intermediate (Figure 2.2.1). The two substrates that we used to probe reactivity are homopropargylic alcohol **2-27** and aniline **2-40**. The use of a homopropargylic alcohol was similar in previous work done in the Ferreira group; however, instead of intramolecular trapping of the carbene, we investigated various potential nucleophiles for their reactivity. Since nitrones have been shown to participate in cycloadditions with these carbenes, we tried isoelectronic nitroso (**2-28**) and hydroxylamine (**2-29**) groups, albeit to no success. Other nucleophiles such as *N*-methylindole (**2-30**), allyl-TMS (**2-31**), nitroalkenes (**2-32**), α,β -unsaturated imines (**2-33**) and allenes (**2-34**) were not competent nucleophiles. Interestingly, azomethine ylides (**2-35**) were able to do cycloadditions with the cycloisomerized substrate; however, this does not go through an α,β -unsaturated platinum carbene

intermediate, as the methyl ether is still present (**2-36**). Using 1,3-dicarbonyl compounds such as 2,4-pentanedione, we were able to form the product (**2-38**) of the attack of the enol into the α,β -unsaturated platinum carbene with the same conditions^{3c} that have been utilized with aniline substrate **2-40**. This experiment showed that the alcohol substrate was capable of generating a platinum carbene that could be intercepted by an external nucleophile. This result only occurred when there was substitution at the propargylic position. When an unsubstituted propargyl ether was used, spirocycle **2-39** was formed instead.

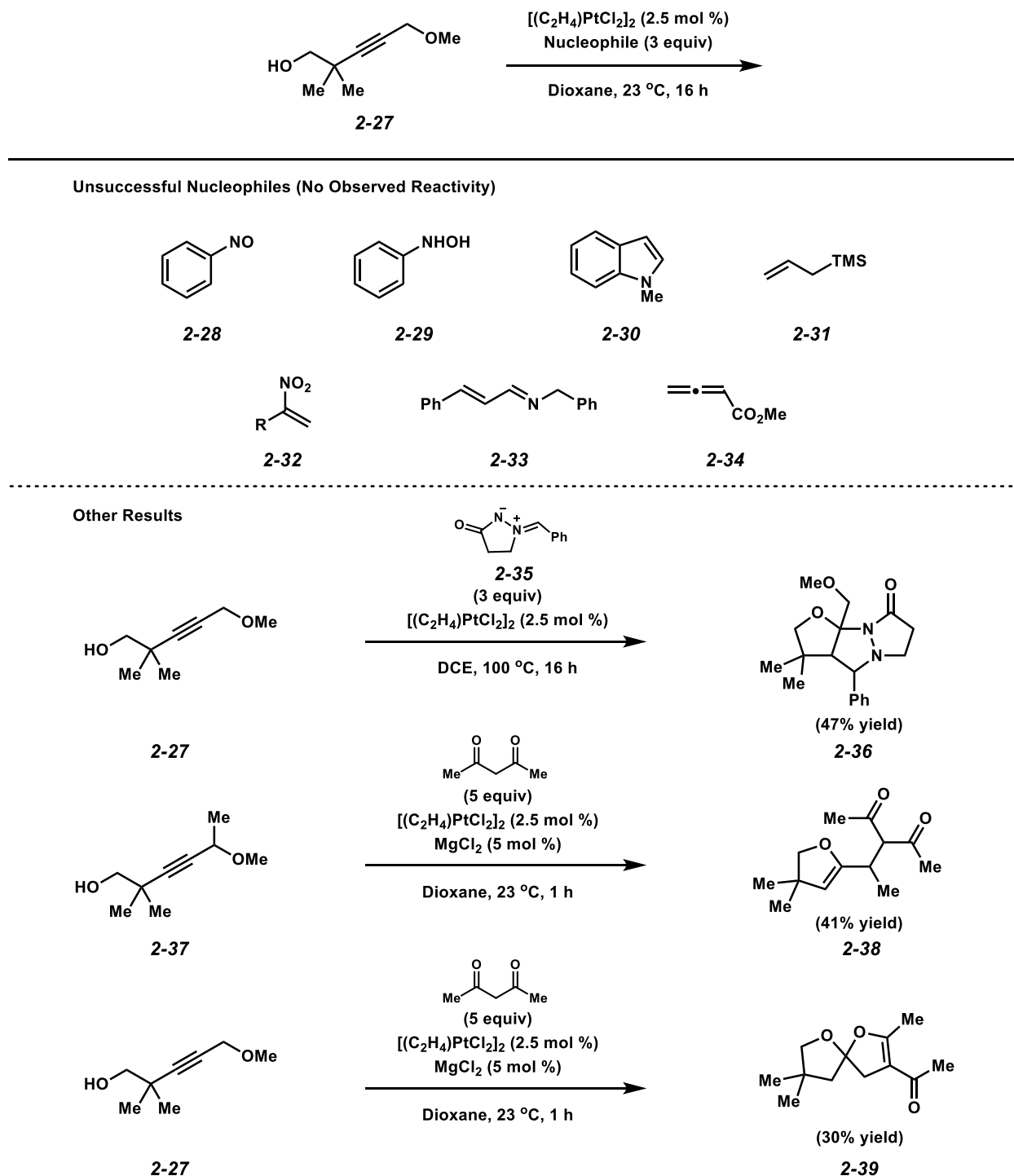


Figure 2.2.1. Nucleophile testing with homopropargylic alcohol substrate **2-27**.

The other substrate we used was the aniline substrate **2-40**, a common substrate class used in platinum carbene chemistry, due to the driving force of forming of an indole ring. Figure 2.2.2 shows the substrates that were tried in this transformation. Like the homopropargyl substrate, we tried nitrosobenzene (**2-28**) and hydroxyaniline (**2-29**), although to no success. We investigated a series of α,β -unsaturated imines (**2-33**, **2-41**, **2-42**, **2-43**) with electron donating groups on them in order to make the imines more nucleophilic. α,β -unsaturated imines tend to be more electrophilic and are used as an electron poor “diene” in a reverse electronic demand Diels-Alder reaction.⁵ Each of these coupling partners proved to be incompatible in the reaction. The next nucleophile we tried was the electron rich oxazole (**2-45**); however, no cycloaddition reaction occurred. When allene **2-34** was used, only indole formation was observed (**2-46**). This indicated that under the reaction conditions the alkyne activation was able to occur; however, the resulting carbene was unreactive with the allene.

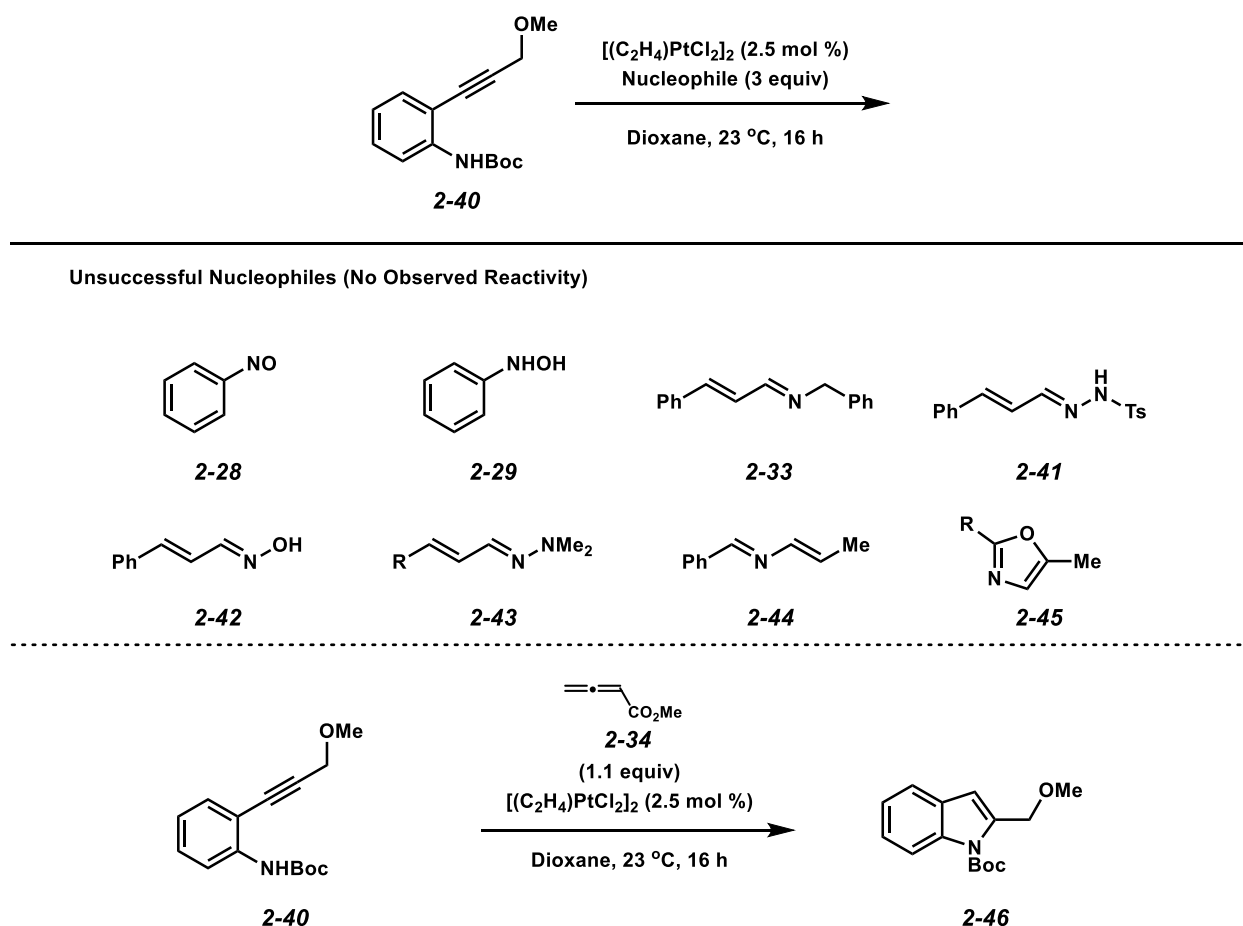


Figure 2.2.2. Nucleophile testing with aniline substrate **2-40**.

2.3 Conclusion

The trapping of α,β -unsaturated platinum carbenes is still a relatively new field where more research is warranted. The examples shown above all use electron rich substrates that can attack the electrophilic unsaturated platinum carbene. Based on the results shown above, there is definitely a threshold of nucleophilicity necessary on the coupling partner to have any interaction with the platinum carbene. In all the attempts we made to make the unsaturated imines and hydrazones more nucleophilic (by installing electron donating groups, for example), we were not able to yield any desired products that utilized the carbene intermediate. Future work in this area

will need to address the concerns of either having a strong enough nucleophile partner, or a more electrophilic platinum carbene in order to achieve the required intermolecular reactivity.

Chapter 2 References

¹ a) Saito, K.; Sogou, H.; Suga, T.; Kusama, H.; Iwasawa, N. *J. Am. Chem. Soc.* **2011**, *133*, 689–691. b) Shu, D.; Song, W.; Li, X.; Tang, W. *Angew. Chem. Int. Ed.* **2013**, *52*, 3237–3240. c) Kusama, H.; Sogo, H.; Saito, K.; Suga, T.; Iwasawa, N. *Synlett* **2013**, *24*, 1364–1370. d) Yang, W.; Wang, T.; Yu, Y.; Shi, S.; Zhang, T.; Hashmi, A. S. K. *Adv. Synth. Catal.* **2013**, *355*, 1523–1528. e) Huynh, K. Q.; Seizert, C. A.; Ozumerzifon, T. J.; Allegretti, P. A.; Ferreira, E. M. *Org. Lett.* **2017**, *19*, 294–297.

² a) Allegretti, P. A.; Ferreira, E. M. *Org. Lett.* **2011**, *13*, 5924–5927. b) Allegretti, P. A.; Ferreira, E. M. *Chem. Sci.* **2013**, *4*, 1053–1058. c) Kwon, Y.; Kim, I.; Kim, S. *Org. Lett.* **2014**, *16*, 4936–4939.

³ a) Allegretti, P. A.; Ferreira, E. M. *J. Am. Chem. Soc.* **2013**, *135*, 17266–17269. b) Shu, D.; Winston-McPherson, G. N.; Song, W.; Tang, W. *Org. Lett.* **2013**, *15*, 4162–4165. c) Allegretti, P. A.; Huynh, K.; Ozumerzifon, T. J.; Ferreira, E. M. *Org. Lett.* **2016**, *18*, 64–67.

⁴ a) Boivin, T. L. B. *Tetrahedron* **1987**, *43*, 3309–3362. b) Faul, M. M.; Huff, B. E. *Chem. Rev.* **2000**, *100*, 2407–2473.

⁵ Boger, D. L. *Tetrahedron* **1983**, *39*, 2869–2939.

CHAPTER 3

ENANTIOSELECTIVE SYNTHESIS OF THE GELSEMIUM ALKALOIDS

3.1 Overview

The purpose of this chapter is to introduce the previous syntheses of the Gelsemium alkaloids (specifically gelsedine-type) as well as highlight the studies towards a novel way to synthesize members of this family enantioselectively. Previous studies in the Ferreira lab on chirality transfer of cycloisomerizations as well as the racemic synthesis of gelsenicine will be discussed briefly. By combining these previous efforts, a strategy towards the enantioselective synthesis of Gelsemium alkaloids via a chirality transfer approach will be explored.

3.2 *Gelsemium* Alkaloids

Gelsemium is a genus of flowering plants that are found in the southeastern United States (*Gelsemium sempervirens* and *G. rankinii*), as well as in South Asia and Oceania (*G. elegans*).¹ Most of the members of this genus have been used in traditional Chinese medicine as well as homeopathic medicines for the treatment of neuralgia, uterine pain, influenza, skin ulcers and cancer pain.² The common bioactive compounds of the genus include over 120 alkaloid natural products which feature either an indole or an oxindole moiety.³ The structures of these complex alkaloids have been classified into six groups: gelsemine, gelsedine, humantenine, koumine, sarpagine, and yohimbane-type. A representative compound from each type is shown in Figure 3.2.1. Only the gelsedine type alkaloids will be discussed further.

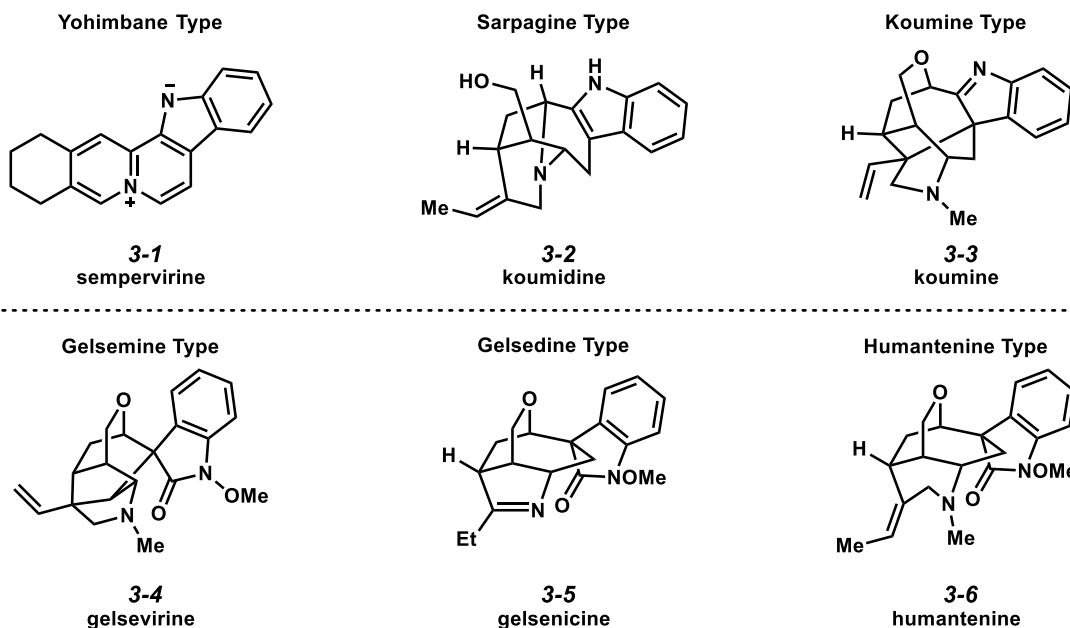


Figure 3.2.1. The six types of *Gelsemium* alkaloids.

3.3 Gelsedine Type Alkaloids

Members of the Gelsedine class of *Gelsemium* alkaloids (gelsedine, gelsenicine, gelsedilam, and gelsemoxonine) were first isolated from *Gelsemium elegans*. Of these natural products, gelsedine and gelsenicine were shown to have efficacy for inflammatory and neuropathic pain, as well as potent cytotoxicity against the A431 human epidermoid carcinoma cell line.⁴ Interestingly, the gelsedine type alkaloids such as gelsedine and 14-acetoxygelsenicine exhibit strong cytotoxicity (EC_{50} values of 0.35 μ M and 0.25 μ M respectively) compared to cisplatin (EC_{50} value of 3.5 μ M). The other classes of *Gelsemium* alkaloids do not show this same level of activity.

The key structures of the Gelsedine-type alkaloids include a cycloheptane-(*N*-methoxy)spiroindole, a [3.2.2]oxabicyclo, *N*-containing 4- or 5-membered heterocycles, and up to 6 contiguous stereocenters. Their compact structures with relatively few functional groups, in

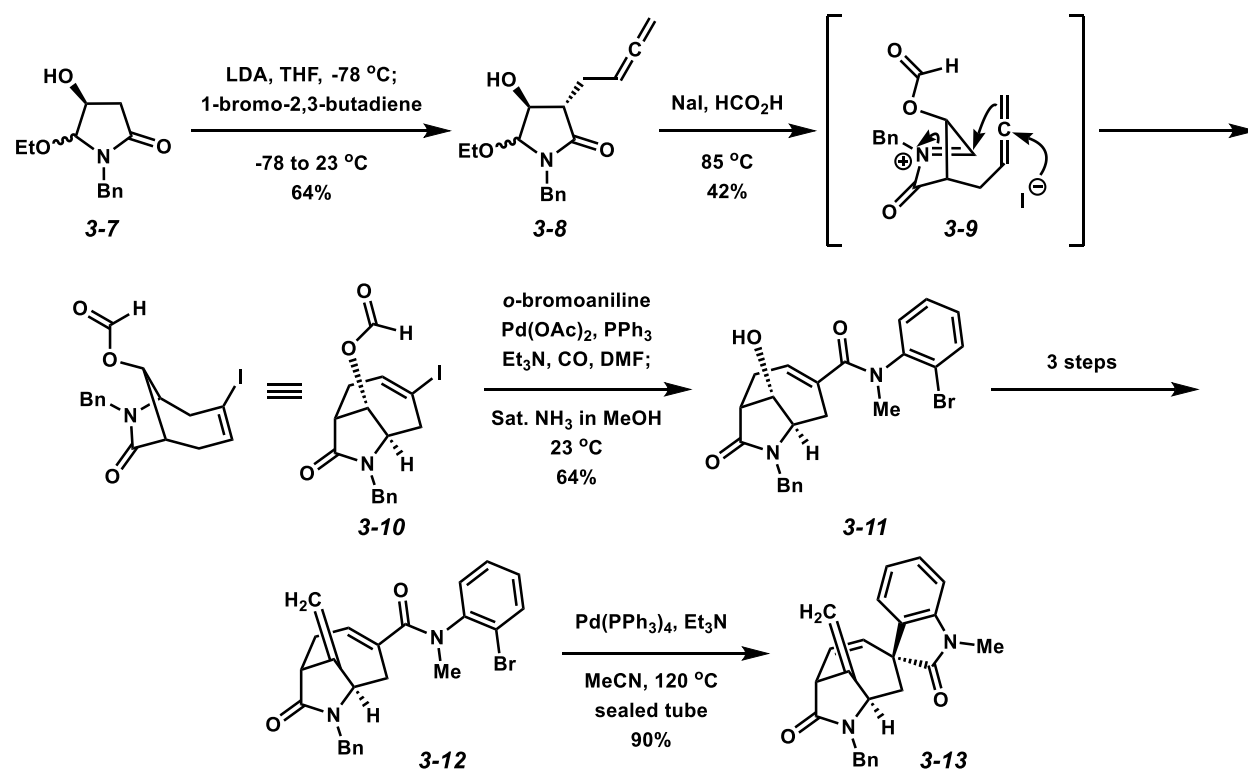
addition to their biological properties, make these natural products interesting to study. There have been a few total syntheses of the gelsedine type alkaloids, and they will be discussed further.

3.4 Syntheses of the Gelsedine-Type Alkaloids

While most of the attention in the synthesis of the Gelsemium alkaloids goes towards the synthesis of gelsemine and other gelsemine-type alkaloids,^{5,6} there have been a few semisyntheses and total syntheses of gelsedine-type alkaloids. From these syntheses one can really start to appreciate both the challenge of making these natural products, as well as the elegant strategies utilized to assemble these natural products. These examples will be shown in chronological order.

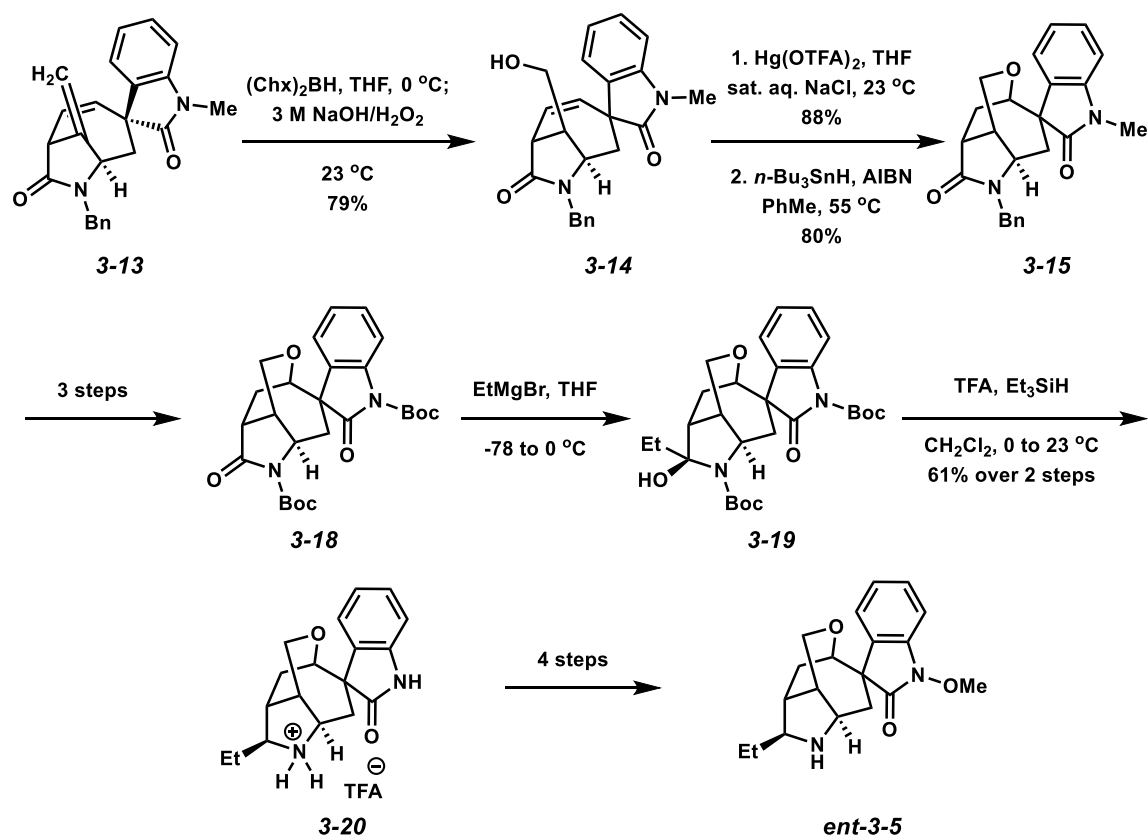
3.4.1 Hiemstra's Synthesis of *ent*-Gelsedine

In 2000, Hiemstra accomplished the total synthesis of *ent*-gelsedine⁷ (*Scheme 3.4.1*) by using a Heck cyclization to form the spiroxindole as was previously done by Overman.⁸ Starting from lactam **3-7** (which was synthesized in 5 steps from (S)-malic acid), alkylation with 1-bromo-2,3-butadiene gave allene **3-8**. Afterwards, treatment with sodium iodide and formic acid gave intermediate **3-10**. Next, a carbonylative Pd-catalyzed cross coupling gave amide **3-11**, which after three steps was ready for the Heck cyclization. Conversion to the spiroxindole occurred with the desired diastereoselectivity, likely due to the carbopalladation occurring on the less sterically hindered convex face.



Scheme 3.4.1. Hiemstra's construction of the spiroindole core.

The oxabicyclic **3-15** was formed in three steps from **3-13**, starting with hydroboration followed by an oxymercuration-reduction of the resulting alcohol (Scheme 3.4.2). With the two main ring systems completed, the next step was to convert the lactam into the pyrrolidine moiety. From **3-18**, addition of ethyl magnesium bromide into the lactam gave hemiaminal **3-19**. Elimination of water by protonation of the alcohol followed by selective reduction of the resulting iminium with triethylsilane led to pyrrolidine salt (**3-20**), which was four steps away from the natural product.



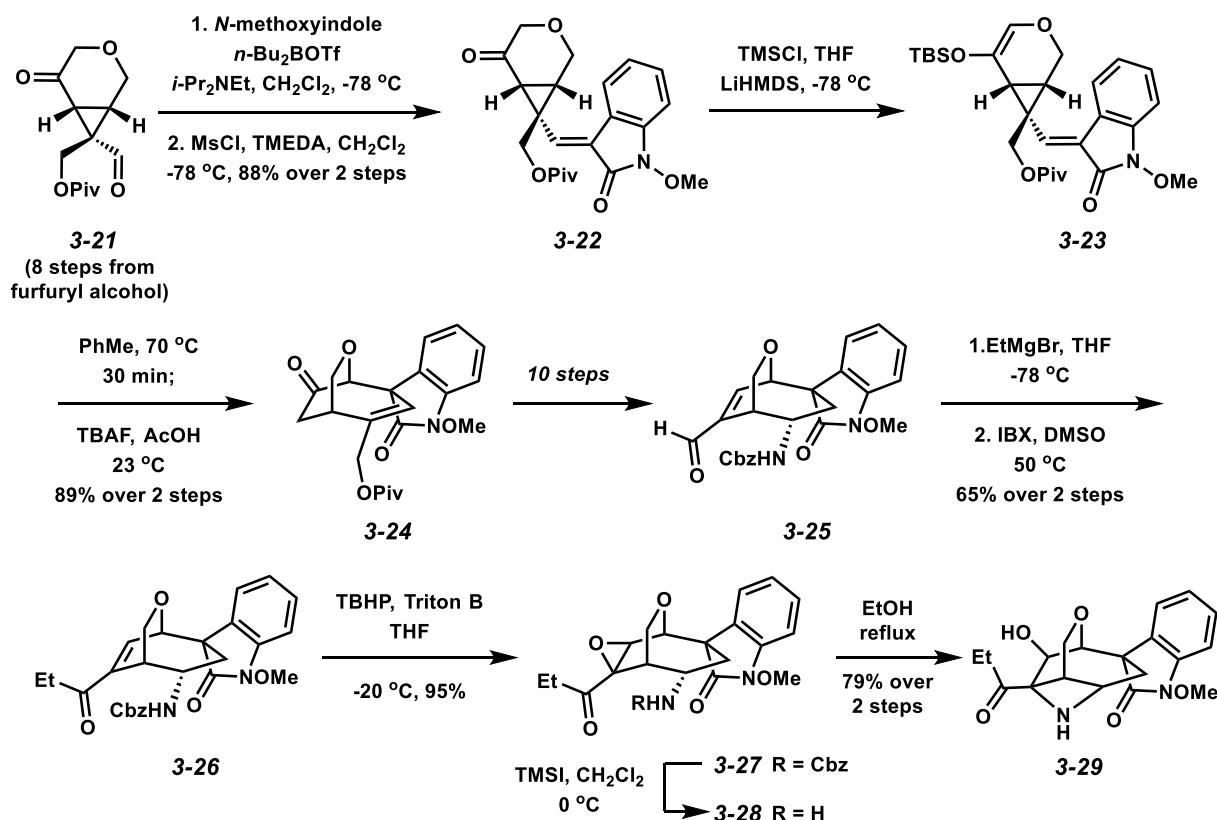
Scheme 3.4.2. Assembly of the oxabicyclic core and pyrrolidine ring of *ent*-gelsedine.

3.4.2 Fukuyama's Enantioselective Synthesis of Gelsemoxonine

In 2011, Fukuyama and coworkers disclosed the enantioselective synthesis of (–)-gelsemoxonine (Scheme 3.4.3).⁹ Starting from furfuryl alcohol, bicycle **3-21** was synthesized in 8 steps. Aldol condensation of *N*-methoxyindole with bicycle **3-21** formed alkene **3-22**, which was converted to silyl enol ether **3-23**. This compound was set up to undergo a divinylcyclopropane-cycloheptadiene rearrangement, forming both the oxabicyclic and spiroindole at the same time.

After ten steps to aldehyde **3-25**, addition of ethylmagnesium bromide and subsequent oxidation with IBX led to **3-26**. Epoxidation of the ethyl ketone followed by deprotection of the secondary amine set up the molecule (**3-28**) for an intramolecular epoxide ring opening with the

amine under reflux in ethanol. This formed the desired azetidine and completed the synthesis of (-)-gelsemoxonine (27 steps, 1.8% overall yield).

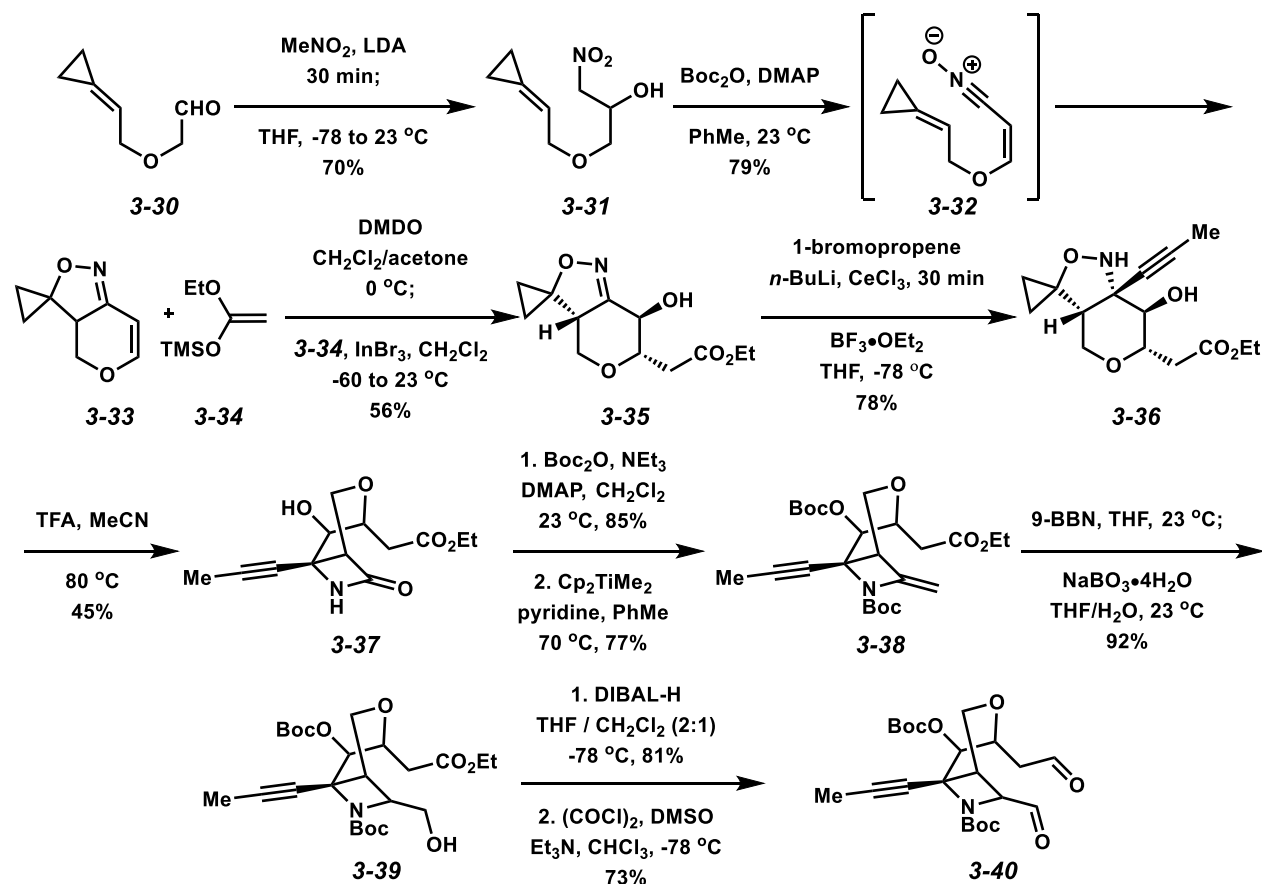


Scheme 3.4.3. Fukuyama's synthesis of (-)-gelsemoxonine.

3.4.3 Carreira's Racemic Synthesis of Gelsemoxonine

In 2013, Carreira and coworkers disclosed a racemic synthesis of gelsemoxonine¹⁰ by using a clever isoxazolidine ring contraction strategy (Scheme 3.4.4).¹¹ A Henry reaction with nitromethane and **3-30** led to alcohol **3-31**. Treatment with di-*tert*-butyl dicarbonate (Boc₂O) and DMAP in toluene formed isoxazolidine **3-33** through alcohol activation, elimination, and dehydration to the nitrile oxide intermediate, which provided the dipole needed for the [3+2] cycloaddition. Epoxide formation with DMDO followed by indium-mediated epoxide ring

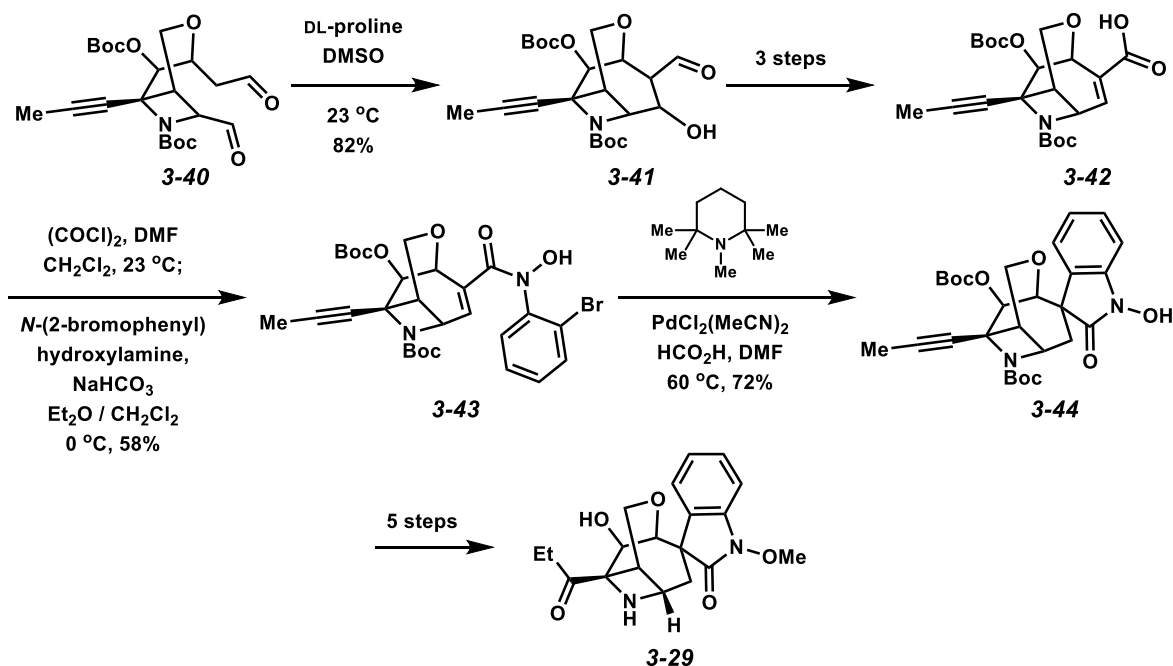
opening with silyl ketene acetal **3-34** led to ester **3-35**. After an addition of *in situ* generated propynyllithium into the imine, a TFA-mediated isoxazolidine ring contraction formed the β -lactam (**3-37**) in modest yield. Protection of the secondary alcohol followed by Petasis olefination led to alkene **3-38**. Hydroboration gave primary alcohol **3-39** which after reduction and Swern oxidation gave the desired dialdehyde (**3-40**).



Scheme 3.4.4. Carreira's synthesis of gelsemoxonine: formation of dialdehyde intermediate **3-40**.

With the dialdehyde in hand, the oxabicyclic was formed using an intramolecular aldol reaction (Scheme 3.4.5). After forming the carboxylic acid (**3-42**), *N*-hydroxyamide was prepared from the corresponding acid chloride, which could undergo a reductive Heck cyclization to form

the spirooxindole (**3-44**). After 5 steps, racemic gelsemoxonine was formed in 26 steps in a 0.1% overall yield.



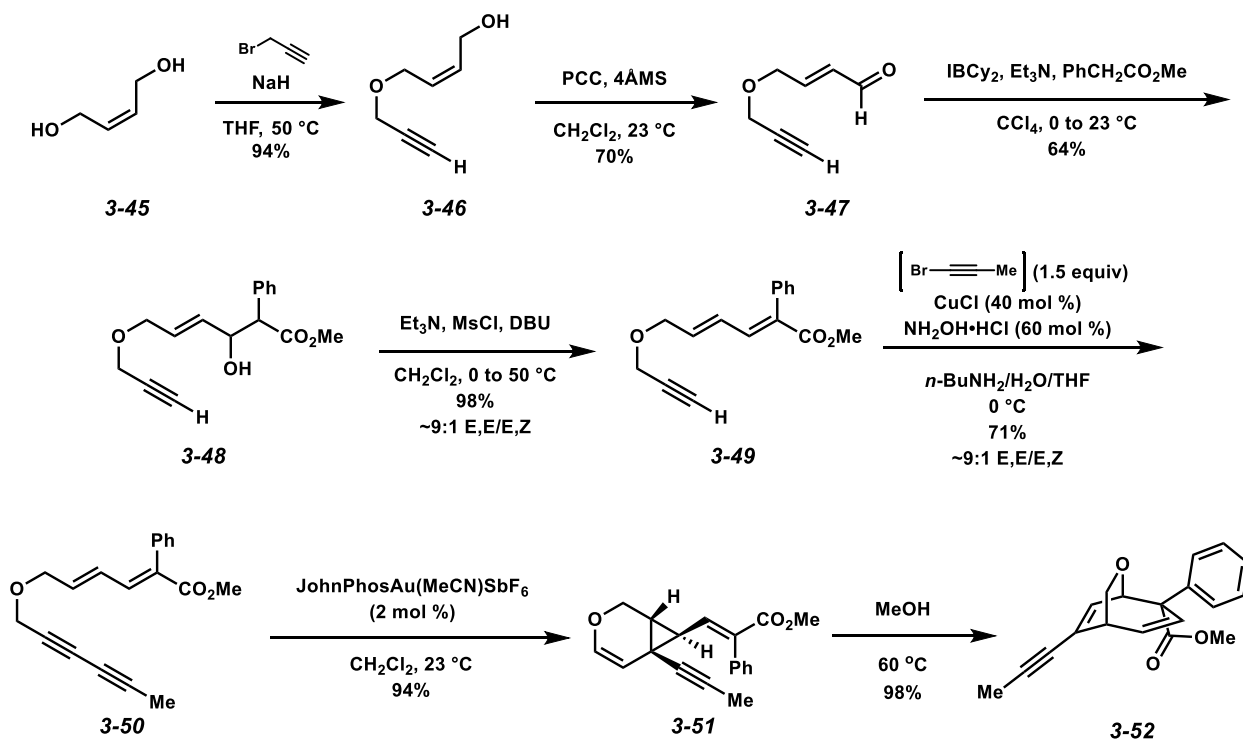
Scheme 3.4.5. Final steps of Carreira's synthesis of gelsemoxonine.

3.4.4 Ferreira's Total Synthesis of Racemic Gelsenicine

Recently, the Ferreira group has completed our own racemic synthesis of gelsenicine¹² featuring a tandem gold-catalyzed cycloisomerization followed by a Cope rearrangement to generate the oxabicyclo with good diastereoselectivity (Scheme 3.4.6). Starting with *cis*-2-butene-1,4-diol, the diol was monoalkylated with propargyl bromide, and oxidized to aldehyde **3-47**. A Lewis acid-mediated aldol condensation using $\text{Cy}_2\text{BI}^{13}$ provided ester **3-49** with good *E,E* selectivity. Alkyne coupling with 1-bromopropyne formed the desired diene-diyne, which would undergo a gold-catalyzed cycloisomerization to afford oxabicycloheptene **3-51** in excellent yield. It was found that removing the catalyst prior to heating the cycloisomerization product was

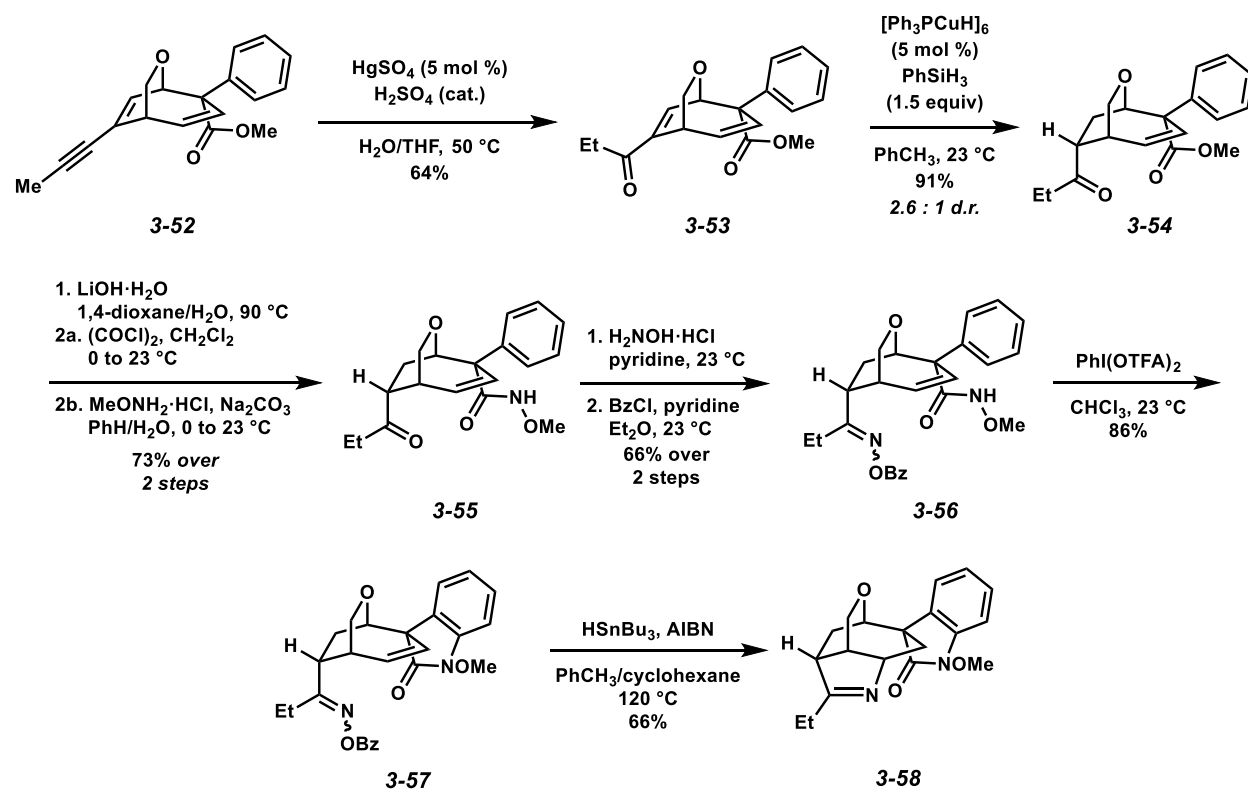
beneficial to increasing the yield and diastereoselectivity of the Cope products in the next step.

The Cope rearrangement formed the oxabicyclic core in excellent yield.



Scheme 3.4.6. Ferreira's generation of the oxabicycle core of gelsenicine.

The final steps, including the formation of the spirooxindole and the radical ring closure of the pyrrolidine ring, can be seen in Scheme 3.4.7. Mercury-catalyzed hydration of the alkyne led to enone **3-53**, providing two electronically different alkenes. Reduction of the enone with Stryker's reagent followed by installation of the *N*-methoxyamide formed compound **3-55**. The ketone was then protected as a benzoyl oxime. Closing the oxindole ring with PIFA followed by closing the pyrrolidine ring by radical cyclization yielded gelsenicine in a 6.8% yield over 14 steps.

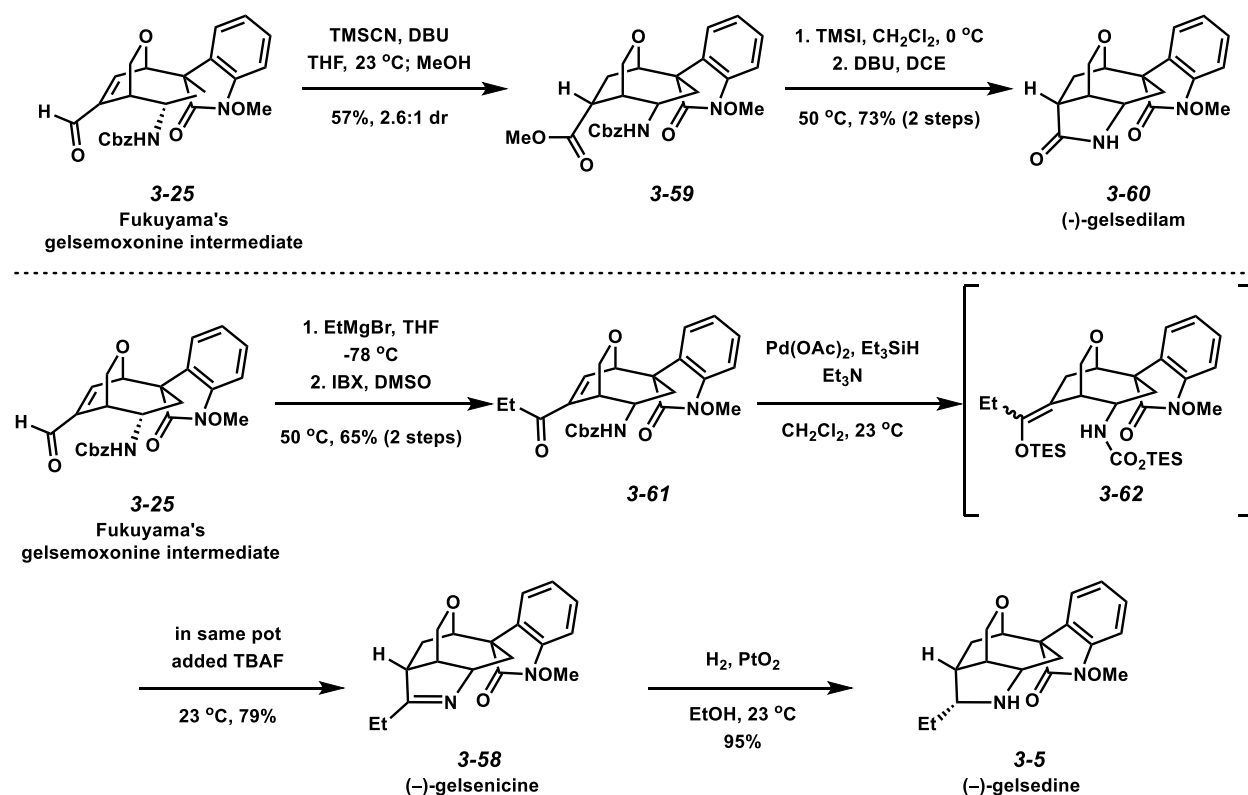


Scheme 3.4.7. Final steps of Ferreira's total synthesis of gelsenicine.

3.4.5 Fukuyama's Divergent Enantioselective Syntheses of Gelsenicine, Gelsedine, and Gelsedilam

In a recent report, Fukuyama was also able to access other members of the Gelsedine-type alkaloids by using a common intermediate approach to introduce the 5-membered nitrogen-containing heterocycles (Scheme 3.4.8).¹⁴ The common intermediate is aldehyde **3-25**, which was one of the intermediates in the gelsemoxonine synthesis that was discussed earlier in Figure 3.4.3.⁹ To make the lactam moiety seen in gelsedilam, aldehyde **3-25** was treated with TMSCN and DBU in THF, followed by MeOH to form methyl ester **3-59** with the required stereochemistry at C15. Subsequent treatment with TMSI, followed by a DBU-promoted ester amidation provided gelsedilam (**3-60**).

Treatment of the same aldehyde intermediate (**3-25**) with EtMgBr followed by oxidation with IBX led to ethyl ketone **3-61**. Pd-catalyzed conjugate reduction of the enone followed by in situ trapping as a silylenol ether led to intermediate **3-62**. In the same pot, gelsenicine could be formed by the addition of TBAF. A hydrogenation of gelsenicine using Adams' catalyst provided gelsedine in excellent yield. Fukuyama's approach highlights the versatility of using a common intermediate to synthesize a library of related natural products (or their derivatives).

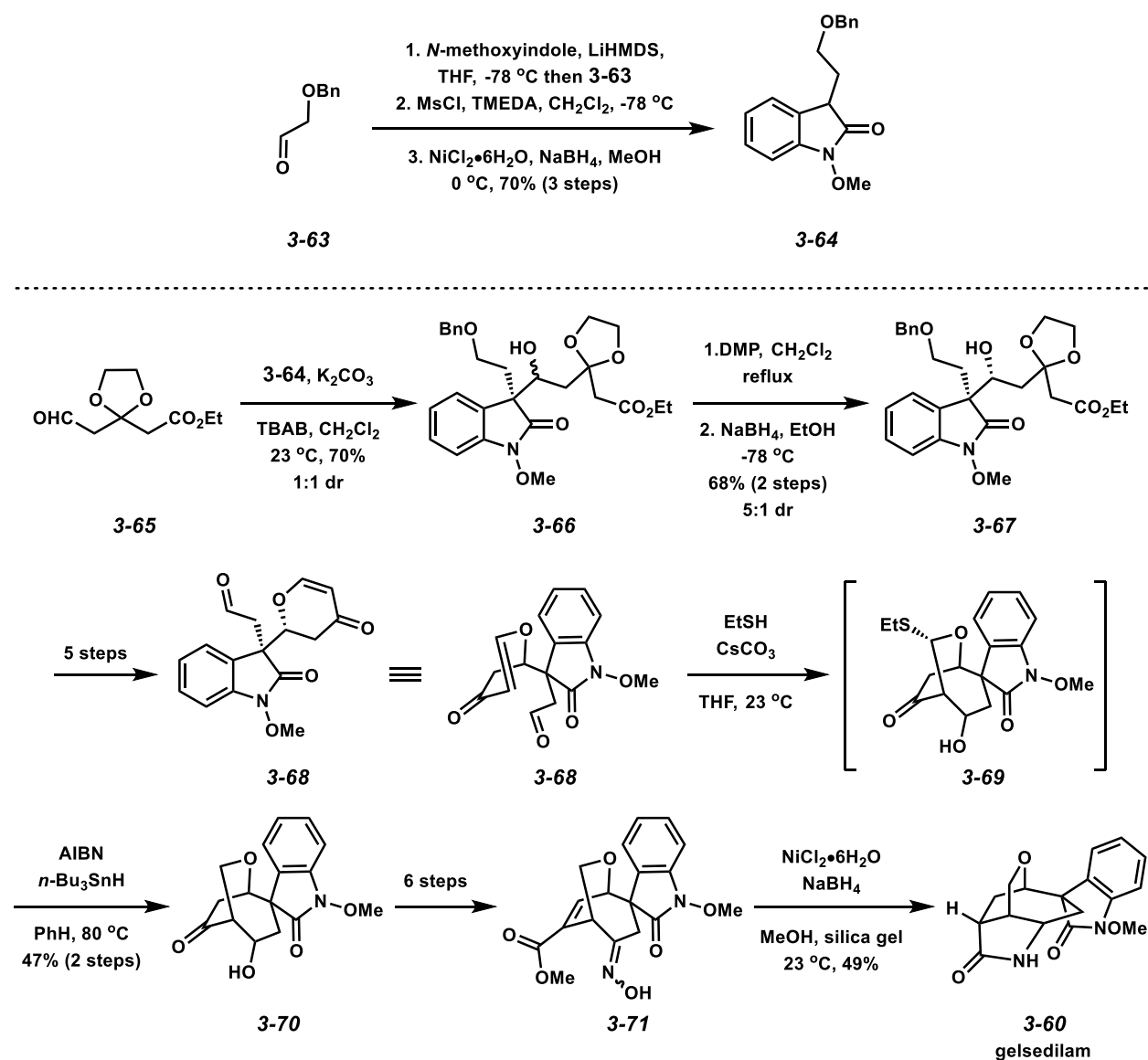


Scheme 3.4.8. Fukuyama's divergent syntheses of the gelsedine-type alkaloids.

3.4.6 Zhao's Racemic Synthesis of Gelsedilam

In 2016, Zhao and coworkers utilized a new strategy to construct the spiroxindole moiety in their total synthesis of gelsedilam (Scheme 3.4.9).¹⁵ In contrast to the commonly used Heck

cyclization strategy, Zhao used an aldol reaction to generate the indole moiety, followed by a thiol mediated Michael addition/aldol cascade to complete the spirocycle. An aldol reaction between aldehyde **3-63** and *N*-methoxyoxindole followed by elimination and reduction led to intermediate **3-64**. The quaternary carbon at C7 was introduced by another aldol reaction with ethyl ester **3-65** to form alcohol **3-66**. Epimerization of the alcohol by a sequence of oxidation followed by reduction allowed the correct stereochemistry of the alcohol to be formed (**3-67**). From this intermediate, keto aldehyde **3-68** was formed in 5 steps. The spirocycle was formed from a thiol-mediated Michael addition onto the aldehyde, forming an unstable intermediate (**3-69**). Immediate reduction with tributyltin hydride formed keto alcohol **3-70**. In 6 steps, **3-70** was converted to methyl ester **3-71**. The lactam moiety was formed from a global reduction of the C=C, C=N, and N-O bonds with $\text{NiCl}_2 \cdot 6\text{H}_2\text{O}$ in the presence of NaBH_4 and silica gel, followed by in situ lactam formation to generate gelsedilam (**3-60**). During the process the desired stereochemistry of C15 was set during a favorable attack of hydride on the less hindered convex face of unsaturated ester **3-71**.

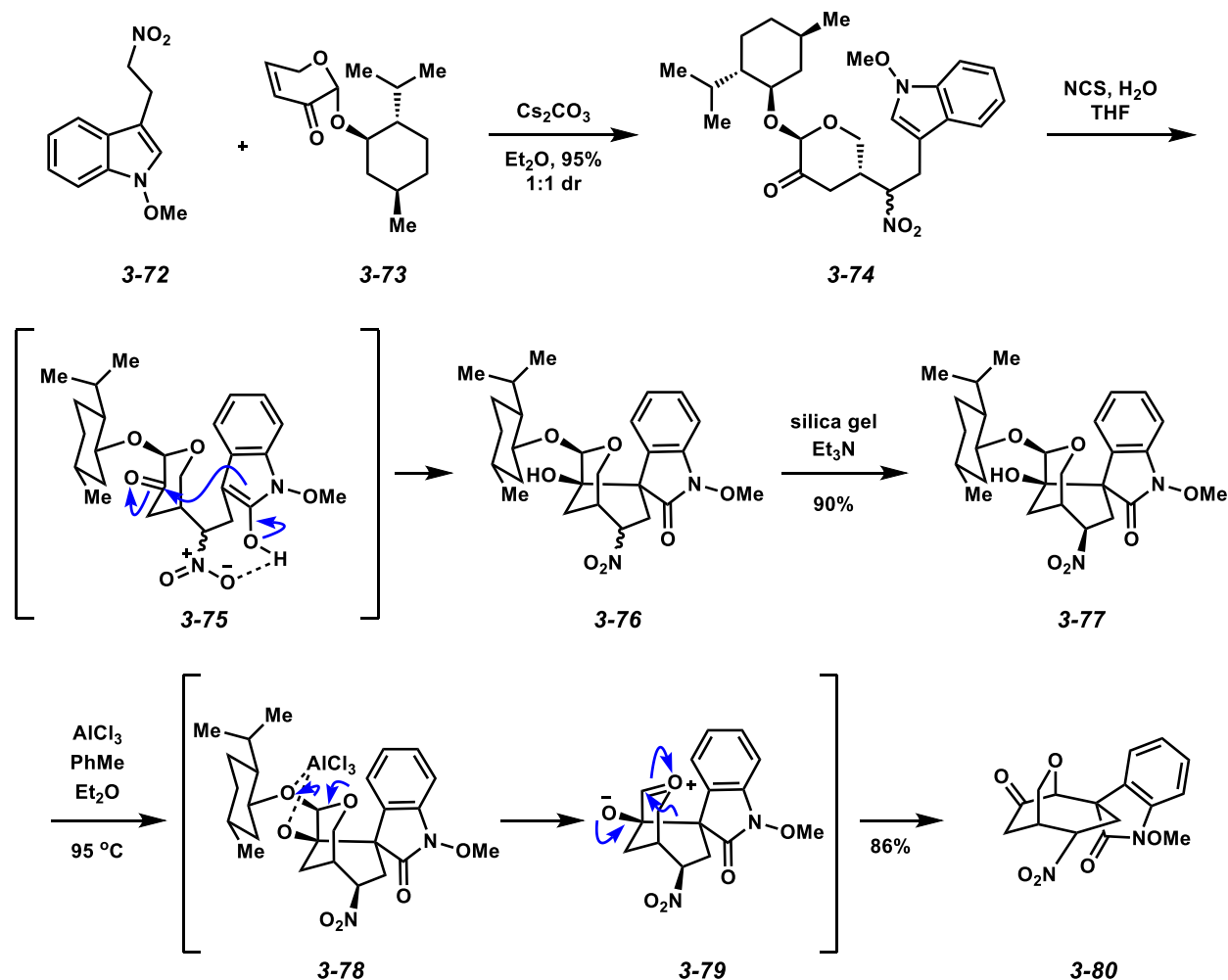


Scheme 3.4.9. Zhao's racemic synthesis of gelsedilam.

3.4.7 Ma's Enantioselective Divergent Syntheses of Gelsedine-Type Alkaloids

Ma and coworkers developed an elegant enantioselective divergent synthesis of four members of the Gelsedine-type alkaloids using common intermediate **3-80** (Scheme 3.4.10).¹⁶ An asymmetric Michael addition of *N*-methoxyindole **3-72** onto (–)-menthol-protected enone **3-73** formed Michael adduct **3-74** as a 1:1 mixture of diastereomers. The quaternary carbon center was

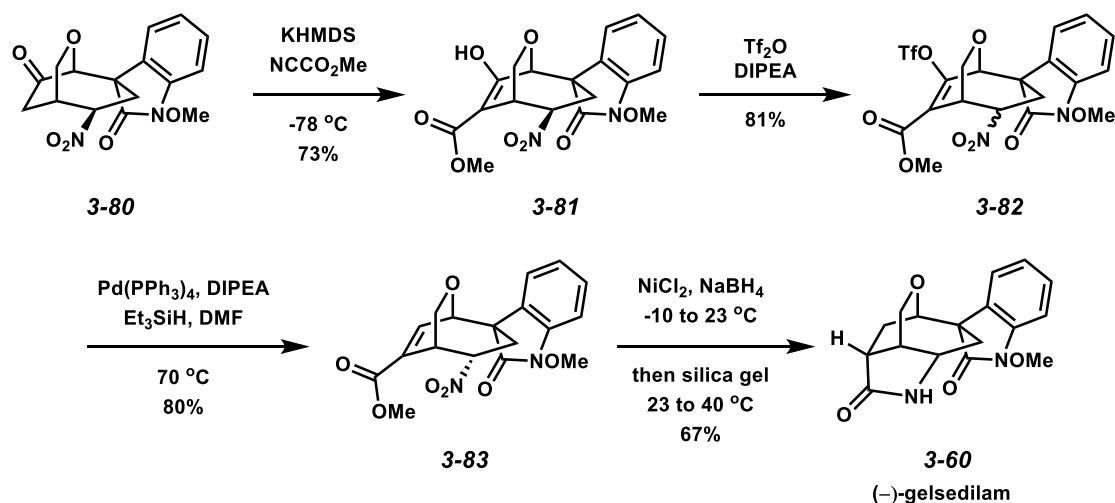
formed from an oxidation of the indole with NCS, followed by an aldol reaction of the oxindole into the ketone. Epimerization of the nitro group with silica gel and trimethylamine was necessary to provide the thermodynamically favored isomer **3-75**. An AlCl_3 -promoted pinacol rearrangement led to the formation of key intermediate **3-80**.



Scheme 3.4.10. Synthesis of Ma's common intermediate.

From intermediate **3-80**, only four steps were needed to synthesize (–)-gelsedilam. Treatment with KHMDS and methyl cyanofornate introduced the methyl ester into the bicyclic ring. After two steps involving the reduction of the enol and epimerization of the nitro group,

unsaturated ester **3-83** underwent a nickel borohydride-mediated global reduction of the alkene and nitro group, furnishing (–)-gelsedilam upon heating with silica gel in 7 steps from **3-72** and **3-73**.

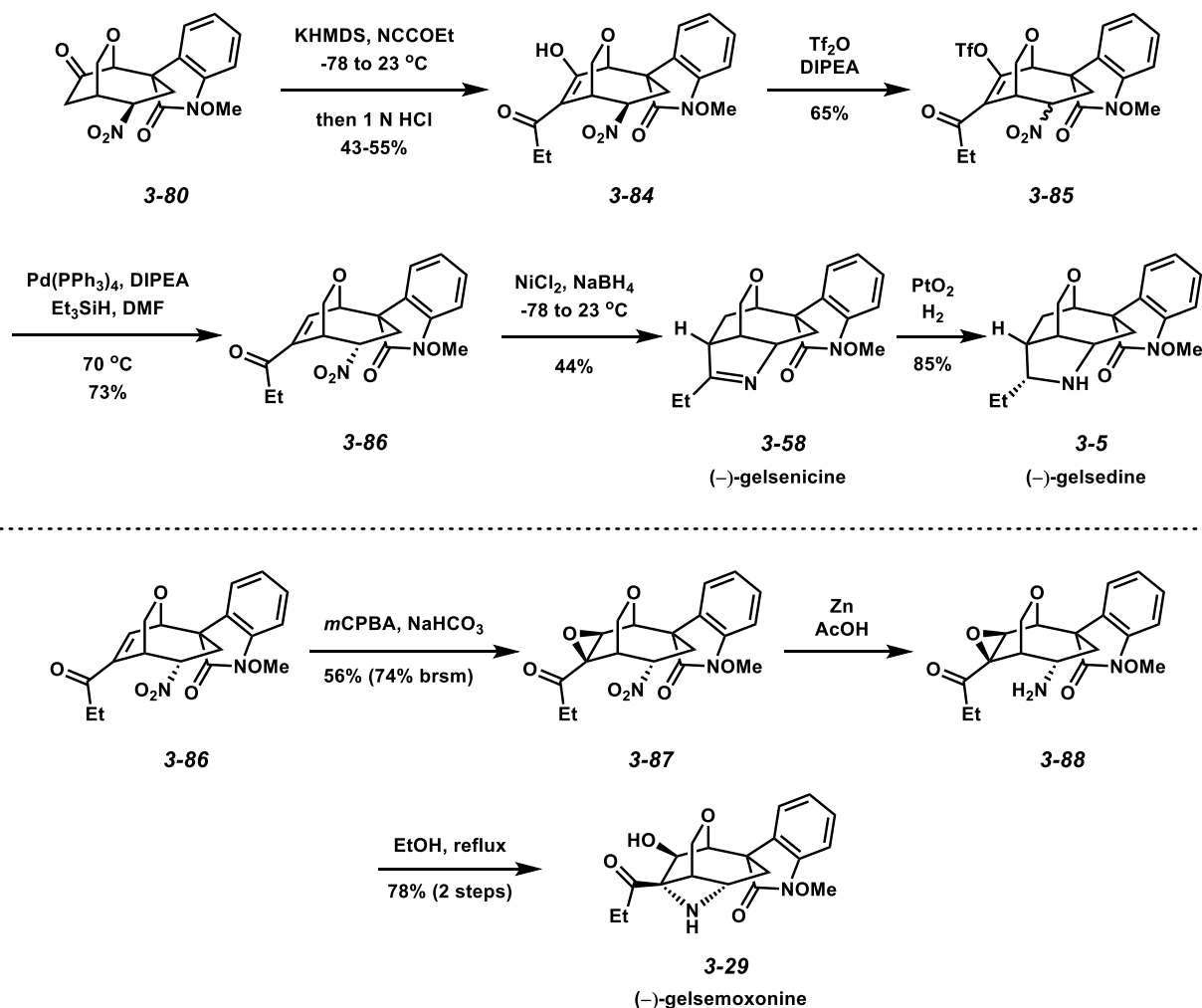


Scheme 3.4.11. Synthesis of (–)-gelsedilam from **3-80**.

The syntheses of (–)-gelsenicine, (–)-gelsedine, and (–)-gelsemoxonine were also possible from intermediate **3-80** (Scheme 3.4.12, top). Treatment with KHMDS and propionyl chloride led to ketone **3-84**. Similarly to the synthesis of (–)-gelsedilam, compound **3-84** was converted to the enone through the two-step formation of the enol triflate and subsequent reduction and epimerization (**3-86**). The synthesis of (–)-gelsenicine (**3-58**, 7 steps from **3-72** and **3-73**, 6.6% yield) was finished by the selective reduction of the alkene and nitro groups using NiCl_2 and NaBH_4 at low temperatures. Catalytic hydrogenation of (–)-gelsenicine with PtO_2 under a hydrogen atmosphere provided (–)-gelsedine (**3-5**, 8 steps, 5.6% yield).

Diverging from the path towards (–)-gelsenicine and (–)-gelsedine, Ma reported that (–)-gelsemoxonine could be made from intermediate **3-86** (Scheme 3.4.12, bottom). Epoxidation of the alkene followed by reduction of the nitro group led to intermediate **3-88**. Refluxing the epoxide

in ethanol allowed the amine to open the epoxide, forming (–)-gelsemoxonine (**3-29**) in 9 steps from known compounds **3-72** and **3-73** in 6.6% yield.



Scheme 3.4.12. Ma's syntheses of (–)-gelsenicine and (–)-gelsedine from intermediate **3-80** (top).

Synthesis of (–)-gelsemoxonine from ethyl ketone **3-86** (bottom).

3.5 Strategies Toward an Enantioselective Synthesis of Gelsenicine

In Section 3.4.4., we have shown that we can access a common core intermediate for the synthesis of gelsenicine, as well as other members in the gelsedine-type alkaloid family (Scheme 3.4.6). In trying to convert this synthesis into an enantioselective synthesis, there are two methods

that we considered: 1) Developing a chiral catalyst system that could achieve the cycloisomerization in an enantioselective manner (Figure 3.5.1, line 2), or 2) Using chirality present in the molecule to achieve an enantioselective cycloisomerization with an achiral catalyst (Figure 3.5.1, line 3). While the easiest option would be to find an enantioselective chiral catalyst for the cycloisomerization, as this would require little changing of the overall synthesis of the natural product, designing a catalyst system to do the cycloisomerization enantioselectively is not so trivial. Typically the catalyst systems and conditions in the literature tend to be successful for a particular substrate meaning asymmetric catalysis might not be a straightforward way to achieve the enantioselective cycloisomerization. We decided to pursue an approach using chirality transfer as a way to do the cycloisomerization. Previous work in the Ferreira lab showed that the enantioselective transformation is possible, if the group at the propargylic position is bulky (i.e., *i*-Pr).¹⁷ However, all of the examples tried were alkyl-based, and ultimately this group would need to be removed after the cycloisomerization if this finding were to be applied to this total synthesis approach.

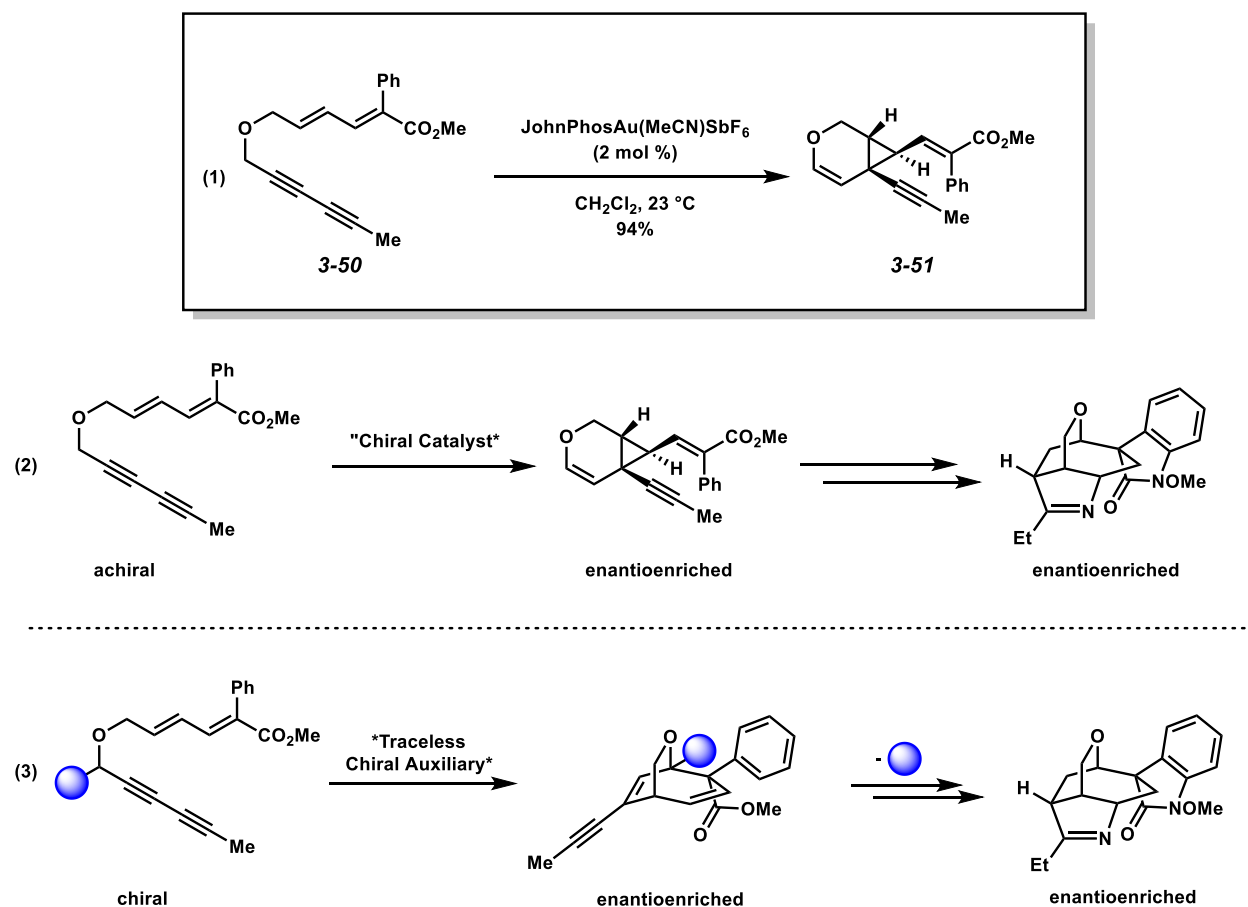


Figure 3.5.1. Strategies to make oxabicyclic core of gelsenicine enantioselectively.

3.5.1 Synthesis of the Reductive Radical Decarboxylation Substrate

In order to investigate whether or not such a strategy could be feasible, we designed a substrate with the oxabicyclic core that is similar to the one present in the gelsenicine synthesis (Scheme 3.5.2). To test the proof of concept, we began our investigation with an achiral substrate first. Starting from *cis*-but-2-ene-1,4-diol, bis-TBS protection followed by ozonolysis led to aldehyde **3-91**. Addition of phenylacetylene and alkylation of the resulting alcohol with sorbyl bromide (generated from sorbitol) formed the 1,6-enyne (**3-94**). After Pt-catalyzed cycloisomerization of the enyne, deprotection of the TBS ether followed by Parikh-Doering oxidation and Pinnick oxidation gave the desired carboxylic acid.

substrate was not the exact substrate we would use to attempt the decarboxylation, further optimization was not pursued. As long as the propargylic “chiral auxiliary” was a functional group that could be transformed into a carboxylic acid, we could use this traceless strategy.

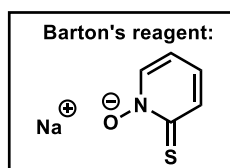
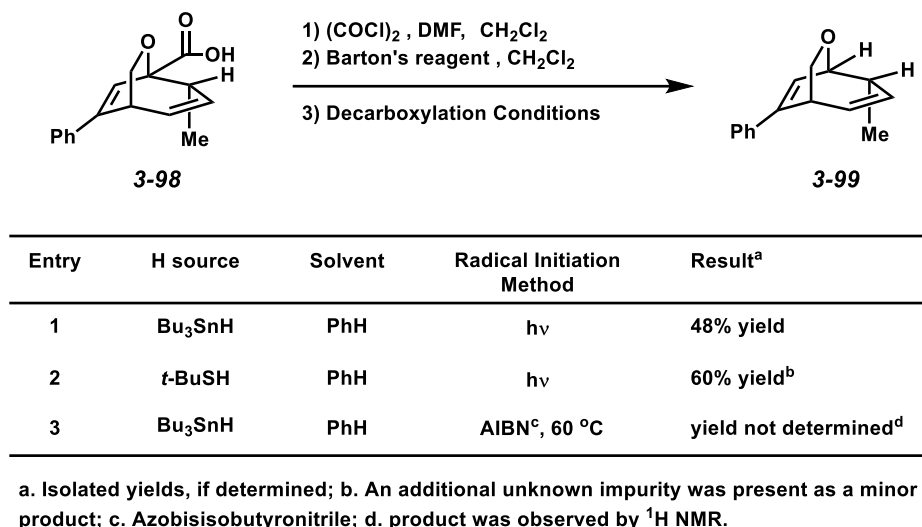
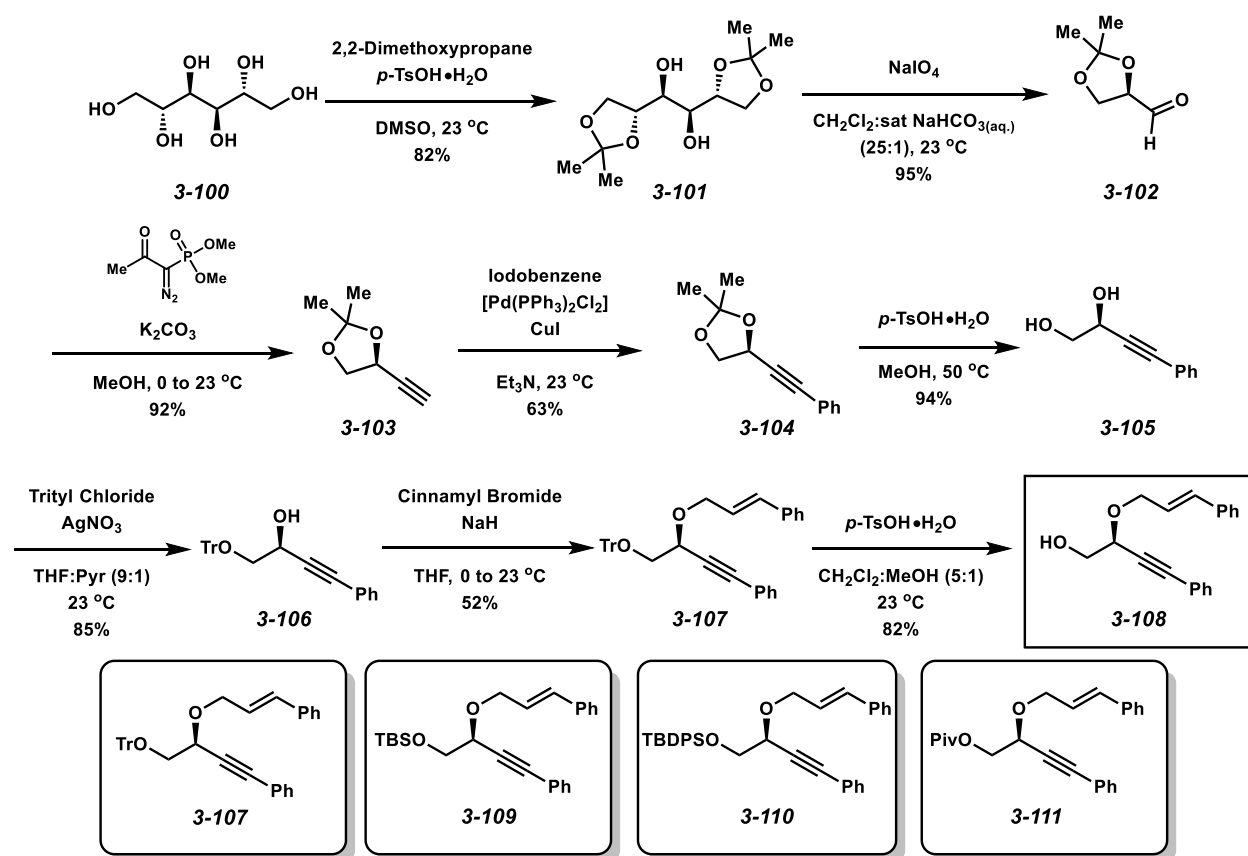


Figure 3.5.3. Preliminary results of the reductive radical decarboxylation of compound **3-98**.

3.5.3 First Generation Traceless Chiral Auxiliaries

With the decarboxylation conditions appearing feasible, the next goal was to get high enantioselectivity in the cycloisomerization reaction. We wanted to stick with –CH₂OPG because of the potential ease of just deprotection, oxidation to the carboxylic acid, and decarboxylation. Also, using substrate **3-108** provides an easy access point to add various protecting groups of various sizes (OTBS, OTBDPS) and types (trityl ethers, pivalate esters).

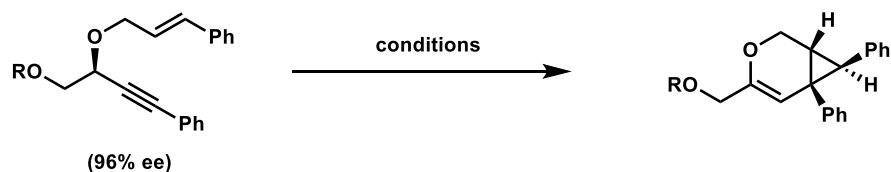


Scheme 3.5.4. Synthesis of first generation substrates for chirality transfer.

Table 3.5.1 shows the enantioselective cycloisomerization attempts on substrates **3-107**, **3-109**, **3-110**, and **3-111** where different catalysts, solvents, and temperatures were tried. The TBS-protected substrate using [JohnPhosAu(MeCN)SbF₆] catalyst (same catalyst used in the natural product synthesis) in dichloromethane at room temperature gave an 82% yield and 74% ee after 4 hours (Figure 3.5.5, entry 1). Excited by this initial result we conducted a quick solvent screen looking at THF and toluene (entries 2-5); however, the yields dropped significantly, while the ee remained about the same. The yield could be slightly recovered after an increase in temperature, but there was not any enantioselectivity enhancement. The reaction was not too successful in a 1:1 hexanes:dichloromethane solvent mixture (48% yield, 74% ee) and increasing the temperature

only caused the yield to drop (entries 6-7). Switching to a platinum-based catalyst gave a modest yield of 35% and 74% ee (entry 8).

While the TBS-protected substrate showed initial promise providing a 74% ee, we had seemed to hit a maximum amount of chirality transfer with this substrate. We next investigated different kinds of protecting groups. The bulkier TBDPS group provided similar reactivity compared to the TBS substrate, with good yields and low 70s ee's (entries 10-11). The same substrate with PtCl_2 as the catalyst was not successful at all, with only 15% yield of product detected (entry 9). The next protecting group we tried was a trityl ether (entries 12-16). Running the trityl ether substrate in THF at 70 °C with PtCl_2 as the catalyst gave a 45% yield and 58% ee. Switching the catalyst to Zeise's dimer ($[(\text{C}_2\text{H}_4)\text{PtCl}_2]_2$) and running the reaction at room temperature saw an enantioselectivity enhancement, but still only at 74% ee. All of the attempts with the JohnPhos Au catalyst were unsuccessful, probably due to the catalyst's incompatibility with the trityl group. The last protecting group we tried was a pivalate ester (entries 17-18). This protecting group offers a chance for a different way for the catalyst to interact with the substrate through possible coordination of the carbonyl of the ester with the catalyst. When we examined the use of gold and platinum catalyst with conditions that have given the best results for these cycloisomerizations. With the platinum conditions we observed a 60% yield and 70% ee, and with gold, a 56% yield and 74% ee.



Entry	R	Catalyst ^b	Solvent	Temp (°C)	Time (h)	Yield (%) ^c	ee (%)
1	TBS	[Au]	CH ₂ Cl ₂	23	4.5	82	74
2	TBS	[Au]	THF	23	3	26	70
3	TBS	[Au]	THF	70	3	49	74
4	TBS	[Au]	PhMe	23	4	35	74
5	TBS	[Au]	PhMe	70	4	60	64
6	TBS	[Au]	1:1 Hexanes:CH ₂ Cl ₂	23	3.5	48	74
7	TBS	[Au]	1:1 Hexanes:CH ₂ Cl ₂	55	3.5	34	72
8	TBS	ZD	PhMe	23	3	35	74
9	TBDPS	PtCl ₂	THF	70	14	15	n.d.
10	TBDPS	[Au]	CH ₂ Cl ₂	23	3	75	70
11	TBDPS	[Au]	PhMe	23	3	90	72
12	Tr	PtCl ₂	THF	70	14	45	58
13	Tr	[Au]	CH ₂ Cl ₂	23	3	<5	n.d.
14	Tr	[Au]	PhMe	23	3	<5	n.d.
15	Tr	[Au]	PhMe	70	3	<5	n.d.
16	Tr	ZD	THF	23	16	45	74
17	Piv	PtCl ₂	THF	70	16	60	70
18	Piv	[Au]	CH ₂ Cl ₂	23	4	56	74

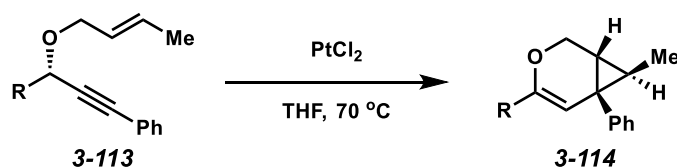
a) Protecting groups: TBS = *tert*-butyldimethylsilyl, TBDPS = *tert*-butyldiphenylsilyl, Tr = trityl, Piv = pivaloyl.

b) Catalyst conditions: [Au] = JohnPhosAu(MeCN)SbF₆ (2 mol %); ZD = Zeise's Dimer, [(C₂H₄)PtCl₂]₂ (2.5 mol%); PtCl₂ @ 7 mol %. c) Yield determined by ¹H NMR with 2-naphthaldehyde as internal standard. d) n.d. = not determined.

Table 3.5.1. Effects of protecting group on observed chirality transfer.

3.5.4 Second Generation Traceless Chiral Auxiliaries

From our studies of $-\text{CH}_2\text{OPG}$ type substrates, we saw that having a functional group at the propargylic position is leading to a transfer of the chirality present in the substrate. Unfortunately though, we had seemed to reach a maximum enantiomeric excess for the substrate at 74% ee. Looking back at the previous work our group had done on chirality transfer,¹³ there was a potential space to explore to enhance enantioselectivity. Two of the best groups for chirality transfer featured α -branching on the group in the propargylic position, such as an isopropyl group, or a cyclohexyl group (Scheme 3.5.7, top). Of course we still needed to consider cleavage of auxiliary after the cycloisomerization, and thus having an all-carbon auxiliary would present a different challenge as it would not be as obvious to cleave. A functional group that could have branching as well as the ability to eventually form a carboxylic acid is the acetonide group. This five membered ring contains the branching that could provide enantioselectivity enhancement, and after deprotection of the acetonide, a 1,2-diol would be formed which could be oxidatively cleaved to the aldehyde, and thus be almost at the stage for decarboxylation (Scheme 3.5.7, bottom). A possible downside to using acetonides as substrates is that now with an extra chiral center in the molecule, each diastereomer would need to be considered separately for these transformations. This is because diastereomers have different physical properties and perhaps one diastereomer could provide the right environment for high levels of chirality transfer, whereas the other diastereomer might not provide as much or any chirality transfer at all. By not separating the diastereomers, we would have two different compounds with potentially varying levels of reactivity, as well as the possibility of forming different products.



Entry	R	ee 3-113	ee 3-114	es ^a
1	Me	97	80	82
2	Cy	99	96	97
3	<i>i</i> -Pr	98	97	99

a) Enantiospecificity (es) = $[(\text{ee}_{\text{product}})/(\text{ee}_{\text{substrate}})] \times 100\%$

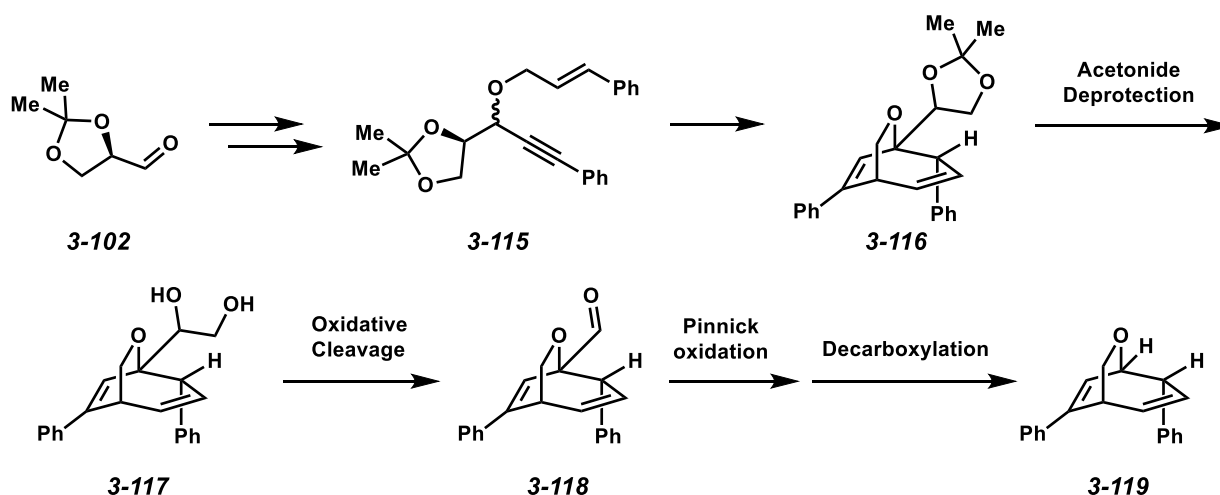
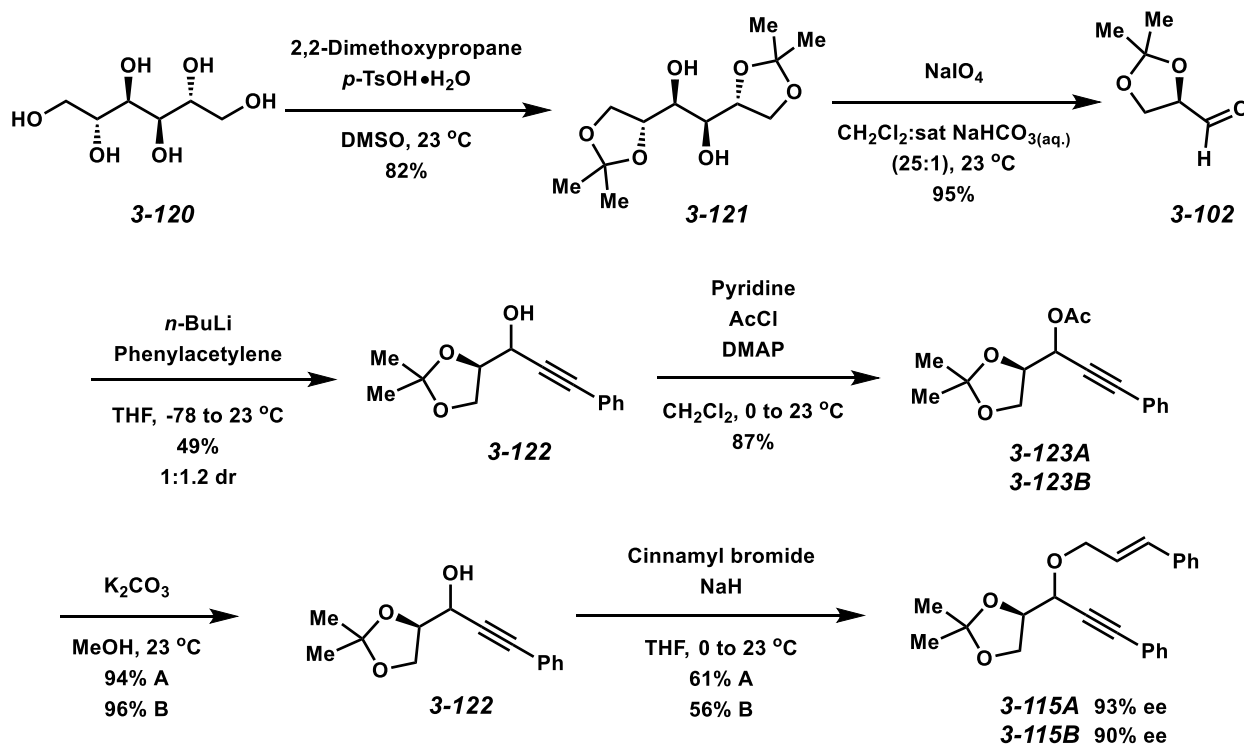


Figure 3.5.7. Previous results involving chirality transfer of substrates with α -branching groups (top). Use of acetonides as a cleavable chiral auxiliary with α -branching (bottom).

The synthesis of the substrates is fairly straightforward, and utilizes another reduced sugar, D-dulcitol, as the starting material (Scheme 3.5.8). Bis-protection of the exterior diols leads to bis-acetonide **3-121**, which underwent oxidative cleavage to give aldehyde **3-102**. Addition of phenylacetylene gave a mixture of two diastereomers, which could be easily separated after acetylation of the alcohol. After alkylation of the diastereomer both substrates were prepared with the diastereomer **3-115A** having 93% ee and the diastereomer **3-115B** having 90% ee. The

potential sources for the erosion of enantiomeric excess probably comes from the basic conditions used for the addition of phenylacetylene into aldehyde **3-102**, which could lead to some epimerization of the adjacent stereocenter.



Scheme 3.5.8. Synthesis of second generation substrates.

For diastereomer A (**3-115A**), using platinum (II) chloride after 14 hours at 70 °C only provided a 50% consumption of the starting material and a 7% yield observed by ¹H NMR (Table 3.5.2, entry 1). Increasing the reaction time to 48 hours only saw a slight increase in conversion with comparable yield (entry 2). Switching to a more soluble platinum catalyst, Zeise's dimer, at room temperature led to total conversion of the starting material after 14 hours, and a slight increase in yield to 20% (entry 3). Changing the catalyst to JohnPhosAu(MeCN)SbF₆ (entries 4-6) allowed for a much faster reaction time; however, there was noticeable decomposition after 4 hours. Shortening the reaction time to 30 minutes led to an enhancement in yield as well as less

noticeable decomposition and similar reactivity was observed after running the reaction in toluene. Lowering the temperature of the reaction to 0 °C led to diminished reactivity (entry 6). For this substrate, ee's were not included due to interference on the HPLC traces from inseparable impurities from the product.

3-115A (93% ee) conditions 3-115A

Entry	Catalyst ^a	Solvent	Temp (°C)	Time (h)	Conversion (%)	Yield (%) ^b
1	PtCl ₂	THF	70	14	50	7
2	PtCl ₂	THF	70	48	65	8
3	ZD	THF	23	14	100	20
4	[Au]	CH ₂ Cl ₂	23	0.5	88	34
5	[Au]	PhMe	23	0.75	80	36
6	[Au]	CH ₂ Cl ₂	0	0.5	45	25

a) Catalyst conditions: [Au] = JohnPhosAu(MeCN)SbF₆ (2 mol%); ZD = Zeise's Dimer, [(C₂H₄)PtCl₂]₂ (2.5 mol%); PtCl₂ @ 7 mol%. b) Yield determined by ¹H NMR with 2-naphthaldehyde as internal standard.

Table 3.5.2. Results of cycloisomerizations of diastereomer (**3-115A**).

3-115B underwent the same analysis as the first diastereomer. Reactions run using platinum (II) chloride showed modest consumption of starting material after 14 and 48 hours, but minimal product was observed (Table 3.5.3, entries 1-2). Switching to the JohnPhosAu(MeCN)SbF₆ catalyst led to a strong increase in yield as well as better conversion (entries 3-8). Running the reaction for a shorter period of time (to keep it consistent with the other diastereomer's experiments) showed an obvious drop in yield and conversion and a 76% ee (entry 4). A quick solvent screen revealed that running the reaction in toluene showed similar yields with

less conversion and a slight drop in ee (68%) (entry 5). Ethereal solvents such as diethyl ether and tetrahydrofuran showed high conversion after 30 minutes; however, yields were very low (entries 6-7). The enantiomeric excess of the reaction run in diethyl ether was appreciably lower compared to the reaction in tetrahydrofuran (37% ee vs. 60% ee). Reducing the temperature of the reaction resulted in less desired product being formed (entry 8).

3-115B
(90% ee)

3-115B

Entry	Catalyst ^a	Solvent	Temp (°C)	Time (h)	Conversion (%)	Yield (%) ^b	ee (%)
1	PtCl ₂	THF	70	14	57	4	**
2	PtCl ₂	THF	70	48	75	<5	**
3	[Au]	CH ₂ Cl ₂	23	4	90	55	**
4	[Au]	CH ₂ Cl ₂	23	0.5	70	32	76
5	[Au]	PhMe	23	0.5	45	30	68
6	[Au]	Et ₂ O	23	0.5	90	6	37
7	[Au]	THF	23	0.5	85	9	60
8	[Au]	CH ₂ Cl ₂	0	0.5	50	4	**

a) Catalyst conditions: [Au] = JohnPhosAu(MeCN)SbF₆ (2 mol%); PtCl₂ @ 7 mol%. b) Yield determined by ¹H NMR with 2-naphthaldehyde as the internal standard.

Table 3.5.3. Results of cycloisomerizations of diastereomer **3-115B**.

3.6 Conclusions from Acetonide-Based Substrate

Alkaloids from the genus *Gelsemium* have been of great interest to chemists for the synthesis of their complex structures as well as understanding the bioactivity of these isolated compounds. Many different approaches presented above have been made to synthesize the

Gelsemium alkaloids. Our original idea was to use a traceless chirality transfer approach to form gelsenicine and other gelsedine type alkaloids enantioselectivity. This idea was based off of previous success of enacting the cycloisomerization reaction with chiral substrates and maintaining high preservation of enantiomeric excess. We also thought this strategy could be a workaround for having to create a new set of chiral catalysis conditions to work on that particular substrate. The first generation of chiral auxiliaries that were based off of protected alcohols showed initial promise of enabling some chirality transfer. Unfortunately, there seemed to be a threshold at 76% ee that we were never able to cross. We then set out to use the acetonide based substrates in order to hopefully add some steric bulk at the propargylic position, and therefore increase the amount of enantioselectivity observed after cycloisomerization. Likewise with the protected alcohol substrates there was an apparent maximum that we seemed to have reached with this type of substrate as well, although more studies need to be done to be conclusive. If such a strategy was able to succeed through the use of chirality transfer and the group was one which could be readily converted to a carboxylic acid, we showed that the reductive radical decarboxylation approach could be a means to remove any traces of the chiral auxiliary. We have since found conditions for the asymmetric cycloisomerization that seem to be very promising, and our research is now focused on optimizing the asymmetric catalyst system further.

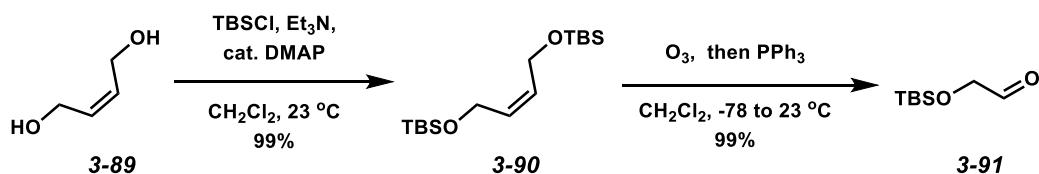
3.7 Experimental

3.7.1 Materials and Methods

Reactions were performed under an argon atmosphere unless otherwise noted. Tetrahydrofuran, dichloromethane, and toluene were purified by passing through activated alumina columns. Deionized water was used for the coupling reactions. All other solvents and reagents were used

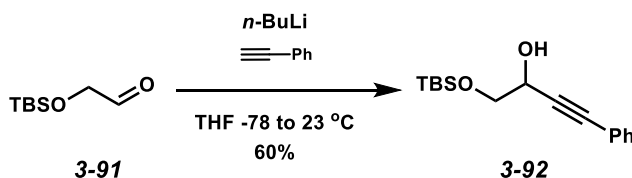
as received unless otherwise noted. Commercially available chemicals and reagents were purchased from Alfa Aesar (Ward Hill, MA), MilliporeSigma (St. Louis, MO), Oakwood Products (West Columbia, SC), Acros Organics (Geel, Belgium), Strem (Newburyport, MA), and TCI America (Portland, OR). Qualitative TLC analysis was performed on 250 mm thick, 60 Å, glass backed, F254 silica (SiliCycle, Quebec City, Canada). Visualization was accomplished with UV light, exposure to *p*-anisaldehyde stain solution followed by heating, exposure to vanillin stain solution followed by heating, or exposure to KMnO₄ stain solution followed by heating. Flash chromatography was performed using SiliCycle silica gel (230-400 mesh). ¹H NMR spectra were acquired on a Varian Mercury Plus NMR (at 400 MHz) and are reported relative to SiMe₄ (δ 0.00). ¹³C NMR spectra were acquired on a Varian Mercury Plus NMR (at 100 MHz) and are reported relative to SiMe₄ (δ 0.0). All IR spectra were obtained on an ATR-ZnSe as thin films with a Nicolet iS-50 FT-IR or Shimadzu IRPrestige-21 FT-IR spectrometer and are reported in wavenumbers (ν). High resolution mass spectrometry (HRMS) data were acquired by the Proteomics and Mass Spectrometry Facility at the University of Georgia on a Thermo Orbitrap Elite. The ee of relevant compounds was determined by HPLC analysis (HPLC: Agilent Technologies 1260 Infinity II Series, Column: Chiral Technologies CHIRALPAK® IA, IB, or IC (250 mm x 4.6 mm i.d.)).

3.8.2 Synthesis of Decarboxylation Substrate 3-98

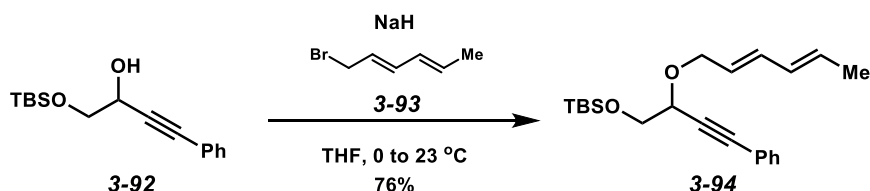


To a stirred solution of TBSCl (3.59 g, 23.8 mmol), imidazole (1.62 g, 23.8 mmol) and DMAP (69.6 mg, 0.570 mmol) in anhydrous CH₂Cl₂ (38.0 mL, 0.300 M) was added diol **3-89** (0.930 mL, 11.4 mmol) dropwise at ambient temperature. The resulting solution was allowed to stir for 15 h. The solvent was removed under reduced pressure, and the resulting crude oil was dissolved in Et₂O (40 mL) and H₂O (40 mL). The layers were separated and the aqueous layer was extracted with Et₂O (2 x 20 mL). The combined organic layers were sequentially washed with 1 M aq. HCl (40 mL) and brine (40 mL), dried over MgSO₄, and filtered. The solvent was removed under reduced pressure and the resulting clear oil was used without further purification (3.61 g, 99% yield, *R*_f: 0.68 in 9:1 hexanes/EtOAc). The spectroscopic data were identical to those previously reported.²⁰

Bis-protected diol **3-90** (1.58 g, 4.98 mmol) was dissolved in anhydrous CH₂Cl₂ (33.2 mL, 0.15 M) and cooled to -78 °C. Ozone was then bubbled through the solution until a pale blue color persisted. Ar gas was then bubbled through the solution until the reaction mixture turned colorless. The reaction mixture was quenched with PPh₃ (1.57 g, 5.98 mmol) at -78 °C and allowed to slowly warm to ambient temperature and stirred for 14 h. The reaction solution was concentrated and then triturated with pentane (3 x 50 mL) to remove triphenylphosphine oxide byproduct. After the removal of pentane under reduced pressure, the crude aldehyde (**3-91**) was taken on without further purification (1.72 g, 99% yield, *R*_f: 0.35 in 9:1 hexanes/EtOAc). The spectroscopic data were in agreement to those previously reported.²¹



To a solution of phenylacetylene (8.07 mL, 73.5 mmol) in anhydrous THF (100 mL) at -78 °C was added *n*-BuLi (30.0 mL, 2.5 M in hexanes, 70.3 mmol) dropwise. The resulting solution was allowed to stir for 15 min followed by the dropwise addition of a solution of aldehyde **3-91** (11.1 g, 63.9 mmol) in THF (100 mL) at -78 °C. The solution was stirred for 30 min before letting the temperature slowly warm to ambient temperature and continue to stir for an additional 14 h. The reaction mixture was quenched with H₂O (100 mL) and the THF was removed under reduced pressure. The resulting crude material was extracted with Et₂O (3 x 150 mL), and the combined organic layers were washed with brine (150 mL), dried over MgSO₄, and filtered. The solvent was removed under reduced pressure and the resulting residue was purified by silica gel chromatography (9:1 hexanes/EtOAc eluent) to afford alcohol **3-92** as a pale yellow oil. (9.45 g, 60% yield, *R*_f: 0.28 in 9:1 hexanes/EtOAc). The spectroscopic data were in agreement to those previously reported.²²



To a solution of alcohol **3-92** (2.19 g, 7.91 mmol) in anhydrous THF (27.0 mL, 0.29 M) at 0 °C was added NaH (348 mg, 60% dispersion in mineral oil, 8.70 mmol) in 2 portions. After the solution stopped bubbling, the reaction was warmed to ambient temperature for 30 min. Sorbyl bromide²³ (**3-93**, 1.40 g, 8.70 mmol) was added dropwise to the solution, and the resulting solution was allowed to stir for 14 h. H₂O (30 mL) was added to the reaction mixture, and the THF was

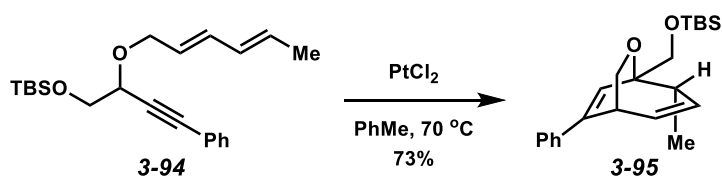
removed under reduced pressure. The resulting crude material was extracted with EtOAc (3 x 30 mL), and the combined organic layers were washed sequentially with H₂O (30 mL) and brine (30 mL), dried over MgSO₄, and filtered. The solvent was removed under reduced pressure and the resulting residue was purified by silica gel chromatography (19:1 hexanes/EtOAc eluent) to afford enyne **3-94** (2.13 g, 76% yield) as a yellow oil. *R*_f: 0.74 (9:1 hexanes/EtOAc).

IR (film): 3021, 2954, 2359, 1661, 1599, 1254 cm⁻¹.

¹H NMR (400 MHz, CDCl₃): δ 7.44 (dd, *J* = 6.5, 3.1 Hz, 2H), 7.31 (dd, *J* = 5.0, 1.7 Hz, 3H), 6.27 (dd, *J* = 15.1, 10.5 Hz, 1H), 6.05 (dd, *J* = 13.3, 2.8 Hz, 1H), 5.80-5.60 (m, 2H), 4.46-4.30 (m, 2H), 4.12 (dd, *J* = 12.4, 6.9 Hz, 1H), 3.86 (dd, *J* = 5.9, 4.7 Hz, 2H), 1.76 (d, *J* = 6.7 Hz, 3H), 0.91 (s, 9H), 0.10 (s, 6H).

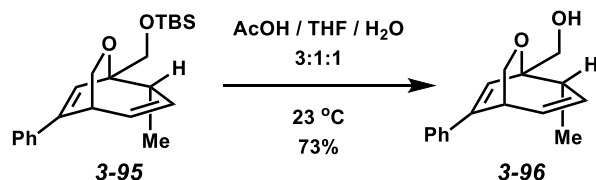
¹³C NMR (100 MHz, CDCl₃): δ 133.8, 131.9, 131.0, 130.3, 128.5, 128.4, 126.5, 122.9, 86.6, 86.4, 70.6, 69.8, 66.4, 26.0, 18.6, 18.3, -5.0, -5.1.

HRMS (ESI⁺): *m/z* calc. for (M + H)⁺ [C₂₂H₃₂O₂Si + H]⁺: 357.2172, found .



To a solution of enyne **3-94** (205 mg, 0.574 mmol) in toluene (8.20 mL, 0.07 M) was added PtCl₂ (10.6 mg, 0.0400 mmol). The reaction mixture was allowed to stir for 14 h. The solution was passed through a silica plug (4 x 0.5 cm, 4:1 hexanes/EtOAc eluent). The crude mixture was concentrated under reduced pressure and diluted with toluene (8.20 mL). The solution was heated

to 70 °C and allowed to stir for 24 h. The solution was cooled to ambient temperature and concentrated under reduced pressure. The resulting crude product was purified by silica gel chromatography (19:1 hexanes/EtOAc eluent) to afford bicycle **3-95** (150 mg, 73% yield, R_f : 0.72 in 9:1 hexanes/EtOAc) as a pale yellow oil.



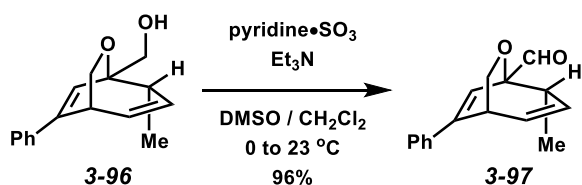
To a solution of bicycle **3-95** (632 mg, 1.77 mmol) in THF (3.54 mL) and H₂O (3.54 mL) was added AcOH (10.6 mL). The solution was allowed to stir for 20 h, and the solvents were then removed under reduced pressure. The crude product was extracted with EtOAc (3 x 20 mL). The combined organic layers were washed with brine (20 mL), dried over MgSO₄, filtered, and concentrated under reduced pressure. Residual AcOH was azeotropically removed prior to purification using heptane (3 x 5 mL). The residue was purified by silica gel chromatography (4:1 hexanes/EtOAc eluent) to afford alcohol **3-96** (313 mg, 73% yield, R_f : 0.05 in 9:1 hexanes/EtOAc) as a pale yellow oil.

IR (film): 3420 (br), 3017, 2960, 2870, 1644, 1074 cm⁻¹.

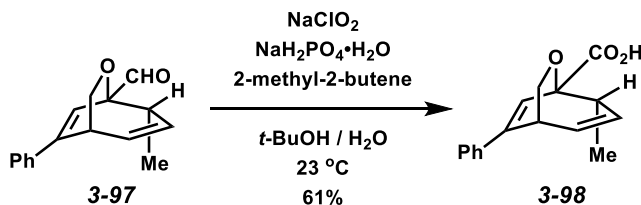
¹H NMR (400 MHz, CDCl₃): δ 7.50-7.27 (comp. m, 5H), 6.08 (dt, J = 11.1, 2.8 Hz, 2H), 5.36 (dd, J = 10.8, 3.7 Hz, 1H), 4.26 (dd, J = 8.3, 1.5 Hz, 1H), 3.80 (dd, J = 10.8, 8.3 Hz, 2H), 3.66 (dd, J = 11.1, 4.6 Hz, 1H), 3.24-3.13 (m, 1H), 2.66-2.55 (m, 1H), 2.33-2.22 (m, 1H), 0.90 (d, J = 7.3 Hz, 3H).

^{13}C NMR (100 MHz, CDCl_3): δ 149.6, 138.2, 135.7, 128.7, 128.0, 126.8, 125.3, 123.1, 79.8, 71.2, 68.6, 41.7, 36.9, 15.5.

HRMS (ESI⁺): m/z calc. for $(\text{M} + \text{H})^+$ [$\text{C}_{16}\text{H}_{18}\text{O}_2 + \text{H}$]⁺: 242.1307, found .



To a solution of alcohol **3-96** (25.0 mg, 0.103 mmol) in CH₂Cl₂ (0.255 mL) and DMSO (0.100 mL) was added Et₃N (43.0 μL , 0.309 mmol) at 0 °C. Pyridine sulfur trioxide complex solution (24.7 mg, 0.155 mmol) in DMSO (0.155 mL) was then added to the solution with the starting material. The resulting reaction mixture was allowed to stir at 0 °C for 10 min before warming to ambient temperature and stirring for an additional 2 h. The reaction mixture was quenched with H₂O (1 mL) and extracted into Et₂O (3 x 3 mL). The combined organic layers were washed with brine (3 mL), dried over MgSO₄, filtered and concentrated. The crude aldehyde was used in the next step without any further purification (23.7 mg, 96% yield, R_f : 0.30 in 9:1 hexanes/EtOAc).



To a solution of aldehyde **3-97** (19.6 mg, 0.0816 mmol) and 2-methyl-2-butene (86.4 μ L, 0.816 mmol) in *t*-BuOH (2.30 mL) at 23 °C was added a solution of NaClO₂ (33.2 mg, 0.367 mmol) and NaH₂PO₄•H₂O (50.6 mg, 0.367 mmol) in H₂O (0.420 mL). The reaction mixture was allowed to stir for 12 h. A 1:1 H₂O/EtOAc mixture (5 mL) was added to dilute the reaction, followed by the addition of 6 N aq. HCl (1 mL). The product was extracted with EtOAc (3 x 3 mL). The combined organic layers were washed with brine (3 mL), dried over MgSO₄, filtered and concentrated. The residue was purified by silica gel chromatography (2:1 hexanes/EtOAc eluent) to afford carboxylic acid **3-98** (13.8 mg, 61% yield, *R*_f: 0.17 (1:1 hexanes/EtOAc) as a white solid.

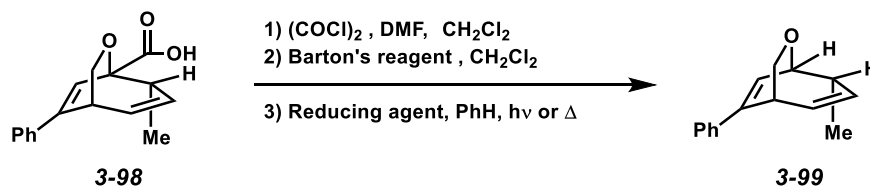
IR (film): 3202 (br), 2965, 2875, 1738, 1093 cm⁻¹.

¹H NMR (400 MHz, CDCl₃): δ 9.40 (bs, 1H), 7.46-7.30 (m, 5H), 6.42 (s, 1H), 6.09 (ddd, *J* = 10.9, 8.4, 1.9 Hz, 1H), 5.33 (dd, *J* = 10.9, 3.7 Hz, 1H), 4.35 (dd, *J* = 8.1, 1.9 Hz, 1H), 3.90 (dd, *J* = 8.1, 1.6 Hz, 1H), 3.20 (dd, *J* = 8.4, 1.6 Hz, 1H), 2.77-2.65 (m, 1H), 1.07 (d, *J* = 7.3 Hz, 3H).

¹³C NMR (100 MHz, CDCl₃): δ 173.3, 149.6, 137.4, 134.3, 128.8, 128.4, 126.1, 125.4, 119.9, 81.3, 70.7, 43.6, 36.2, 15.5.

HRMS (ESI⁺): *m/z* calc. for (M + H)⁺ [C₁₆H₁₆O₃ + H]⁺: 256.1099, found .

3.8.3 Decarboxylation of Substrate 3-98.



General Procedure for Reductive Radical Decarboxylation.

Notes: A 20:1 CH₂Cl₂:DMF solution was prepared prior to reaction setup in order to ensure a catalytic amount of DMF would be added for the generation of the acid chloride.

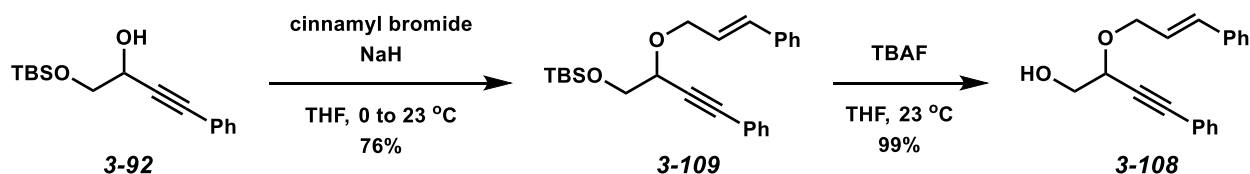
To a solution of carboxylic acid **3-98** (10.0 mg, 0.0400 mmol) in CH₂Cl₂ (0.40 mL, 0.1 M) was added DMF solution (approx. 5% v/v in CH₂Cl₂, 10 μ L), followed by dropwise addition of (COCl)₂ (7.2 μ L, 0.0800 mmol). The solution was allowed to stir for 30 min at 23 °C. The solvent was then removed under reduced pressure on a Schlenk line. The crude acid chloride was dissolved in CH₂Cl₂ (0.40 mL) and added to a flask containing Barton's reagent (5.8 mg, 0.0400 mmol) under Ar. The flask was covered in aluminum foil and allowed to stir for 2 h. (*Note: After addition of the acid chloride to the Barton reagent, care must be taken to avoid any unnecessary exposure to light until the reducing reagent has been added*). The solvent was then removed under reduced pressure by the use of the Schlenk line. Benzene (0.400 mL) was added to the crude Barton ester, followed by addition of the reducing reagent (5 equiv). (*Note: At this stage exposure to light is not detrimental to the reaction*). The solution was then irradiated by light from a 250 W halogen lamp for 1 h. The reaction mixture was concentrated and the residue was purified by silica gel chromatography (hexanes to 19:1 hexanes/EtOAc eluent) to afford bicycle **3-99** (3.9 mg, 46% yield over 3 steps, R_f: 0.35 in 10:1 hexanes/EtOAc). The spectroscopic data were in agreement to those previously reported.²⁴

Physical State: colorless oil

¹H NMR (400 MHz, CDCl₃): δ .

Synthesis of First Generation Chirality Transfer Substrate

Racemic



To a solution of alcohol **3-92** (440 mg, 1.60 mmol) in anhydrous THF (6.00 mL, 0.27 M) at 0 °C was added NaH (70.0 mg, 60% dispersion in mineral oil, 1.76 mmol) in 2 portions. After the solution stopped bubbling, the reaction was warmed to ambient temperature for 30 min. Cinnamyl bromide (260 μ L, 1.76 mmol) was added dropwise to the solution and the resulting solution was allowed to stir for 14 h. H₂O (10 mL) was added to the reaction mixture and the THF was removed under reduced pressure. The resulting material was extracted with EtOAc (3 x 10 mL), and the combined organic layers were washed sequentially with H₂O (10 mL) and brine (10 mL), dried over MgSO₄, and filtered. The solvent was removed under reduced pressure and the resulting residue was purified by silica gel chromatography (19:1 hexanes/EtOAc eluent) to afford enyne **3-109** (628 mg, 76% yield, *R_f*: 0.53 in 9:1 hexanes/EtOAc) as a yellow oil.

IR (film): 3026, 2927, 2210, 1490, 1135cm⁻¹.

¹H NMR (400 MHz, CDCl₃): δ 7.48-7.43 (m, 2H), 7.42-7.37 (m, 2H), 7.32 (td, *J* = 6.1, 5.5, 3.9 Hz, 6H), 6.68 (d, *J* = 15.9 Hz, 1H), 6.34 (ddd, *J* = 15.9, 6.5, 5.6 Hz, 1H), 4.56-4.40 (m, 2H), 4.30 (ddd, *J* = 12.6, 6.5, 1.4 Hz, 1H), 3.97-3.84 (m, 2H), 0.92 (s, 9H), 0.12 (s, 6H).

¹³C NMR (100 MHz, CDCl₃): δ 136.9, 132.9, 132.0, 128.7, 128.6, 128.4, 127.8, 126.7, 125.9, 122.8, 86.6, 86.4, 71.0, 70.0, 66.4, 26.0, 18.6, -5.0, -5.1.

HRMS (ESI⁺): *m/z* calc. for (M + H)⁺ [C₂₅H₃₂O₂Si + H]⁺: 392.2172, found .

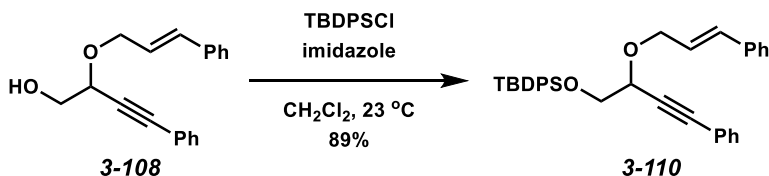
To a solution of enyne **3-109** (500 mg, 1.27 mmol) in THF (21.0 mL, 0.06 M) was added TBAF (1.91 mL, 1.0 M in THF, 1.91 mmol) dropwise at ambient temperature. The reaction mixture was allowed to stir for 2 h before saturated aq. NH₄Cl solution (20 mL) was added. The reaction mixture was extracted with EtOAc (3 x 20 mL). The combined organic layers were washed with brine (20 mL), dried over MgSO₄, and filtered. The solvent was removed under reduced pressure, and the resulting crude product was purified by silica gel chromatography (4:1 hexanes/EtOAc to 1:1 hexanes/EtOAc eluent) to afford alcohol **3-108** (352 mg, 99% yield, R_f: 0.16 in 4:1 hexanes/EtOAc) as a white solid.

IR (film): 3404 (br), 3027, 2927, 2220, 1490 cm⁻¹.

¹H NMR (400 MHz, CDCl₃): δ 7.46 (dd, *J* = 7.4, 2.2 Hz, 2H), 7.43-7.38 (m, 2H), 7.37-7.27 (m, 6H), 6.69 (d, *J* = 15.9 Hz, 1H), 6.35 (ddd, *J* = 15.9, 6.8, 5.7 Hz, 1H), 4.60-4.46 (m, 2H), 4.28 (ddd, *J* = 12.3, 6.8, 1.3 Hz, 1H), 3.89-3.82 (m, 2H).

¹³C NMR (100 MHz, CDCl₃): δ 136.6, 133.6, 132.0, 128.9, 128.7, 128.5, 128.0, 126.7, 125.3, 122.3, 87.5, 84.9, 70.4, 70.0, 65.5.

HRMS (ESI⁺): *m/z* calc. for (M + H)⁺ [C₁₉H₁₈O₂ + H]⁺: 278.1307, found .



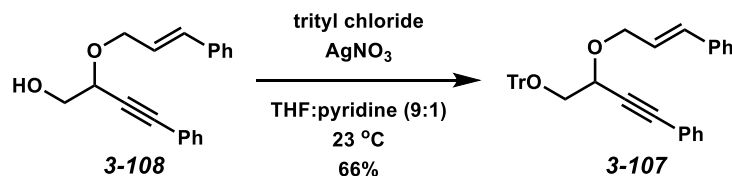
To a stirred solution of alcohol **3-108** (50.0 mg, 0.180 mmol) in anhydrous CH₂Cl₂ (1.80 mL, 0.1 M) were added imidazole (12.9 mg, 1.89 mmol) and TBDPSCl (49.1 μ L, 1.89 mmol) at ambient temperature. The resulting solution was allowed to stir for 15 h. The solvent was removed under reduced pressure, and the resulting crude oil was dissolved in Et₂O (5 mL) and H₂O (5 mL). The layers were separated, and the aqueous layer was extracted with Et₂O (2 x 5 mL). The combined organic layers were washed sequentially with 1 M aq. HCl (5 mL), water (5 mL), and brine (5 mL), dried over MgSO₄, and filtered. The solvent was removed under reduced pressure and the resulting oil was purified by silica gel chromatography (19:1 hexanes/EtOAc eluent) to afford silyl ether **3-110** as a pale yellow oil (82.4 mg, 89% yield, *R*_f: 0.66 in 9:1 hexanes/EtOAc).

IR (film): 3071, 2926, 2855, 2384, 1113 cm⁻¹.

¹H NMR (400 MHz, CDCl₃): δ 7.78-7.70 (m, 4H), 7.48-7.30 (m, 16H), 6.68 (dd, *J* = 16.0, 1.6 Hz, 1H), 6.32 (dt, *J* = 16.0, 6.0 Hz, 1H), 4.58-4.45 (m, 2H), 4.35-4.25 (m, 1H), 3.96 (qd, *J* = 10.4, 6.0 Hz, 2H), 1.10 (s, 9H).

¹³C NMR (100 MHz, CDCl₃): δ 136.9, 135.8, 133.6, 132.9, 131.9, 129.8, 128.7, 128.5, 128.4, 127.8, 126.7, 125.9, 122.8, 86.6, 86.5, 70.8, 69.9, 66.7, 26.9, 19.5.

HRMS (ESI⁺): *m/z* calc. for (M + H)⁺ [C₃₅H₃₆O₂Si + H]⁺: 516.2485, found .



To a solution of alcohol **3-108** (40.0 mg, 0.144 mmol) in THF:pyridine (9:1, 0.72 mL, 0.2 M) were added AgNO₃ (29.4 mg, 0.173 mmol) and trityl chloride (48.2 mg, 0.173 mmol) at 23 °C.

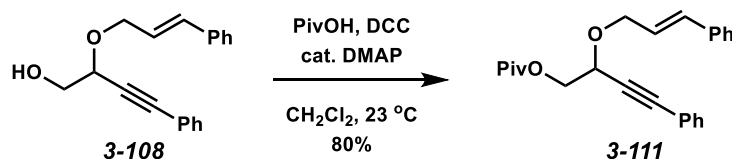
The reaction mixture was allowed to stir for 2 h. After the reaction was complete, CH₂Cl₂ (2 mL) and saturated aq. NaHCO₃ (2 mL) were added. The layers were separated and the aqueous layer was extracted by CH₂Cl₂ (3 x 2 mL). The combined organic layers were washed sequentially with saturated aq. NaHCO₃ (2 mL) and brine (2 mL), dried over MgSO₄, and filtered. After removal of the solvent under reduced pressure, the crude product was purified by silica gel chromatography (19:1 hexanes/EtOAc eluent) to afford trityl ether **3-107** (49.5 mg, 66% yield, R_f: 0.62 in 9:1 hexanes/EtOAc) as a colorless oil.

IR (film): 3058, 2927, 1954, 1881, 1597, 1490, 1448 cm⁻¹.

¹H NMR (400 MHz, CDCl₃): δ 7.57-7.51 (m, 6H), 7.48-7.44 (m, 2H), 7.43-7.38 (m, 2H), 7.35-7.21 (m, 15H), 6.72 (d, *J* = 15.9 Hz, 1H), 6.36 (dt, *J* = 15.9, 5.9 Hz, 1H), 4.62 – 4.45 (m, 2H), 4.33 (ddd, *J* = 12.8, 6.5, 1.4 Hz, 1H), 3.49 (dd, *J* = 9.4, 6.9 Hz, 1H), 3.38 (dd, *J* = 9.4, 5.0 Hz, 1H).

¹³C NMR (100 MHz, CDCl₃): δ 144.0, 136.9, 132.9, 131.9, 128.9, 128.8, 128.7, 128.6, 128.4, 128.0, 127.8, 127.2, 126.7, 125.9, 122.7, 86.9, 86.6, 86.5, 77.4, 69.8, 69.2, 66.5.

HRMS (ESI⁺): *m/z* calc. for (M + H)⁺ [C₃₈H₃₂O₂ + H]⁺: 520.2402, found .



To a solution of alcohol **3-108** (50.0 mg, 0.180 mmol) in CH₂Cl₂ (1.00 mL, 0.18 M) were added DCC (40.8 mg, 0.198 mmol), DMAP (0.2 mg, 0.00180 mmol), and PivOH (22.0 μL, 0.189 mmol) at ambient temperature. The reaction mixture was heated to 50 °C and allowed to stir for 24 h. H₂O (2 mL) was added to the reaction mixture and extracted into CH₂Cl₂ (3 x 3 mL). The combined organic layers were washed with brine (3 mL), dried over MgSO₄, and filtered. After

removal of the solvent under reduced pressure, the crude product was purified by silica gel chromatography (19:1 hexanes:EtOAc eluent) to afford pivaloyl ester **3-111** (52.2 mg, 80% yield, R_f : 0.48 in 9:1 hexanes/EtOAc) as a colorless oil.

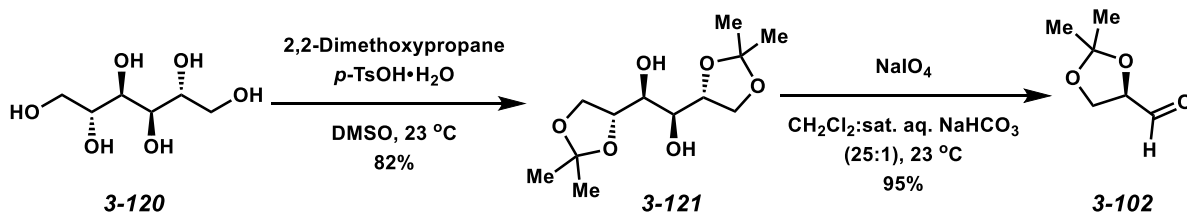
IR (film): 3027, 2971, 1731, 1280, 1153 cm^{-1} .

^1H NMR (400 MHz, CDCl_3): δ 7.45 (dd, $J = 7.2, 2.5$ Hz, 2H), 7.42-7.37 (m, 2H), 7.37-7.29 (m, 5H), 6.68 (d, $J = 15.9$ Hz, 1H), 6.31 (ddd, $J = 15.9, 6.7, 5.6$ Hz, 1H), 4.64 (dd, $J = 6.7, 4.9$ Hz, 1H), 4.49 (ddd, $J = 12.6, 5.6, 1.5$ Hz, 1H), 4.44-4.22 (m, 3H), 1.24 (s, 9H).

^{13}C NMR (100 MHz, CDCl_3): δ 178.3, 136.7, 133.3, 132.0, 128.8, 128.7, 128.5, 127.9, 126.7, 125.4, 122.4, 87.2, 84.8, 77.4, 69.7, 67.6, 65.6, 39.0, 27.3, 26.7.

HRMS (ESI $^{+}$): m/z calc. for $(\text{M} + \text{H})^{+}$ [$\text{C}_{24}\text{H}_{26}\text{O}_3 + \text{H}$] $^{+}$: 362.1882, found .

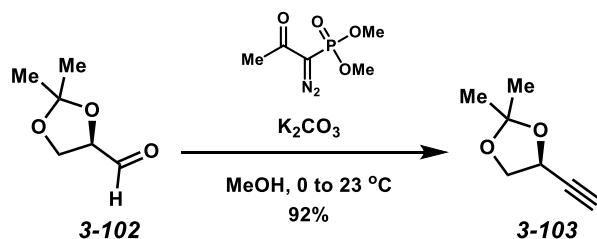
First Generation Chirality Transfer Substrates – Chiral



To a solution of d-mannitol **3-120** (1.04 g, 5.73 mmol) in DMSO (2.10 mL, 2.75 M) were added 2,2-dimethoxypropane (1.55 mL, 12.6 mmol) and $p\text{-TsOH}\cdot\text{H}_2\text{O}$ (10.3 mg, 0.0600 mmol) at 23 °C. The reaction mixture was allowed to stir for 20 h. After the reaction was complete, EtOAc (10 mL) and H_2O (10 mL) was added. The layers were separated and the aqueous layer was extracted by EtOAc (3 x 5 mL). The combined organic layers were washed sequentially with 5%

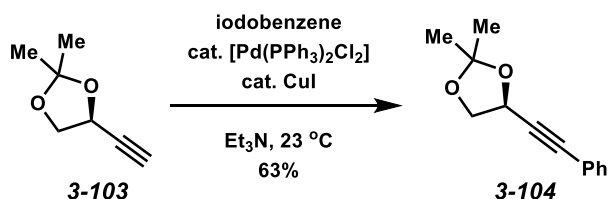
aq. NaHCO_3 (10 mL) and brine (10 mL), dried over MgSO_4 , and filtered. After removal of the solvent under reduced pressure, the crude product was purified by silica gel chromatography (1:1 hexanes/EtOAc eluent) to afford diol **3-121** (1.23 g, 82% yield) as a white solid. R_f : 0.18 (1:1 hexanes/EtOAc), The spectroscopic data were in agreement to those previously reported.²⁵

To a solution of diol **3-121** (200 mg, 0.762 mmol) in CH_2Cl_2 (2.5 mL, 0.3 M) and saturated NaHCO_3 (aq) solution (0.1 mL) was added NaIO_4 (326 mg, 1.53 mmol) at ambient temperature. The reaction mixture was allowed to stir for 4 h. The reaction mixture was filtered through a plug of silica (4 x 2 cm, CH_2Cl_2 eluent). The filtrate was carefully concentrated under reduced pressure in a 0 °C bath to afford pure aldehyde **3-102** (188 mg, 95% yield, R_f : 0.12 in 4:1 hexanes/EtOAc) as a clear oil that did not need further purification. The spectroscopic data were in agreement to those previously reported.²⁶

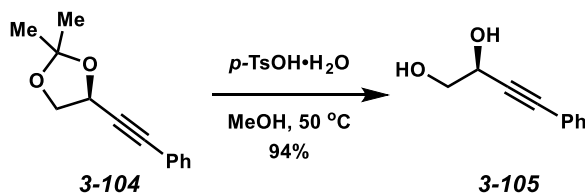


To a solution of aldehyde **3-102** (100 mg, 0.790 mmol) in MeOH (5.00 mL, 0.16 M) was added Ohira-Bestmann reagent²⁷ (242 mg, 1.26 mmol) at 0 °C. K_2CO_3 (233 mg, 1.68 mmol) was added in 3 portions over 30 min. The cooling bath was removed and the solution was allowed to warm to ambient temperature and stir for 16 h. Saturated aq. NH_4Cl (5 mL) was added to the reaction mixture and the reaction mixture was extracted into pentane (3 x 5 mL). The combined organic layers were washed with brine (3 mL), dried over Na_2SO_4 , filtered and concentrated with

a 0 °C cooling bath. The residue was purified by silica gel chromatography (10:1 hexanes/Et₂O eluent) to afford alkyne **3-103** (91.7 mg, 92% yield, *R*_f: 0.61 in 4:1 hexanes/EtOAc)) as a colorless oil. The spectroscopic data were in agreement to those previously reported.²⁸

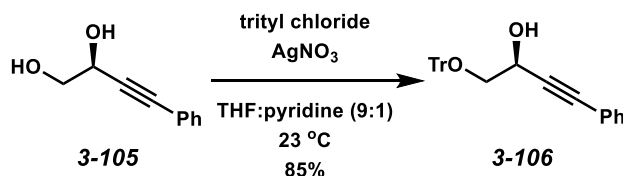


To a solution of alkyne **3-103** (50.0 mg, 0.400 mmol) in Et₃N (1.20 mL, 0.33 M) was added iodobenzene (67.0 μ L, 0.600 mmol) at 23 °C. Argon was bubbled through the solution for 30 min. [Pd(PPh₃)₂Cl₂] (14.0 mg, 0.0200 mmol) and CuI (7.6 mg, 0.0400 mmol) were then added, and the resulting solution was allowed to stir for 14 h. The reaction was passed through a plug of silica (2 cm x 1 cm, 1:1 hexanes/EtOAc eluent). The solvent was removed under reduced pressure and the resulting residue was purified by silica gel chromatography (19:1 hexanes/EtOAc eluent) to afford product **3-104** (50.7 mg, 63% yield, *R*_f: 0.68 in 4:1 hexanes/EtOAc) as a yellow oil. The spectroscopic data were in agreement to those previously reported.²⁹

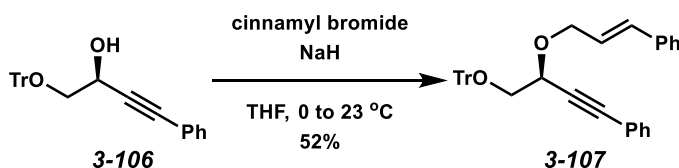


To a solution of alkyne **3-104** (46.1 mg, 0.230 mmol) in MeOH (2.3 mL, 0.1 M) was added *p*-TsOH·H₂O (4.0 mg, 0.0230 mmol) at 23 °C. The reaction was heated to 50 °C and was allowed

to stir for 24 h. After the reaction was complete, the solvent was removed under reduced pressure and the crude product was purified by silica gel chromatography (2:1 hexanes/EtOAc eluent) to afford diol **3-105** (35.0 mg, 94% yield, R_f : 0.21 in 2:1 hexanes/EtOAc) as a white solid. The spectroscopic data were in agreement to those previously reported.³⁰

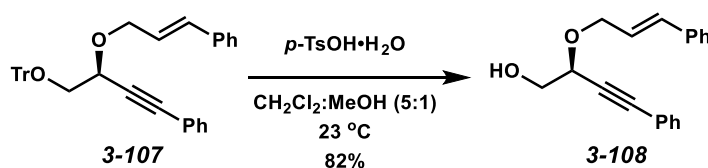


To a solution of diol **3-105** (25.0 mg, 0.150 mmol) in THF:pyridine (9:1, 0.75 mL, 0.2 M) were added AgNO_3 (30.6 mg, 0.180 mmol) and trityl chloride (51.6 mg, 0.180 mmol) at 23 °C. The reaction was allowed to stir for 2 h. After the reaction was complete, CH_2Cl_2 (2.0 mL) and saturated aq. NaHCO_3 (2 mL) were added. The layers were separated and the aqueous layer was extracted by CH_2Cl_2 (3 x 2 mL). The combined organic layers were washed sequentially with saturated aq. NaHCO_3 (2 mL) and brine (2 mL), dried over MgSO_4 , and filtered. After removal of the solvent under reduced pressure, the crude product was purified by silica gel chromatography (19:1 hexanes/EtOAc eluent) to afford secondary alcohol **3-106** (51.6 mg, 85% yield, R_f : 0.48 in 4:1 hexanes/EtOAc) as a colorless oil. The spectroscopic data were in agreement to those previously reported.³¹



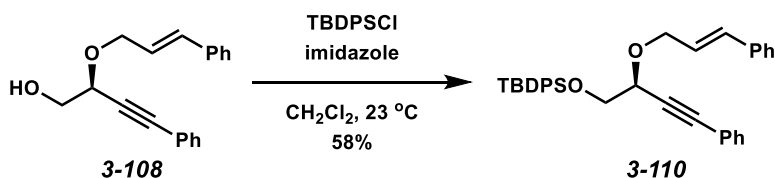
To a solution of alcohol **3-106** (319 mg, 0.789 mmol) in anhydrous THF (5.00 mL, 0.16 M) at 0 °C was added NaH (21.0 mg, 60% dispersion in mineral oil, 0.867 mmol) in 2 portions. After the solution stopped bubbling, the reaction was warmed to ambient temperature over 30 min. Cinnamyl bromide (260 μ L, 1.76 mmol) was added dropwise to the solution and the solution was allowed to stir for 14 h. H₂O (10 mL) was added to the reaction mixture and the THF was removed under reduced pressure. The resulting material was extracted with EtOAc (3 x 10 mL), and the combined organic layers were washed sequentially with H₂O (10 mL) and brine (10 mL), dried over MgSO₄, and filtered. The solvent was removed under reduced pressure and the resulting residue was purified by silica gel chromatography (19:1 hexanes/EtOAc eluent) to afford enyne **3-107** (213 mg, 52% yield, *R*_f: 0.18 in 1:1 hexanes/EtOAc).

¹H NMR (400 MHz, CDCl₃): δ 7.57-7.51 (m, 6H), 7.48-7.44 (m, 2H), 7.43-7.38 (m, 2H), 7.35-7.21 (m, 15H), 6.72 (d, *J* = 15.9 Hz, 1H), 6.36 (dt, *J* = 15.9, 5.9 Hz, 1H), 4.62 – 4.45 (m, 2H), 4.33 (ddd, *J* = 12.8, 6.5, 1.4 Hz, 1H), 3.49 (dd, *J* = 9.4, 6.9 Hz, 1H), 3.38 (dd, *J* = 9.4, 5.0 Hz, 1H).



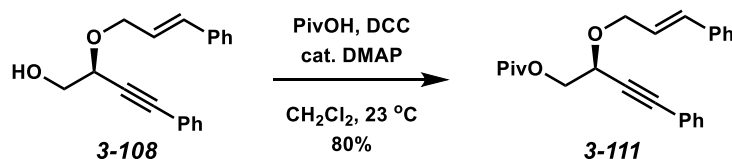
To a solution of enyne **3-107** (121 mg, 0.230 mmol) in CH₂Cl₂:MeOH (5:1, 2.4 mL, 0.1 M) was added *p*-TsOH·H₂O (22.0 mg, 0.115 mmol) at 23 °C. The reaction was allowed to stir for 14 h. After the reaction was complete, the solvent was removed under reduced pressure and the crude product was purified by silica gel chromatography (2:1 hexanes/EtOAc eluent) to afford primary alcohol **3-108** (52.5 mg, 82% yield, *R*_f: 0.08 in 9:1 hexanes/EtOAc) as a white solid.

¹H NMR (400 MHz, CDCl₃): δ 7.46 (dd, *J* = 7.4, 2.2 Hz, 2H), 7.43-7.38 (m, 2H), 7.37-7.27 (m, 6H), 6.69 (d, *J* = 15.9 Hz, 1H), 6.35 (ddd, *J* = 15.9, 6.8, 5.7 Hz, 1H), 4.60-4.46 (m, 2H), 4.28 (ddd, *J* = 12.3, 6.8, 1.3 Hz, 1H), 3.89-3.82 (m, 2H).



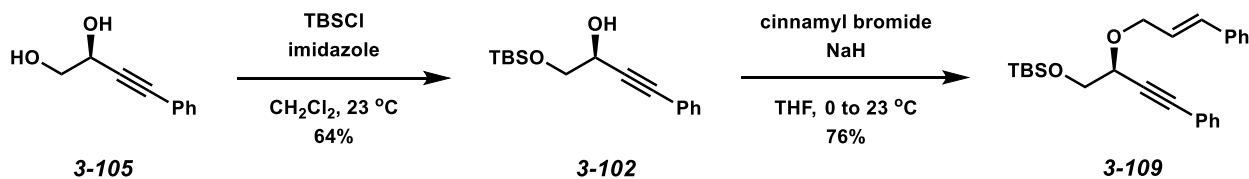
To a stirred solution of alcohol **3-108** (33.2 mg, 0.120 mmol) in anhydrous CH₂Cl₂ (1.20 mL, 0.100 M) were added imidazole (8.2 mg, 1.20 mmol) and TBDPSCl (31.2 μL, 1.20 mmol) at ambient temperature. The resulting solution was allowed to stir for 15 h. The solvent was removed under reduced pressure, and the resulting crude oil was dissolved in Et₂O (5 mL) and H₂O (5 mL). The layers were separated and the aqueous layer was extracted with Et₂O (2 x 5 mL). The combined organic layers were washed sequentially with 1 M aq. HCl (5 mL), water (5 mL), and brine (5 mL), dried over MgSO₄, and filtered. The solvent was removed under reduced pressure and the resulting oil was purified by silica gel chromatography (19:1 hexanes/EtOAc eluent) to afford silyl ether **3-110** (36.0 mg, 58% yield, *R*_f: 0.60 in 9:1 hexanes/EtOAc) as a pale yellow oil.

¹H NMR (400 MHz, CDCl₃): δ 7.78-7.70 (m, 4H), 7.48-7.30 (m, 16H), 6.68 (dd, *J* = 16.0, 1.6 Hz, 1H), 6.32 (dt, *J* = 16.0, 6.0 Hz, 1H), 4.58-4.45 (m, 2H), 4.35-4.25 (m, 1H), 3.96 (qd, *J* = 10.4, 6.0 Hz, 2H), 1.10 (s, 9H).



To a solution of alcohol **3-108** (35.5 mg, 0.130 mmol) in CH_2Cl_2 (1.00 mL, 0.15 M) was added DCC (29.5 mg, 0.143 mmol), DMAP (0.1 mg, 0.00130 mmol), and PivOH (16.0 μL , 0.137 mmol) at ambient temperature. The reaction was heated to 50 $^\circ\text{C}$ and allowed to stir for 24 h. H_2O (2 mL) was added to the reaction mixture and extracted into CH_2Cl_2 (3 x 3 mL). The combined organic layers were washed with brine (3 mL), dried over MgSO_4 , and filtered. After removal of the solvent under reduced pressure, the crude product was purified by silica gel chromatography (19:1 hexanes/EtOAc eluent) to afford pivaloyl ester **3-111** (37.7 mg, 80% yield, R_f : 0.46 in 9:1 hexanes/EtOAc) as a colorless oil.

^1H NMR (400 MHz, CDCl_3): δ 7.45 (dd, $J = 7.2, 2.5$ Hz, 2H), 7.42-7.37 (m, 2H), 7.37-7.29 (m, 5H), 6.68 (d, $J = 15.9$ Hz, 1H), 6.31 (ddd, $J = 15.9, 6.7, 5.6$ Hz, 1H), 4.64 (dd, $J = 6.7, 4.9$ Hz, 1H), 4.49 (ddd, $J = 12.6, 5.6, 1.5$ Hz, 1H), 4.44-4.22 (m, 3H), 1.24 (s, 9H).



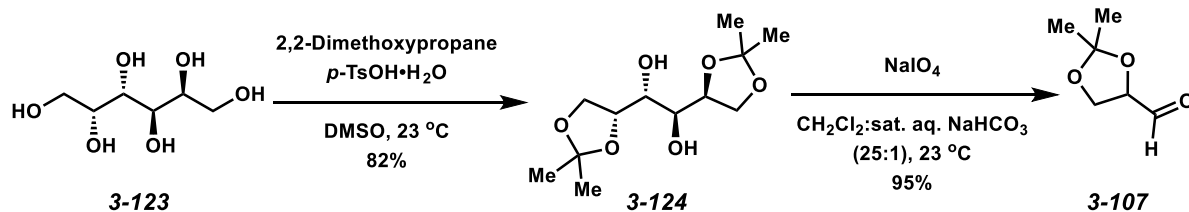
To a stirred solution of diol **3-105** (860 mg, 5.30 mmol) in anhydrous CH_2Cl_2 (18.0 mL, 0.3 M) were added imidazole (379 mg, 5.57 mmol) and TBSCl (839 mg, 5.57 mmol) at ambient temperature. The resulting solution was allowed to stir for 15 h. The solvent was removed under

reduced pressure, and the resulting crude oil was dissolved in Et₂O (20 mL) and H₂O (20 mL). The layers were separated and the aqueous layer was extracted with Et₂O (2 x 20 mL). The combined organic layers were washed sequentially with 1 M aq. HCl (20 mL), water (20 mL), and brine (20 mL), dried over MgSO₄, and filtered. The solvent was removed under reduced pressure and the resulting oil was purified by silica gel chromatography (19:1 hexanes/EtOAc eluent) to afford secondary alcohol **3-102** (938 mg, 64% yield, R_f: 0.55 (9:1 hexanes/EtOAc) as a pale yellow oil.

To a solution of alcohol **3-102** (500 mg, 1.81 mmol) in anhydrous THF (6.00 mL, 0.3 M) at 0 °C was added NaH (80.0 mg, 60% dispersion in mineral oil, 1.99 mmol) in 2 portions. After the solution stopped bubbling, the reaction mixture was warmed to ambient temperature over 30 min. Cinnamyl bromide (268 µL, 1.81 mmol) was added dropwise to the solution and the resulting solution was allowed to stir for 14 h. H₂O (10 mL) was added to the reaction mixture, and the THF was removed under reduced pressure. The resulting crude material was extracted with EtOAc (3 x 10 mL), and the combined organic layers were washed sequentially with H₂O (10 mL) and brine (10 mL), dried over MgSO₄, and filtered. The solvent was removed under reduced pressure and the resulting residue was purified by silica gel chromatography (19:1 hexanes/EtOAc eluent) to afford enyne **3-109** (540 mg, 76% yield, R_f: 0.64 (9:1 hexanes/EtOAc) as a pale yellow oil.

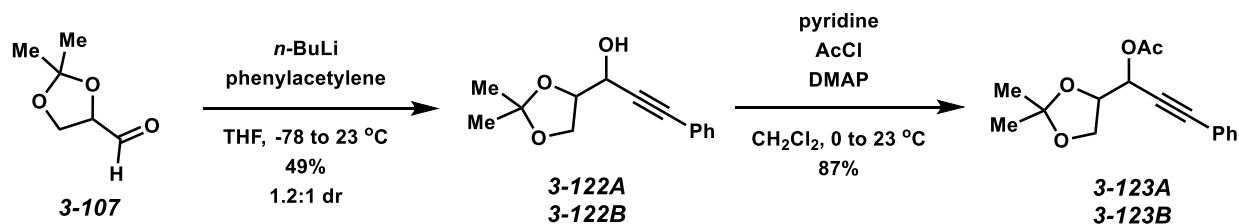
¹H NMR (400 MHz, CDCl₃): δ 7.48-7.43 (m, 2H), 7.42-7.37 (m, 2H), 7.32 (td, *J* = 6.1, 5.5, 3.9 Hz, 6H), 6.68 (d, *J* = 15.9 Hz, 1H), 6.34 (ddd, *J* = 15.9, 6.5, 5.6 Hz, 1H), 4.56-4.40 (m, 2H), 4.30 (ddd, *J* = 12.6, 6.5, 1.4 Hz, 1H), 3.97-3.84 (m, 2H), 0.92 (s, 9H), 0.12 (s, 6H).

Synthesis of Second Generation Chiral Auxiliars – Racemic Acetonides



To a solution of D-dulcitol **3-123** (10.0 g, 54.8 mmol) in DMSO (20.0 mL, 2.75 M) was added 2,2-dimethoxypropane (14.9 mL, 121 mmol) and *p*-TsOH·H₂O (94.0 mg, 0.549 mmol) at 23 °C. The reaction was allowed to stir for 20 h. After the reaction was complete, EtOAc (50 mL) and H₂O (50 mL) were added. The layers were separated, and the aqueous layer was extracted by EtOAc (3 x 50 mL). The combined organic layers were washed sequentially with 5% aq. NaHCO₃ (50 mL) and brine (50 mL), dried over MgSO₄, and filtered. After removal of the solvent under reduced pressure, the crude product was purified by silica gel chromatography (1:1 hexanes/EtOAc eluent) to afford diol **3-124** (11.8 g, 82% yield, *R*_f: 0.08 in 4:1 hexanes/EtOAc) as a white solid. The spectroscopic data were in agreement to those previously reported.³²

To a solution of diol **3-124** (374 mg, 1.42 mmol) in CH₂Cl₂ (5.0 mL, 0.3 M) and saturated aq. NaHCO₃ (0.2 mL) was added NaIO₄ (530 mg, 2.84 mmol) at ambient temperature. The reaction mixture was allowed to stir for 4 h. The reaction mixture was then filtered through a plug of silica (4 x 2 cm, CH₂Cl₂ eluent). The filtrate was carefully concentrated under reduced pressure in a 0 °C bath to afford pure aldehyde **3-107** (188 mg, 95% yield, *R*_f: 0.12 in 4:1 hexanes/EtOAc) as a clear oil that did not need further purification. The spectroscopic data were in agreement to those previously reported.²⁰



To a solution of phenylacetylene (0.928 mL, 8.45 mmol) in anhydrous THF (15.6 mL, 0.3 M) was added *n*-BuLi (3.68 mL, 2.5 M in hexanes, 9.22 mmol) dropwise at -78 °C. After stirring for 10 min, a solution of aldehyde **3-107** (1.00 g, 7.68 mmol) in THF (10.0 mL) was added dropwise. The cooling bath was removed and the reaction was allowed to stir for 14 h and slowly warm to ambient temperature. The reaction was then quenched with saturated aq. NH₄Cl (15 mL) and extracted with Et₂O (3 x 25 mL). The combined organic layers were washed with brine (35 mL), dried over MgSO₄, filtered and concentrated. The residue was purified by silica gel chromatography (4:1 hexanes/EtOAc eluent) to afford inseparable diastereomeric alcohols **3-122A** and **3-122B** (962 mg, 1.2:1 dr, 49% yield, R_f: 0.16 in 4:1 hexanes/EtOAc) as a colorless oil. The spectroscopic data were in agreement to those previously reported.³³

To a stirred solution of alcohol **3-122** (71.6 mg, 0.31 mmol) in anhydrous CH₂Cl₂ (1.24 mL, 0.25 M) were added DMAP (3.8 mg, 0.031 mmol) and pyridine (50.0 μL, 0.62 mmol) at 0 °C. Acetyl chloride (33.0 μL, 0.46 mmol) was then added dropwise to the reaction mixture. The solution was allowed to warm to ambient temperature and stir for 1 h. The reaction was quenched with H₂O (3 mL) and extracted with EtOAc (5 x 5 mL). The combined organic layers were washed with brine (5 mL), dried over Na₂SO₄, and filtered. The solvent was removed under reduced pressure and the resulting oil was purified by silica gel chromatography (8:1:1 hexanes/EtOAc:MTBE eluent) to afford acetates **3-123A** (36.3 mg, 43% yield, R_f: 0.28 in 8:1:1

hexanes/EtOAc/MTBE) and **3-123B** (33.0 mg, 39% yield, R_f : 0.24 in 8:1:1 hexanes/EtOAc/MTBE)) as pale yellow oils.

3-123A

IR (film): 2987, 2937, 2229, 1748, 1372, 1226 cm^{-1} .

^1H NMR (400 MHz, CDCl_3): δ 7.48-7.41 (m, 2H), 7.41-7.28 (m, 3H), 5.65 (d, $J = 7.6$ Hz, 1H), 4.37 (ddd, $J = 7.6, 6.5, 5.3$ Hz, 1H), 4.19 (dd, $J = 9.0, 6.5$ Hz, 1H), 4.09 (dd, $J = 9.0, 5.3$ Hz, 1H), 2.16 (s, 3H), 1.46 (s, 3H), 1.39 (s, 3H).

^{13}C NMR (100 MHz, CDCl_3): δ 169.9, 132.1, 129.1, 128.5, 121.8, 111.0, 86.7, 83.3, 76.6, 66.5, 66.0, 26.7, 25.6, 21.1.

HRMS (ESI⁺): m/z calc. for $(\text{M} + \text{H})^+ [\text{C}_{16}\text{H}_{18}\text{O}_4 + \text{H}]^+$: 274.1205, found .

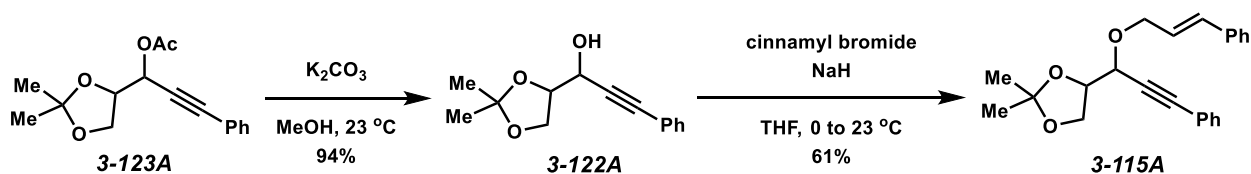
3-123B

IR (film): 2988, 2936, 2231, 1748, 1372, 1227 cm^{-1} .

^1H NMR (400 MHz, CDCl_3): δ 7.48-7.39 (m, 2H), 7.35-7.28 (m, 3H), 5.75 (d, $J = 3.7$ Hz, 1H), 4.41 (td, $J = 6.5, 3.7$ Hz, 1H), 4.18 (dd, $J = 8.6, 6.5$ Hz, 1H), 4.06 (dd, $J = 8.6, 6.5$ Hz, 1H), 2.16 (s, 3H), 1.48 (s, 3H), 1.40 (s, 3H).

^{13}C NMR (100 MHz, CDCl_3): δ 169.9, 132.1, 129.1, 128.4, 121.9, 110.8, 86.7, 83.1, 76.7, 65.8, 64.3, 26.4, 25.6, 21.1.

HRMS (ESI⁺): m/z calc. for $(\text{M} + \text{H})^+ [\text{C}_{16}\text{H}_{18}\text{O}_4 + \text{H}]^+$: 274.1205, found.



To a solution of acetate **3-123A** (306 mg, 1.12 mmol) in MeOH (5.6 mL, 0.2 M) was added K_2CO_3 (185 mg, 1.34 mmol) at ambient temperature. The reaction mixture was allowed to stir for 2 h. After consumption of the starting material was observed, the solution was diluted with Et_2O (15 mL) and H_2O (15 mL). After the layers were separated, the aqueous layer was extracted with Et_2O (2 x 10 mL). The combined organic layers were washed with brine (20 mL), dried over MgSO_4 , and filtered. The solvent was removed under reduced pressure yielding alcohol **3-122A** (278 mg, 94% yield, R_f : 0.16 in 4:1 hexanes/ EtOAc) as a colorless oil. Alcohol **3-122A** was sufficiently pure to be carried on to the next reaction.

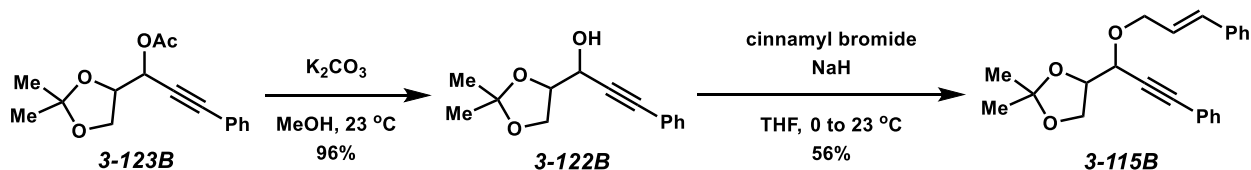
To a solution of alcohol **3-122A** (278 mg, 1.20 mmol) in anhydrous THF (4.00 mL, 0.3 M) at 0 $^\circ\text{C}$ was added NaH (50.2 mg, 60% dispersion in mineral oil, 1.26 mmol) in 2 portions. After the solution stopped bubbling, the reaction was warmed to ambient temperature over 30 min. Cinnamyl bromide (177 μL , 1.20 mmol) was added dropwise to the solution, and the resulting solution was allowed to stir for 14 h. H_2O (10 mL) was added to the reaction mixture and the THF was removed under reduced pressure. The resulting crude material was extracted with EtOAc (3 x 10 mL), and the combined organic layers were washed sequentially with H_2O (10 mL) washed with brine (10 mL), dried over MgSO_4 , and filtered. The solvent was removed under reduced pressure, and the resulting residue was purified by silica gel chromatography (19:1 hexanes/ EtOAc eluent) to afford enyne **3-115A** (255 mg, 61% yield, R_f : 0.49 in 9:1 hexanes/ EtOAc) as a pale yellow oil.

IR (film): 3058, 2985, 2231, 1598, 1489 cm^{-1} .

^1H NMR (400 MHz, CDCl_3): δ 7.39-7.10 (m, 10H), 6.58 (d, $J = 15.9$ Hz, 1H), 6.24 (ddd, $J = 15.9$, 7.0, 5.6 Hz, 1H), 4.47-4.33 (m, 2H), 4.33-4.15 (m, 2H), 4.09 (dd, $J = 8.7$, 6.5 Hz, 1H), 3.95 (dd, $J = 8.7$, 6.1 Hz, 1H), 1.38 (s, 3H), 1.30 (s, 3H).

^{13}C NMR (100 MHz, CDCl_3): δ 136.7, 133.6, 132.0, 128.9, 128.7, 128.5, 127.9, 126.7, 125.4, 122.3, 110.6, 87.6, 84.8, 77.4, 71.3, 70.0, 66.8, 26.9, 25.6.

HRMS (ESI $^+$): m/z calc. for $(\text{M} + \text{H})^+$ [$\text{C}_{23}\text{H}_{24}\text{O}_3 + \text{H}$] $^+$: 348.1725, found .



To a solution of acetate **3-123B** (245 mg, 0.894 mmol) in MeOH (4.5 mL, 0.2 M) was added K_2CO_3 (148 mg, 1.07 mmol) at ambient temperature. The reaction was allowed to stir for 2 h. After consumption of the starting material was observed, the solution was diluted with Et_2O (15 mL) and H_2O (15 mL). After the layers were separated, the aqueous layer was extracted with Et_2O (2 x 10 mL). The combined organic layers were washed with brine (20 mL), dried over MgSO_4 , and filtered. The solvent was removed under reduced pressure yielding alcohol **3-122B** (221 mg, 96% yield, R_f : 0.16 in 4:1 hexanes/ EtOAc) as a colorless oil. Alcohol **3-122B** was sufficiently pure to be carried on to the next reaction.

To a solution of alcohol **3-122B** (221 mg, 0.952 mmol) in anhydrous THF (3.20 mL, 0.3 M) at 0 °C was added NaH (40.0 mg, 60% dispersion in mineral oil, 1.00 mmol) in 2 portions. After the solution stopped bubbling, the reaction mixture was warmed to ambient temperature over 30 min. Cinnamyl bromide (141 μ L, 0.952 mmol) was added dropwise to the solution, and the resulting solution was allowed to stir for 14 h. H₂O (10 mL) was added to the reaction mixture, and the THF was removed under reduced pressure. The resulting crude material was extracted with EtOAc (3 x 10 mL), and the combined organic layers were sequentially washed with H₂O (10 mL) and brine (10 mL), dried over MgSO₄, and filtered. The solvent was removed under reduced pressure, and the resulting residue was purified by silica gel chromatography (19:1 hexanes/EtOAc eluent) to afford enyne **3-115B** (186 mg, 56% yield, *R_f*: 0.46 in 9:1 hexanes/EtOAc) as a pale yellow oil.

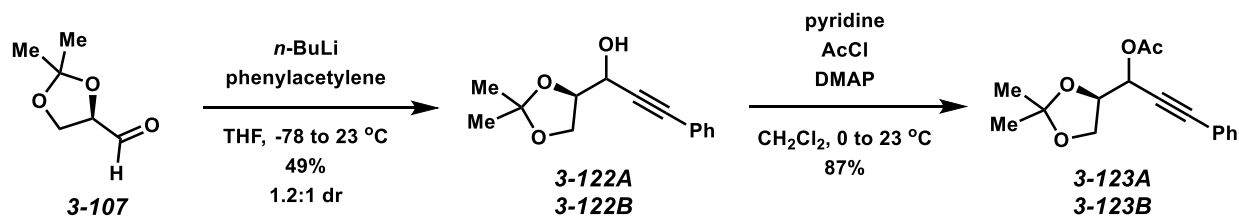
IR (film): 3027, 2987, 2226, 1490, 1073 cm⁻¹.

¹H NMR (400 MHz, CDCl₃): δ 7.40-7.34 (m, 2H), 7.33-7.10 (m, 8H), 6.57 (d, *J* = 15.9 Hz, 1H), 6.22 (ddd, *J* = 15.9, 6.8, 5.6 Hz, 1H), 4.43 (ddd, *J* = 12.5, 5.6, 1.4 Hz, 1H), 4.33-4.22 (m, 2H), 4.18 (ddd, *J* = 12.5, 6.8, 1.4 Hz, 1H), 4.05 (dd, *J* = 8.5, 6.2 Hz, 1H), 3.97 (dd, *J* = 8.5, 5.8 Hz, 1H), 1.40 (s, 3H), 1.30 (s, 3H).

¹³C NMR (100 MHz, CDCl₃): δ 136.7, 133.4, 132.1, 128.7, 128.5, 128.4, 127.9, 126.7, 125.4, 122.5, 110.3, 87.3, 85.3, 77.7, 70.3, 70.1, 65.5, 26.7, 25.7.

HRMS (ESI⁺): *m/z* calc. for (M + H)⁺ [C₂₃H₂₄O₃ + H]⁺: 348.1725, found.

Synthesis of Second Generation Chiral Auxiliarys – Chiral Acetonides



To a solution of phenylacetylene (0.928 mL, 8.45 mmol) in anhydrous THF (15.6 mL, 0.3 M) was added *n*-BuLi (3.68 mL, 2.5 M in hexanes, 9.22 mmol) dropwise at -78 °C. After stirring for 10 min, a solution of aldehyde **3-107** (1.00 g, 7.68 mmol) in THF (10 mL) was added dropwise. The cooling bath was removed and the reaction mixture was allowed to stir for 14 h and slowly warm to ambient temperature. The reaction was then quenched with saturated aq. NH₄Cl (15 mL) and extracted with Et₂O (3 x 25 mL). The combined organic layers were washed with brine (35 mL), dried over MgSO₄, filtered and concentrated. The residue was purified by silica gel chromatography (4:1 hexanes/EtOAc eluent) to afford inseparable diastereomeric alcohols **3-122A** and **3-122B** as a colorless oil (962 mg, 49% yield, *R_f*: 0.16 in 4:1 hexanes/EtOAc). The spectroscopic data were in agreement to those previously reported.³²

To a stirred solution of alcohol **3-122** (71.6 mg, 0.310 mmol) in anhydrous CH₂Cl₂ (1.24 mL, 0.25 M) were added DMAP (3.8 mg, 0.0310 mmol) and pyridine (50.0 μL, 0.620 mmol) at 0 °C. Acetyl chloride (33.0 μL, 0.460 mmol) was added dropwise to the reaction mixture. The solution was allowed to warm to ambient temperature and stir for 1 h. H₂O (3 mL) was added to the reaction mixture and extracted with EtOAc (5 x 5 mL). The combined organic layers were washed with brine (5 mL), dried over Na₂SO₄, and filtered. The solvent was removed under reduced pressure, and the resulting oil was purified by silica gel chromatography (8:1:1 hexanes/EtOAc/MTBE eluent) to afford acetates **3-123A** (36.3 mg, 43% yield, *R_f*: 0.28 in 8:1:1

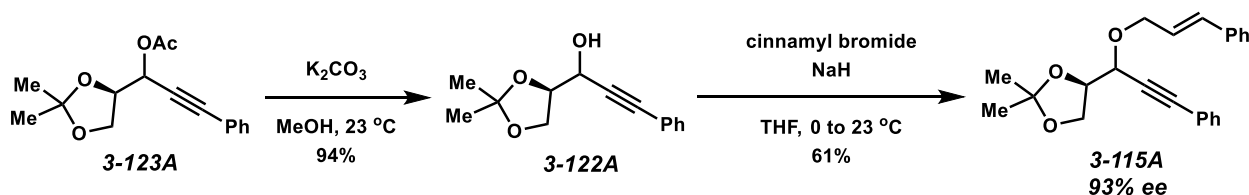
hexanes/EtOAc:MTBE) and **3-123B** (33.0 mg, 39% yield, R_f : 0.24 in 8:1:1 hexanes/EtOAc:MTBE) as pale yellow oils.

3-123A

$^1\text{H NMR}$ (400 MHz, CDCl_3): δ 7.48-7.41 (m, 2H), 7.41-7.28 (m, 3H), 5.65 (d, $J = 7.6$ Hz, 1H), 4.37 (ddd, $J = 7.6, 6.5, 5.3$ Hz, 1H), 4.19 (dd, $J = 9.0, 6.5$ Hz, 1H), 4.09 (dd, $J = 9.0, 5.3$ Hz, 1H), 2.16 (s, 3H), 1.46 (s, 3H), 1.39 (s, 3H).

3-123B

$^1\text{H NMR}$ (400 MHz, CDCl_3): δ 7.48-7.39 (m, 2H), 7.35-7.28 (m, 3H), 5.75 (d, $J = 3.7$ Hz, 1H), 4.41 (td, $J = 6.5, 3.7$ Hz, 1H), 4.18 (dd, $J = 8.6, 6.5$ Hz, 1H), 4.06 (dd, $J = 8.6, 6.5$ Hz, 1H), 2.16 (s, 3H), 1.48 (s, 3H), 1.40 (s, 3H).

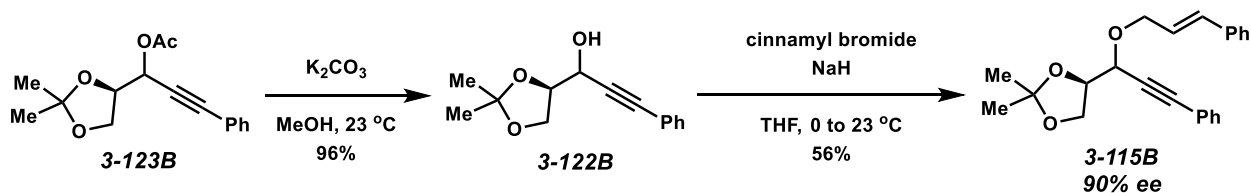


To a solution of acetate **3-123A** (52.3 mg, 0.191 mmol) in MeOH (0.955 mL, 0.2 M) was added K_2CO_3 (31.6 mg, 0.229 mmol) at ambient temperature. The reaction mixture was allowed to stir for 2 h. After consumption of the starting material was observed, the solution was diluted with Et_2O (3 mL) and H_2O (3 mL). The layers were separated, and the aqueous layer was extracted with Et_2O (2 x 3 mL). The combined organic layers were washed with brine (3 mL), dried over MgSO_4 , and filtered. The solvent was removed under reduced pressure, yielding alcohol **3-122A**.

(41.7 mg, 94% yield, R_f : 0.16 in 4:1 hexanes/EtOAc) as a colorless oil. Alcohol **3-122A** was sufficiently pure to be carried on to the next reaction.

To a solution of alcohol **3-122A** (22.4 mg, 0.096 mmol) in anhydrous THF (1.00 mL, 0.3 M) at 0 °C was added NaH (4.0 mg, 60% dispersion in mineral oil, 0.101 mmol) in 2 portions. After the solution stopped bubbling, the reaction was warmed to ambient temperature for 30 min. Cinnamyl bromide (14.0 μ L, 0.0960 mmol) was added dropwise to the solution, and the resulting solution was allowed to stir for 14 h. H₂O (2 mL) was added to the reaction mixture, and the THF was removed under reduced pressure. The resulting crude material was extracted with EtOAc (3 x 3 mL), and the combined organic layers were washed sequentially with H₂O (3 mL) and brine (3 mL), dried over MgSO₄, and filtered. The solvent was removed under reduced pressure, and the resulting residue was purified by silica gel chromatography (19:1 hexanes/EtOAc eluent) to afford enyne **3-115A** (18.3 mg, 61% yield, R_f : 0.49 in 9:1 hexanes/EtOAc) as a pale yellow oil.

¹H NMR (400 MHz, CDCl₃): δ 7.39-7.10 (m, 10H), 6.58 (d, J = 15.9 Hz, 1H), 6.24 (ddd, J = 15.9, 7.0, 5.6 Hz, 1H), 4.47-4.33 (m, 2H), 4.33-4.15 (m, 2H), 4.09 (dd, J = 8.7, 6.5 Hz, 1H), 3.95 (dd, J = 8.7, 6.1 Hz, 1H), 1.38 (s, 3H), 1.30 (s, 3H).



To a solution of acetate **3-123B** (47.8 mg, 0.174 mmol) in MeOH (0.870 mL, 0.2 M) was added K₂CO₃ (28.9 mg, 0.209 mmol) at ambient temperature. The reaction was allowed to stir for 2 h. After consumption of the starting material was observed, the solution was diluted with Et₂O (3 mL) and H₂O (3 mL). The layers were separated, and the aqueous layer was extracted with Et₂O (2 x 3 mL). The combined organic layers were washed with brine (20 mL), dried over MgSO₄, and filtered. The solvent was removed under reduced pressure yielding alcohol **3-122B** (38.8 mg, 96% yield, R_f: 0.16 in 4:1 hexanes/EtOAc) as a colorless oil. Alcohol **3-122B** was sufficiently pure to be carried on to the next reaction.

To a solution of alcohol **3-122B** (31.9 mg, 0.137 mmol) in anhydrous THF (1.0 mL, 0.137 M) at 0 °C was added NaH (5.8 mg, 60% dispersion in mineral oil, 0.144 mmol) in 2 portions. After the solution stopped bubbling, the reaction mixture was warmed to ambient temperature for 30 min. Cinnamyl bromide (20.3 µL, 0.137 mmol) was added dropwise to the solution, and the solution was allowed to stir for 14 h. H₂O (3 mL) was added to the reaction mixture, and the THF was removed under reduced pressure. The resulting crude material was extracted with EtOAc (3 x 3 mL), and the combined organic layers were washed sequentially with H₂O (3 mL) and brine (3 mL), dried over MgSO₄, and filtered. The solvent was removed under reduced pressure, and the resulting residue was purified by silica gel chromatography (19:1 hexanes/EtOAc eluent) to afford enyne **3-115B** (21.0 mg, 56% yield, R_f: 0.46 in 9:1 hexanes/EtOAc) as a pale yellow oil.

¹H NMR (400 MHz, CDCl₃): δ 7.40-7.34 (m, 2H), 7.33-7.10 (m, 8H), 6.57 (d, *J* = 15.9 Hz, 1H), 6.22 (ddd, *J* = 15.9, 6.8, 5.6 Hz, 1H), 4.43 (ddd, *J* = 12.5, 5.6, 1.4 Hz, 1H), 4.33-4.22 (m, 2H), 4.18

(ddd, $J = 12.5, 6.8, 1.4$ Hz, 1H), 4.05 (dd, $J = 8.5, 6.2$ Hz, 1H), 3.97 (dd, $J = 8.5, 5.8$ Hz, 1H), 1.40 (s, 3H), 1.30 (s, 3H)..

General Cycloisomerization Procedures



General Procedure A

To a flask containing JohnPhosAu(MeCN)SbF₆ (0.4 mg, 0.000600 mmol) under argon was added a solution of enyne (10.0 mg, 0.0290 mmol) in solvent (1.0 mL, 0.03 M). The solution was allowed to stir for the indicated time before being passed through a plug of neutral alumina (2 x 0.5 cm, 4:1 hexanes/EtOAc eluent). The solvent was removed under reduced pressure. The resulting residue was purified by silica gel chromatography (97:2:1 hexanes/EtOAc/Et₃N eluent) to afford oxabicycloheptene as a pale yellow oil.

General Procedure B

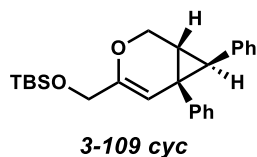
To a flask containing PtCl₂ (0.5 mg, 0.00200 mmol) under argon was added a solution of enyne (10.0 mg, 0.0290 mmol) in solvent (1.0 mL, 0.03 M). The solution was allowed to stir for the indicated time before being passed through a plug of neutral alumina (2 x 0.5 cm, 4:1 hexanes/EtOAc eluent). The solvent was removed under reduced pressure. The resulting residue

was purified by silica gel chromatography (97:2:1 hexanes/EtOAc/Et₃N eluent) to afford oxabicycloheptene as a pale yellow oil.

General Procedure C

To a flask containing [(C₂H₄)PtCl₂]₂ (0.4 mg, 0.000700 mmol) under argon was added a solution of enyne (10.0 mg, 0.0290 mmol) in solvent (1.0 mL, 0.03 M). The solution was allowed to stir for the indicated time before being run through a plug of neutral alumina (2 x 0.5 cm, 4:1 hexanes/EtOAc eluent). The solvent was removed under reduced pressure. The resulting residue was purified by silica gel chromatography (97:2:1 hexanes/EtOAc/Et₃N eluent) to afford oxabicycloheptene as a pale yellow oil.

Cycloisomerization Products

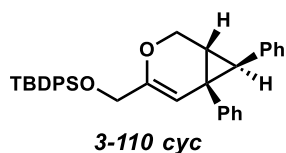


IR (film): 3027, 2954, 1598, 1490, 1254cm⁻¹.

¹H NMR (400 MHz, C₆D₆): δ 7.06-6.84 (m, 8H), 6.72-6.63 (m, 2H), 5.58 (s, 1H), 4.19 (dd, *J* = 10.4, 1.4 Hz, 1H), 4.11 (s, 2H), 3.88 (dd, *J* = 10.4, 2.1 Hz, 1H), 2.86 (d, *J* = 5.9 Hz, 1H), 2.10-2.03 (m, 1H), 0.97 (s, 9H), 0.09 (s, 6H).

¹³C NMR (100 MHz, C₆D₆): δ 150.7, 140.5, 138.2, 130.2, 128.5, 128.2, 128.0, 126.7, 125.9, 107.5, 63.4, 62.5, 37.2, 32.2, 29.7, 26.1, 18.6, -5.1.

HRMS (ESI⁺): *m/z* calc. for (M + H)⁺ [C₂₅H₃₂O₂Si + H]⁺: 392.2172, found.

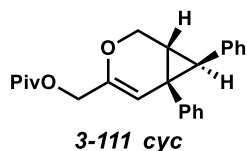


IR (film): 3020, 2929, 2820, 1590, 1130 cm^{-1} .

^1H NMR (400 MHz, C_6D_6): δ 7.88-7.80 (m, 3H), 7.21 (p, $J = 3.6$ Hz, 5H), 7.00 (d, $J = 4.3$ Hz, 4H), 6.98-6.80 (m, 6H), 6.67 (dd, $J = 7.0, 1.8$ Hz, 2H), 5.53 (s, 1H), 4.22 (d, $J = 4.6$ Hz, 2H), 4.15 (dd, $J = 10.5, 1.3$ Hz, 1H), 3.83 (dd, $J = 10.5, 2.1$ Hz, 1H), 2.80 (d, $J = 5.9$ Hz, 1H), 2.03 (d, $J = 6.0$ Hz, 1H), 1.18 (s, 9H).

^{13}C NMR (100 MHz, C_6D_6): δ .

HRMS (ESI⁺): m/z calc. for $(\text{M} + \text{H})^+$ [$\text{C}_{35}\text{H}_{36}\text{O}_2\text{S} + \text{H}$]⁺: 516.2485, found.

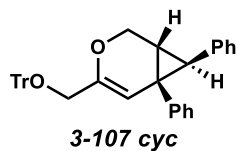


IR (film): 3025, 2987, 1727, 1293, 1165 cm^{-1} .

^1H NMR (400 MHz, C_6D_6): δ 7.11-6.81 (m, 8H), 6.66-6.59 (m, 2H), 5.43 (s, 1H), 4.61 (d, $J = 12.7$ Hz, 1H), 4.48 (d, $J = 12.7$ Hz, 1H), 4.13 (dd, $J = 10.5, 1.3$ Hz, 1H), 3.79 (dd, $J = 10.5, 2.0$ Hz, 1H), 2.80 (d, $J = 6.2$ Hz, 1H), 2.01 (d, $J = 6.2$ Hz, 1H), 1.19 (s, 9H).

^{13}C NMR (100 MHz, C_6D_6): δ .

HRMS (ESI⁺): m/z calc. for $(\text{M} + \text{H})^+$ [$\text{C}_{24}\text{H}_{26}\text{O}_3 + \text{H}$]⁺: 362.1882, found.

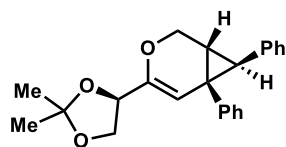


IR (film): 3058, 2924, 2360, 1670, 1602, 1491, 1448 cm^{-1} .

^1H NMR (400 MHz, C_6D_6): δ 7.73-7.59 (m, 7H), 7.14-6.82 (m, 20H), 6.70-6.59 (m, 2H), 5.52 (s, 1H), 4.22 (dd, $J = 10.5, 1.3$ Hz, 1H), 3.90 (dd, $J = 10.5, 2.0$ Hz, 1H), 3.81 (d, $J = 11.7$ Hz, 1H), 3.70 (d, $J = 11.7$ Hz, 1H), 2.85 (d, $J = 5.9$ Hz, 1H), 2.05 (d, $J = 5.9$ Hz, 1H).

^{13}C NMR (100 MHz, C_6D_6): δ 149.0, 144.7, 140.4, 138.1, 130.3, 129.3, 128.5, 128.2, 127.9, 127.3, 126.7, 125.9, 109.2, 87.3, 64.8, 62.5, 37.1, 35.0, 29.8.

HRMS (ESI⁺): m/z calc. for $(\text{M} + \text{H})^+$ [$\text{C}_{38}\text{H}_{32}\text{O}_2 + \text{H}$]⁺: 520.2402, found .



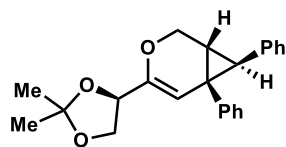
3-115A cyc

IR (film): 3026, 2985, 1599, 1490, 1213, 1072 cm^{-1} .

^1H NMR (400 MHz, C_6D_6): Due to instability of the product during chromatography, the product was unable to be isolated. Key signals: δ 5.60 (s, 1H), 2.79 (d, 1H), 2.01 (d, 1H).

^{13}C NMR (100 MHz, C_6D_6): δ .

HRMS (ESI⁺): m/z calc. for $(\text{M} + \text{H})^+$ [$\text{C}_{23}\text{H}_{24}\text{O}_3 + \text{H}$]⁺: 348.1725, found.



3-115B cyc

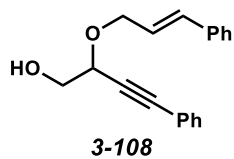
IR (film): 3026, 2986, 1599, 1490, 1217, 1073 cm^{-1} .

^1H NMR (400 MHz, C_6D_6): Due to instability of the product during chromatography, the product was unable to be isolated. Key signals: δ 5.63 (s, 1H), 2.79 (d, 1H), 2.03 (d, 1H).

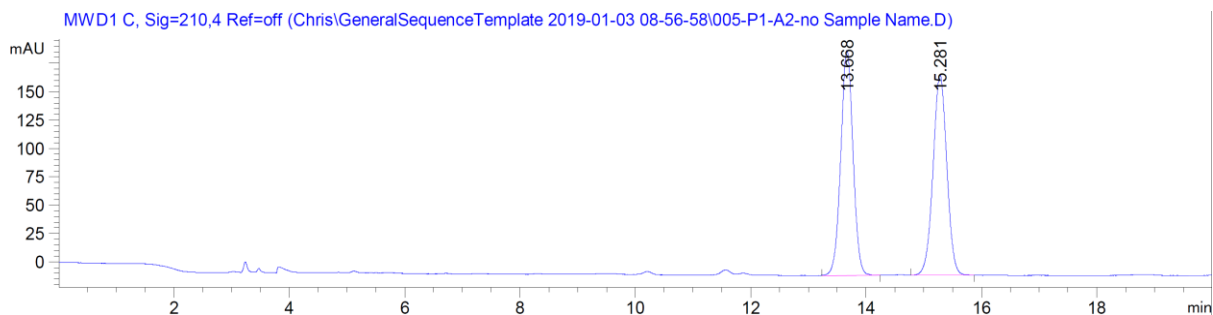
^{13}C NMR (100 MHz, C_6D_6): δ .

HRMS (ESI $^{+}$): m/z calc. for $(\text{M} + \text{H})^{+}$ [$\text{C}_{23}\text{H}_{24}\text{O}_3 + \text{H}$] $^{+}$: 348.1725, found.

HPLC Chromatograms



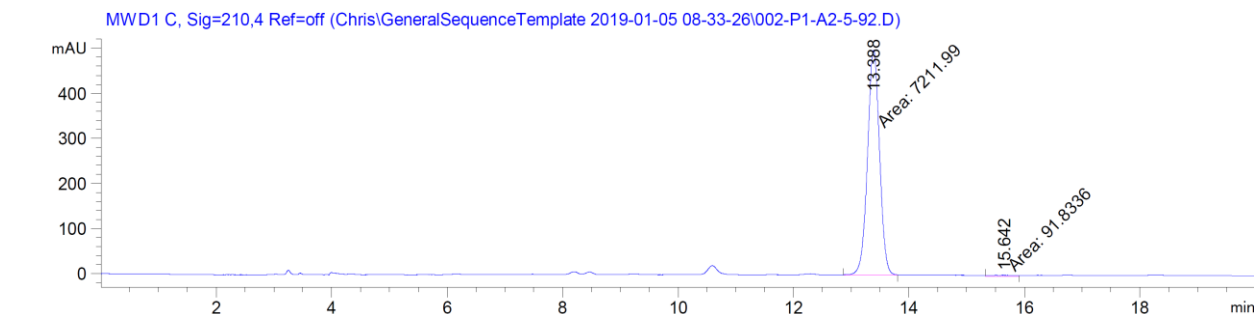
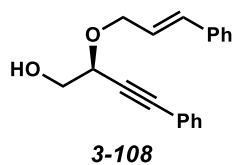
Column: CHIRALPAK IB, (2% EtOH, 98% Hexanes), 210 nm



Signal 3: MWD1 C, Sig=210,4 Ref=off

Peak #	RetTime [min]	Type	Width [min]	Area [mAU*s]	Height [mAU]	Area %
1	13.668	VV R	0.2239	2937.11279	198.20619	50.0248
2	15.281	VV R	0.2448	2934.19507	176.59589	49.9752

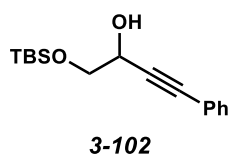
Totals : 5871.30786 374.80208



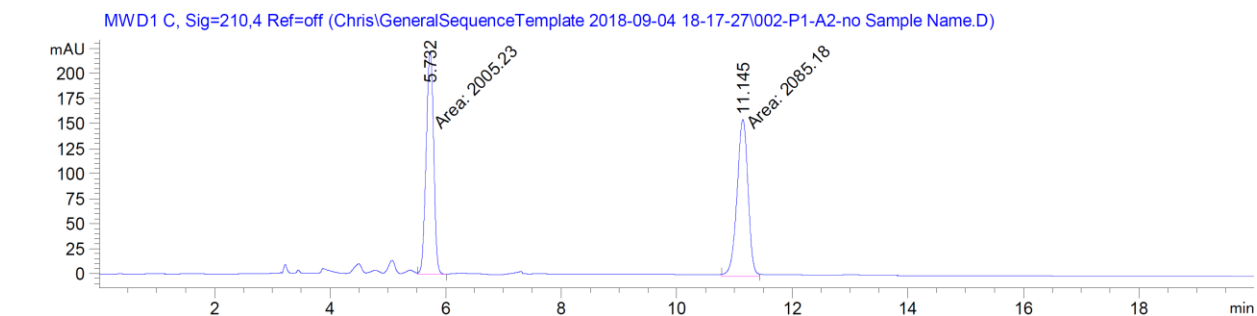
Signal 3: MWD1 C, Sig=210,4 Ref=off

Peak #	RetTime [min]	Type	Width [min]	Area [mAU*s]	Height [mAU]	Area %
1	13.388	MM	0.2409	7211.99023	498.87613	98.7427
2	15.642	MM	0.5492	91.83365	2.78686	1.2573

Totals : 7303.82388 501.66299



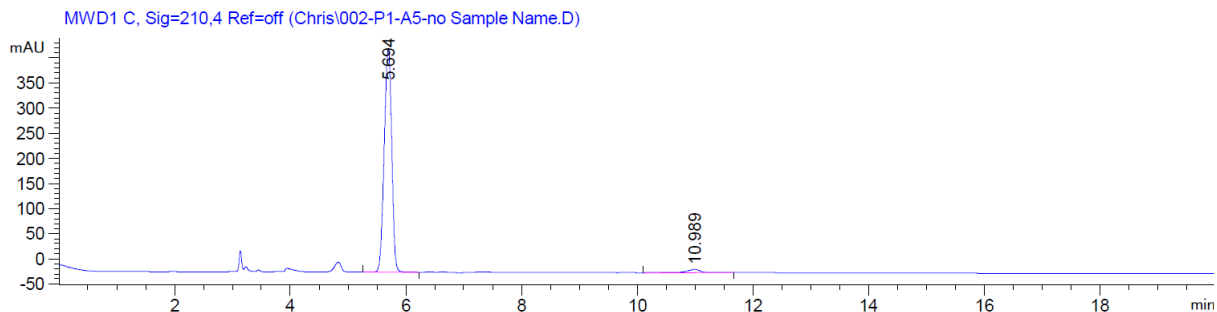
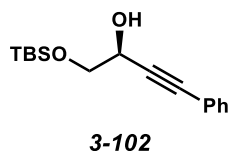
Column: CHIRALPAK IB, 2% EtOH / 98% Hexanes, 210 nm



Signal 3: MWD1 C, Sig=210,4 Ref=off

Peak #	RetTime [min]	Type	Width [min]	Area [mAU*s]	Height [mAU]	Area %
1	5.732	MM	0.1499	2005.22961	222.90631	49.0228
2	11.145	MM	0.2217	2085.17505	156.73003	50.9772

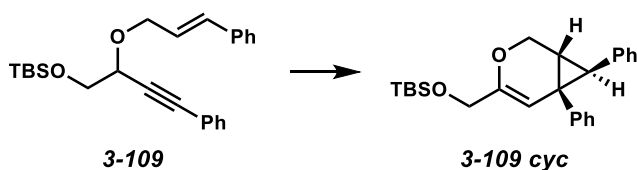
Totals : 4090.40466 379.63634



Signal 3: MWD1 C, Sig=210,4 Ref=off

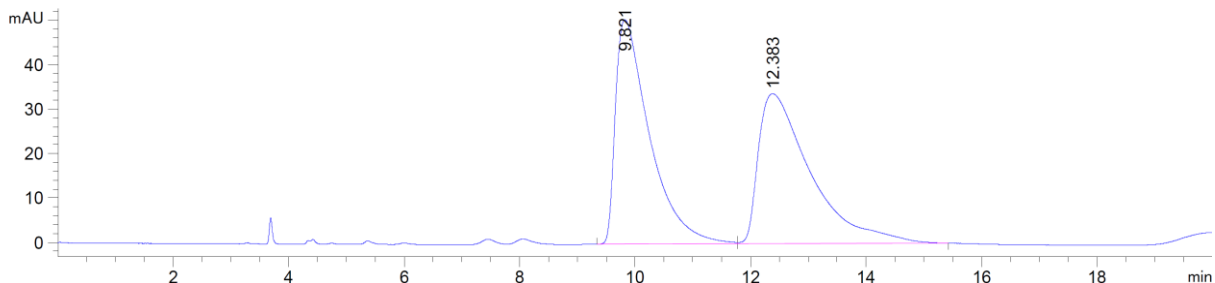
Peak #	RetTime [min]	Type	Width [min]	Area [mAU*s]	Height [mAU]	Area %
1	5.694	BB	0.1448	4021.08252	443.46747	97.5779
2	10.989	VV R	0.2254	99.81361	6.31617	2.4221

Totals : 4120.89613 449.78363



Column: CHIRALPAK IC, (100% Hexanes), 254 nm

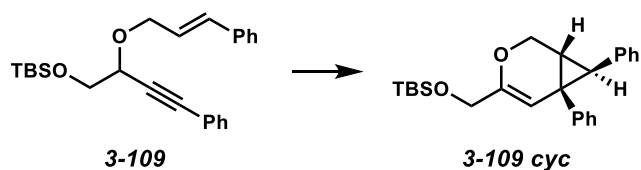
MWD1 B, Sig=254,4 Ref=off (Chris\GeneralSequenceTemplate 2018-10-02 10-47-36\002-P1-A2-no Sample Name.D)



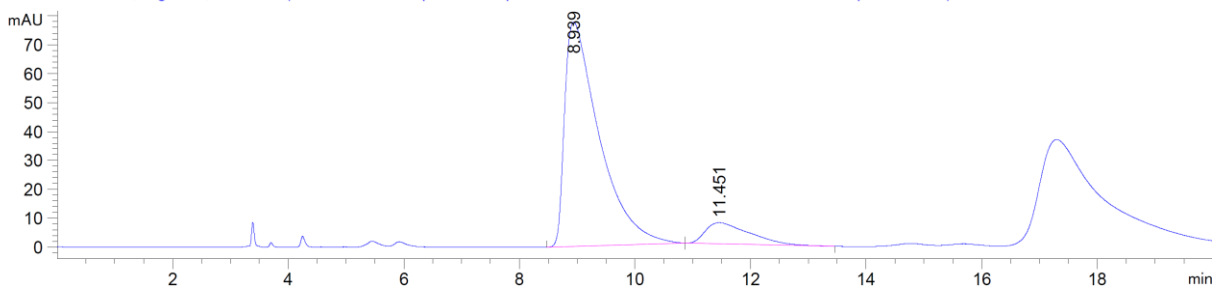
Signal 2: MWD1 B, Sig=254,4 Ref=off

Peak #	RetTime [min]	Type	Width [min]	Area [mAU*s]	Height [mAU]	Area %
1	9.821	VV R	0.5661	2071.53979	50.50011	49.3853
2	12.383	VB	0.7357	2123.11279	33.75793	50.6147

Totals : 4194.65259 84.25804



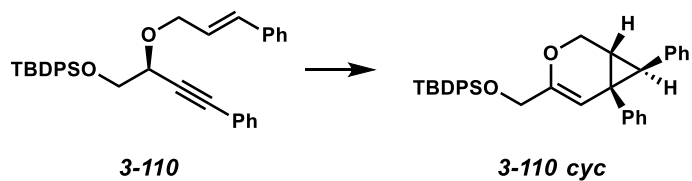
MWD1 B, Sig=254,4 Ref=off (Chris\GeneralSequenceTemplate 2018-10-16 11-09-07\002-P1-A2-no Sample Name.D)



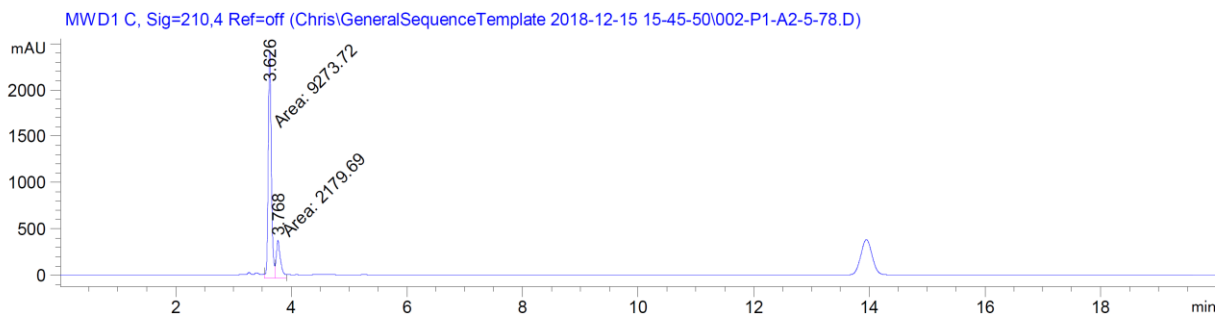
Signal 2: MWD1 B, Sig=254,4 Ref=off

Peak #	RetTime [min]	Type	Width [min]	Area [mAU*s]	Height [mAU]	Area %
1	8.939	BB	0.5866	3230.95093	77.70293	89.1295
2	11.451	BB	0.6322	394.05511	7.36535	10.8705

Totals : 3625.00604 85.06829



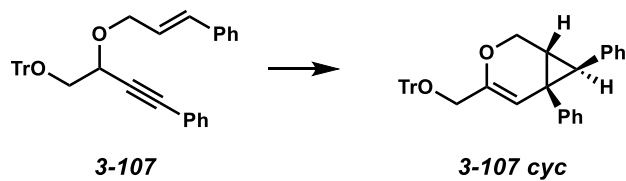
Column: CHIRALPAK IC, (1% *i*PrOH, 99% Hexanes), 210 nm



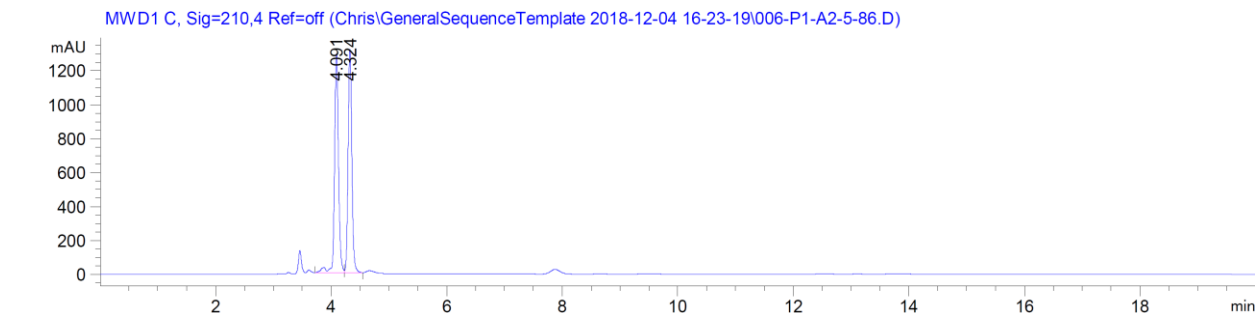
Signal 3: MWD1 C, Sig=210,4 Ref=off

Peak #	RetTime [min]	Type	Width [min]	Area [mAU*s]	Height [mAU]	Area %
1	3.626	MF	0.0626	9273.72168	2467.63379	80.9690
2	3.768	FM	0.0887	2179.69482	409.66141	19.0310

Totals : 1.14534e4 2877.29520



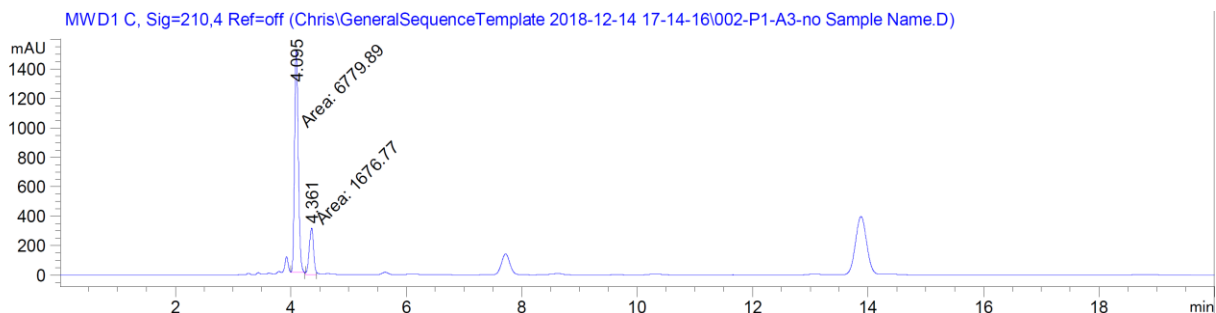
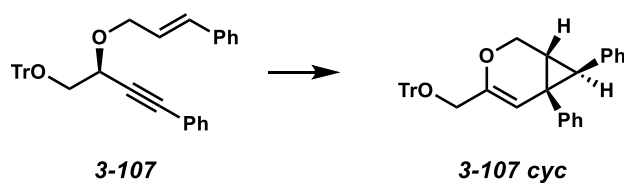
Column: CHIRALPAK IC, (1% *i*PrOH, 99% Hexanes), 210 nm



Signal 3: MWD1 C, Sig=210,4 Ref=off

Peak #	RetTime [min]	Type	Width [min]	Area [mAU*s]	Height [mAU]	Area %
1	4.091	VV R	0.0713	6173.73682	1292.43042	51.1547
2	4.324	VB	0.0691	5895.01416	1319.21533	48.8453

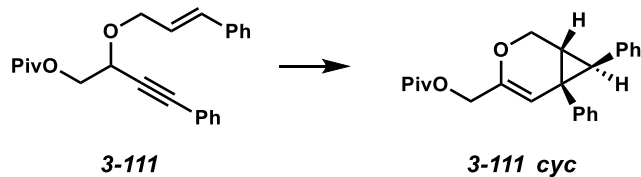
Totals : 1.20688e4 2611.64575



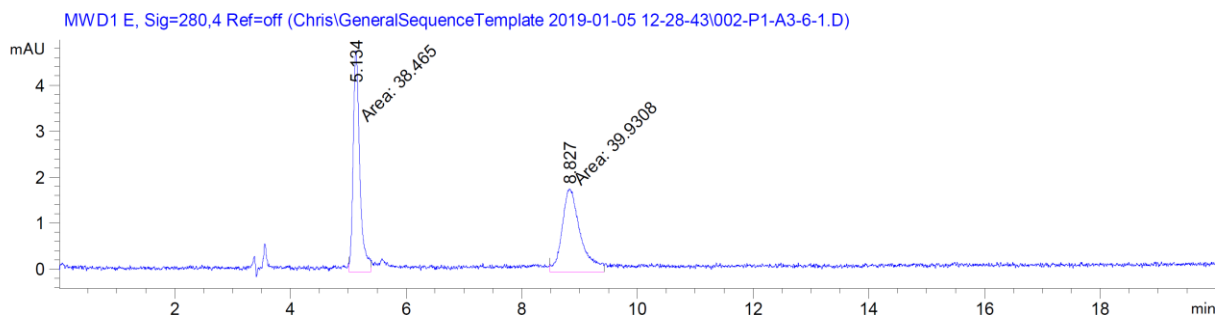
Signal 3: MWD1 C, Sig=210,4 Ref=off

Peak #	RetTime [min]	Type	Width [min]	Area [mAU*s]	Height [mAU]	Area %
1	4.095	MM	0.0747	6779.89307	1512.33545	80.1722
2	4.361	MM	0.0881	1676.77124	317.13654	19.8278

Totals : 8456.66431 1829.47198



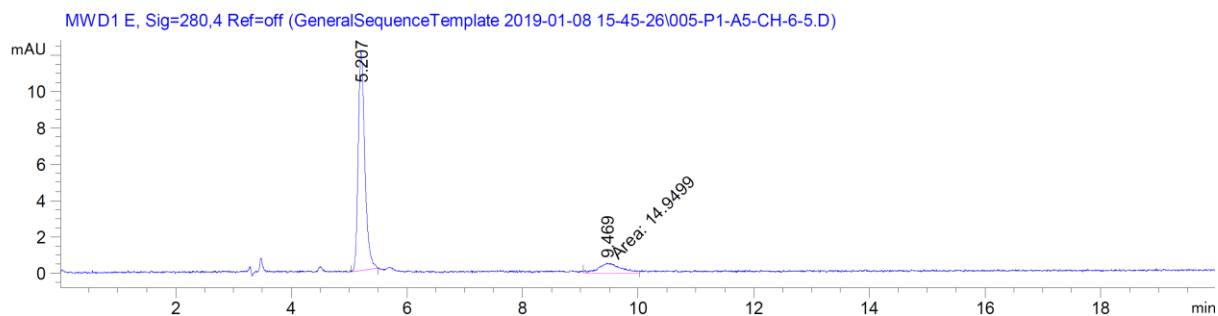
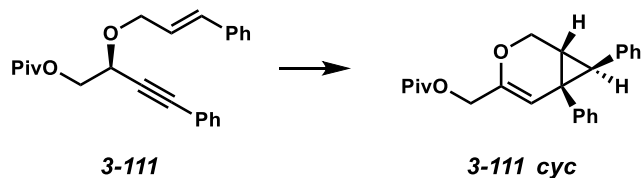
Column: CHIRALPAK IC, (100% Hexanes), 280 nm



Signal 5: MWD1 E, Sig=280,4 Ref=off

Peak #	RetTime [min]	Type	Width [min]	Area [mAU*s]	Height [mAU]	Area %
1	5.134	MM	0.1331	38.46502	4.81486	49.0652
2	8.827	MM	0.3684	39.93079	1.80672	50.9348

Totals : 78.39581 6.62158

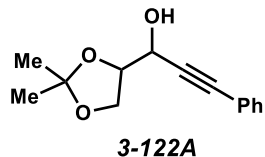


Signal 5: MWD1 E, Sig=280,4 Ref=off

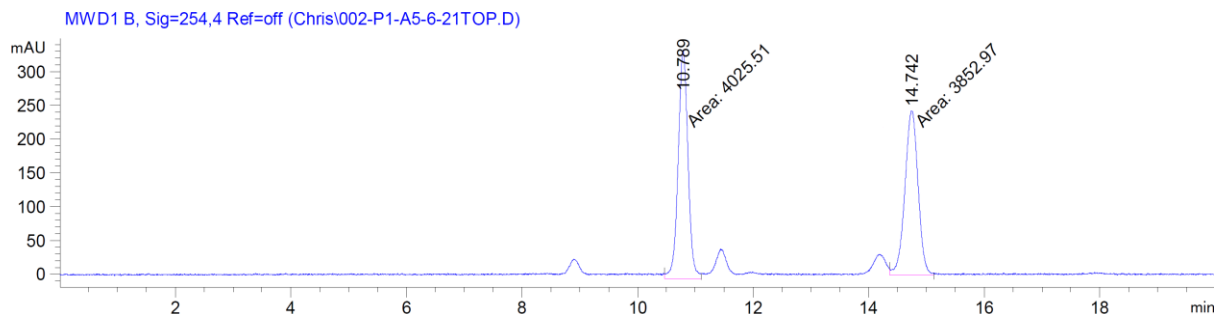
Peak #	RetTime [min]	Type	Width [min]	Area [mAU*s]	Height [mAU]	Area %
1	5.207	BV R	0.1187	96.11079	12.09072	86.5390
2	9.469	MM	0.4487	14.94988	5.55349e-1	13.4610

Totals : 111.06067 12.64607

Second Generation Substrate Chirality Transfer HPLC Data:



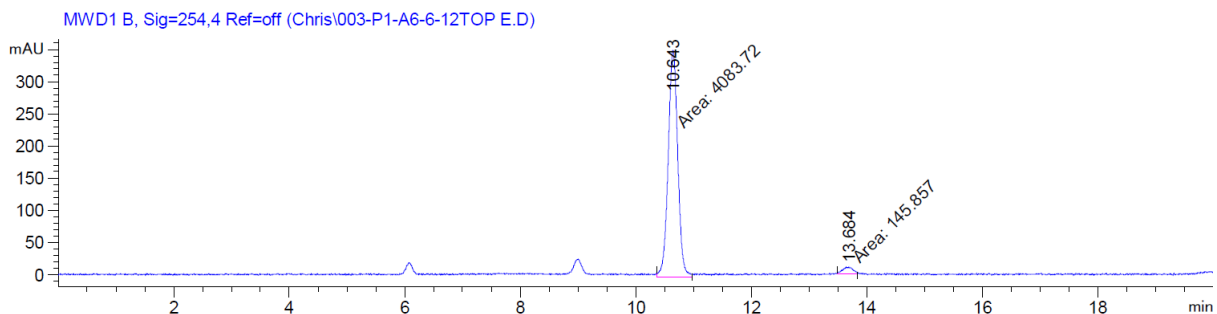
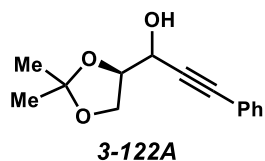
Column: CHIRALPAK IB, (2% EtOH, 98% Hexanes), 254 nm



Signal 2: MWD1 B, Sig=254,4 Ref=off

Peak #	RetTime [min]	Type	Width [min]	Area [mAU*s]	Height [mAU]	Area %
1	10.789	MM	0.1973	4025.51196	339.97565	51.0950
2	14.742	MM	0.2643	3852.97412	242.98613	48.9050

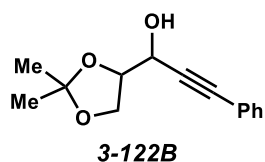
Totals : 7878.48608 582.96178



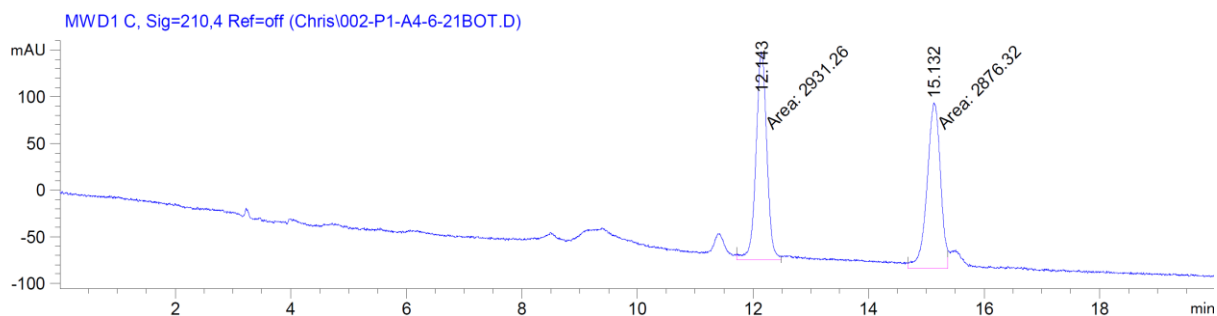
Signal 2: MWD1 B, Sig=254,4 Ref=off

Peak #	RetTime [min]	Type	Width [min]	Area [mAU*s]	Height [mAU]	Area %
1	10.643	MM	0.1927	4083.71875	353.22931	96.5515
2	13.684	MM	0.2159	145.85718	11.25828	3.4485

Totals : 4229.57593 364.48759



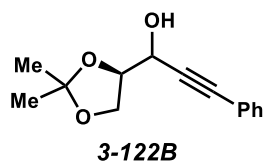
Column: CHIRALPAK IB, (2% EtOH, 98% Hexanes), 210 nm

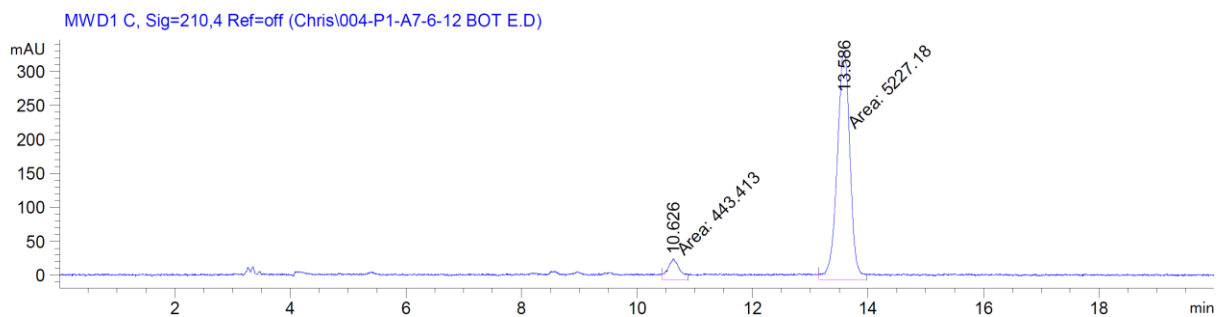


Signal 3: MWD1 C, Sig=210,4 Ref=off

Peak #	RetTime [min]	Type	Width [min]	Area [mAU*s]	Height [mAU]	Area %
1	12.143	MM	0.2185	2931.25757	223.61221	50.4730
2	15.132	MM	0.2705	2876.32324	177.19771	49.5270

Totals : 5807.58081 400.80992





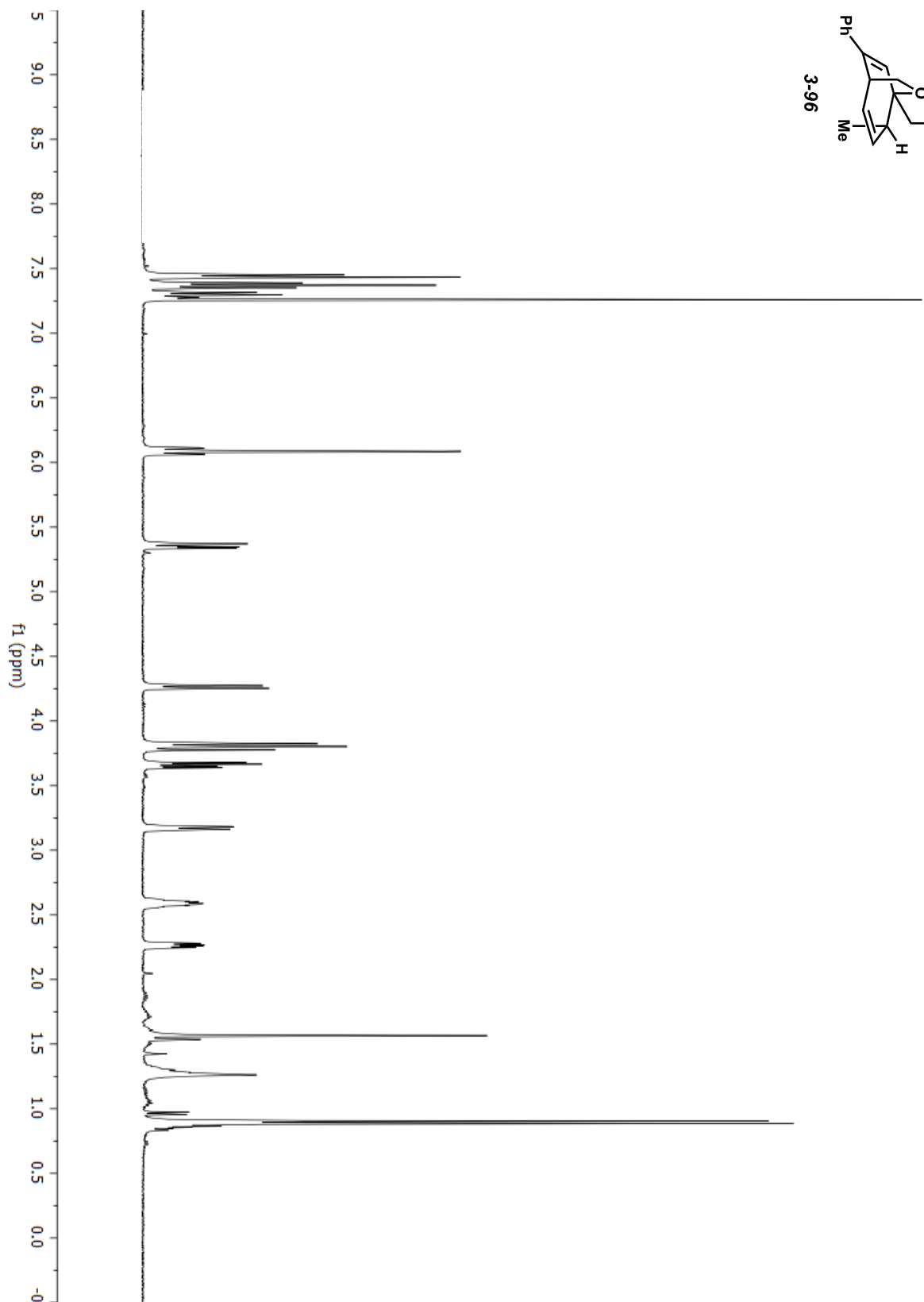
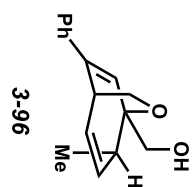
Signal 2: MWD1 B, Sig=254,4 Ref=off

Peak #	RetTime [min]	Type	Width [min]	Area [mAU*s]	Height [mAU]	Area %
1	10.624	MM	0.1831	288.35565	26.24571	4.5616
2	13.587	MM	0.2449	6032.98389	410.59183	95.4384

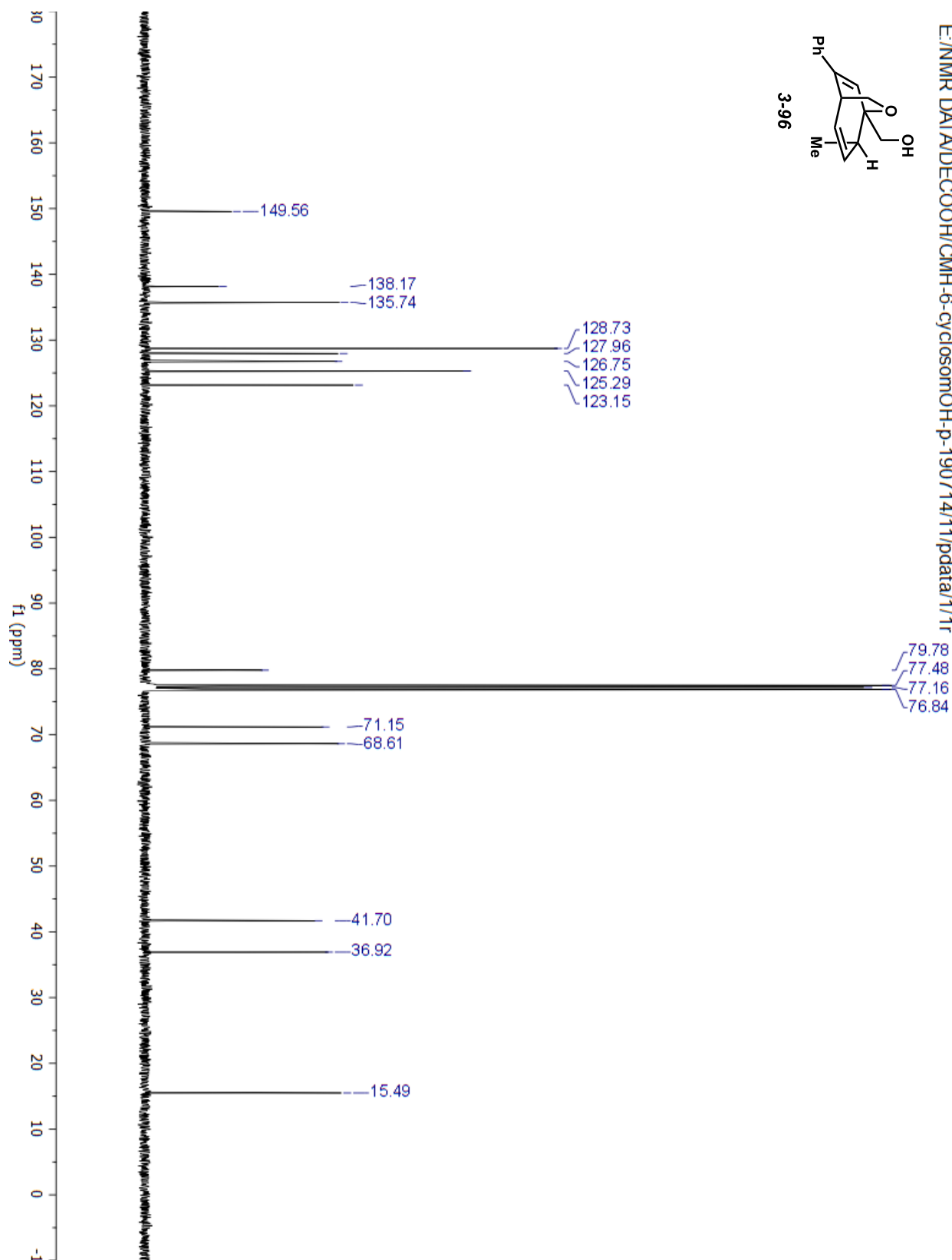
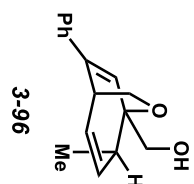
Totals : 6321.33954 436.83754

NMR Spectra

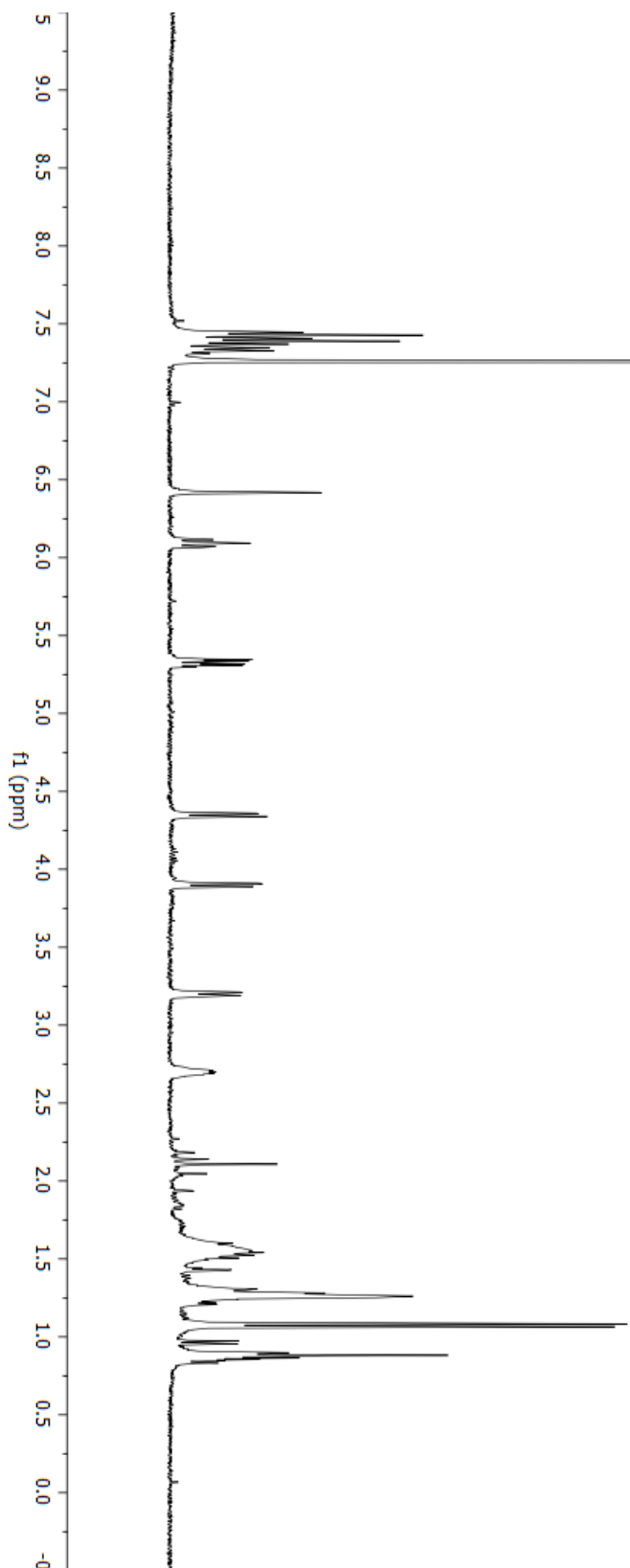
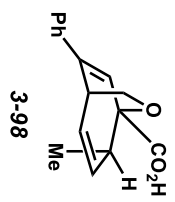
E:/NMR DATA/DECOOH/CMH-4-24-p-180414/10/pdata/1/1r



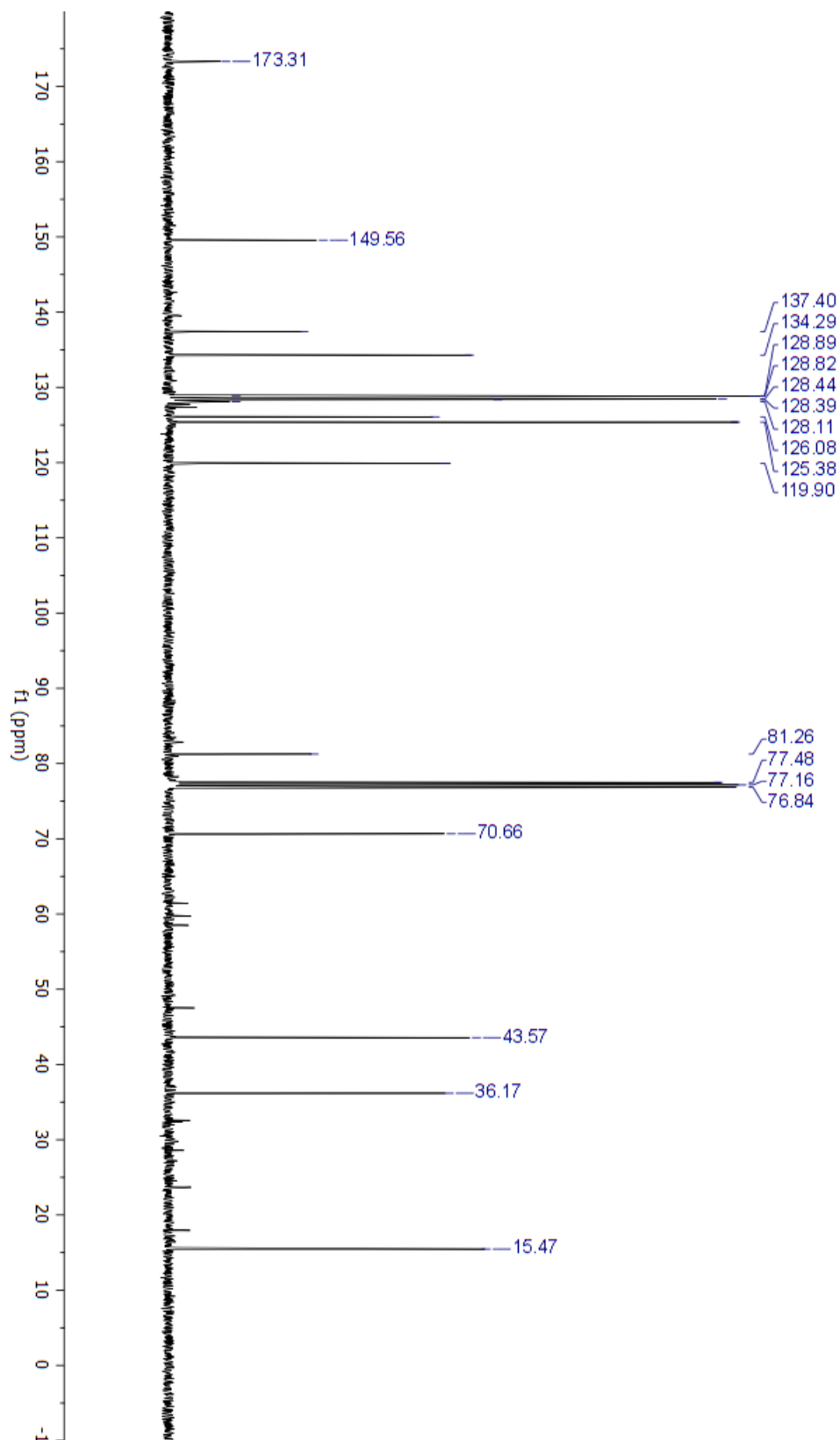
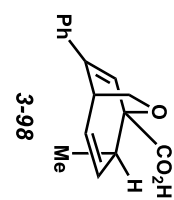
E:/NMR DATA/DECOOH/CMH-6-cyclosomOH-p-190714/1/pdata/1/1r



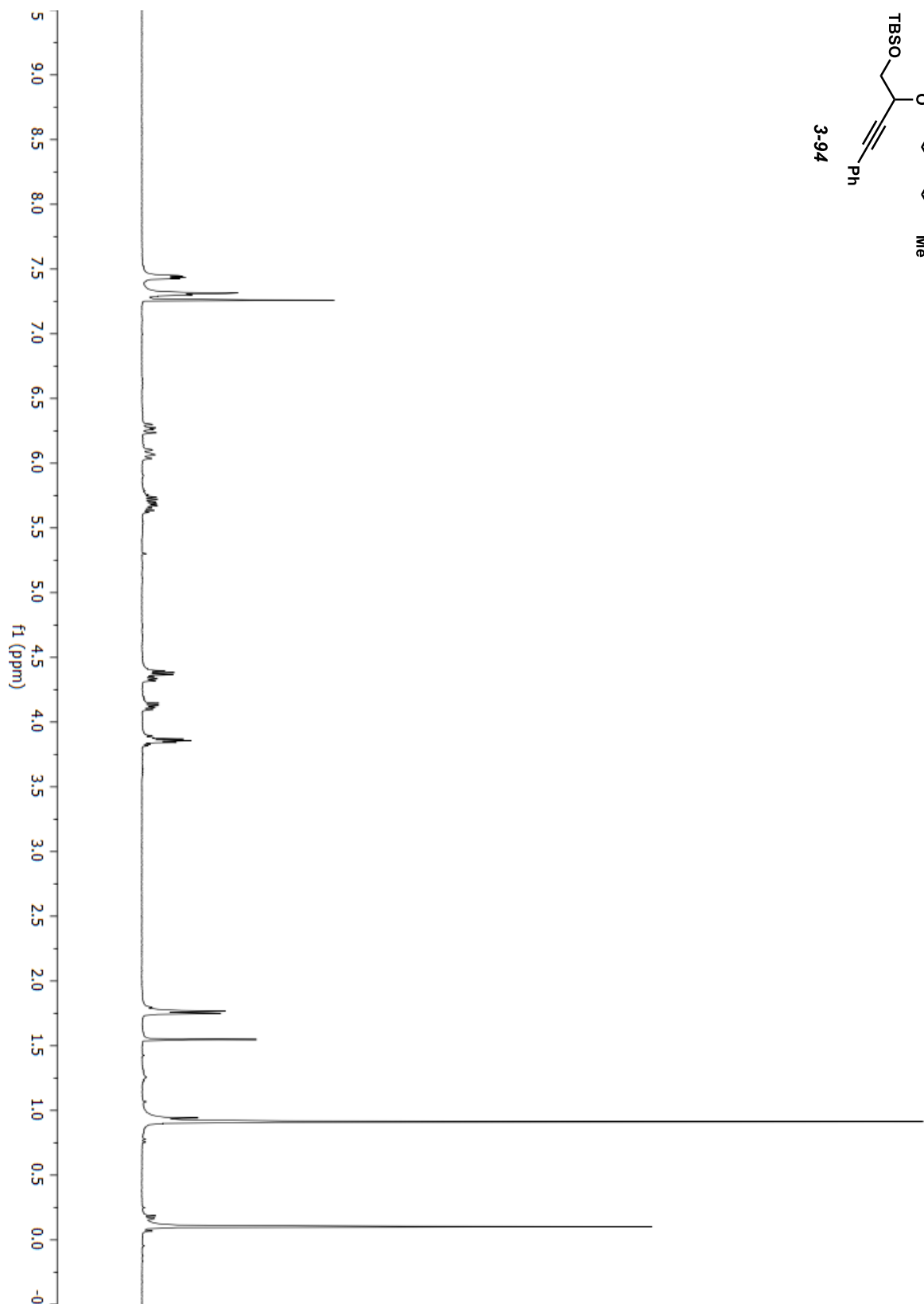
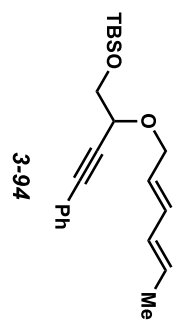
E:/NMR DATA/DECOOH/CMH-4-26-p-180416/10/pdata/1/1r



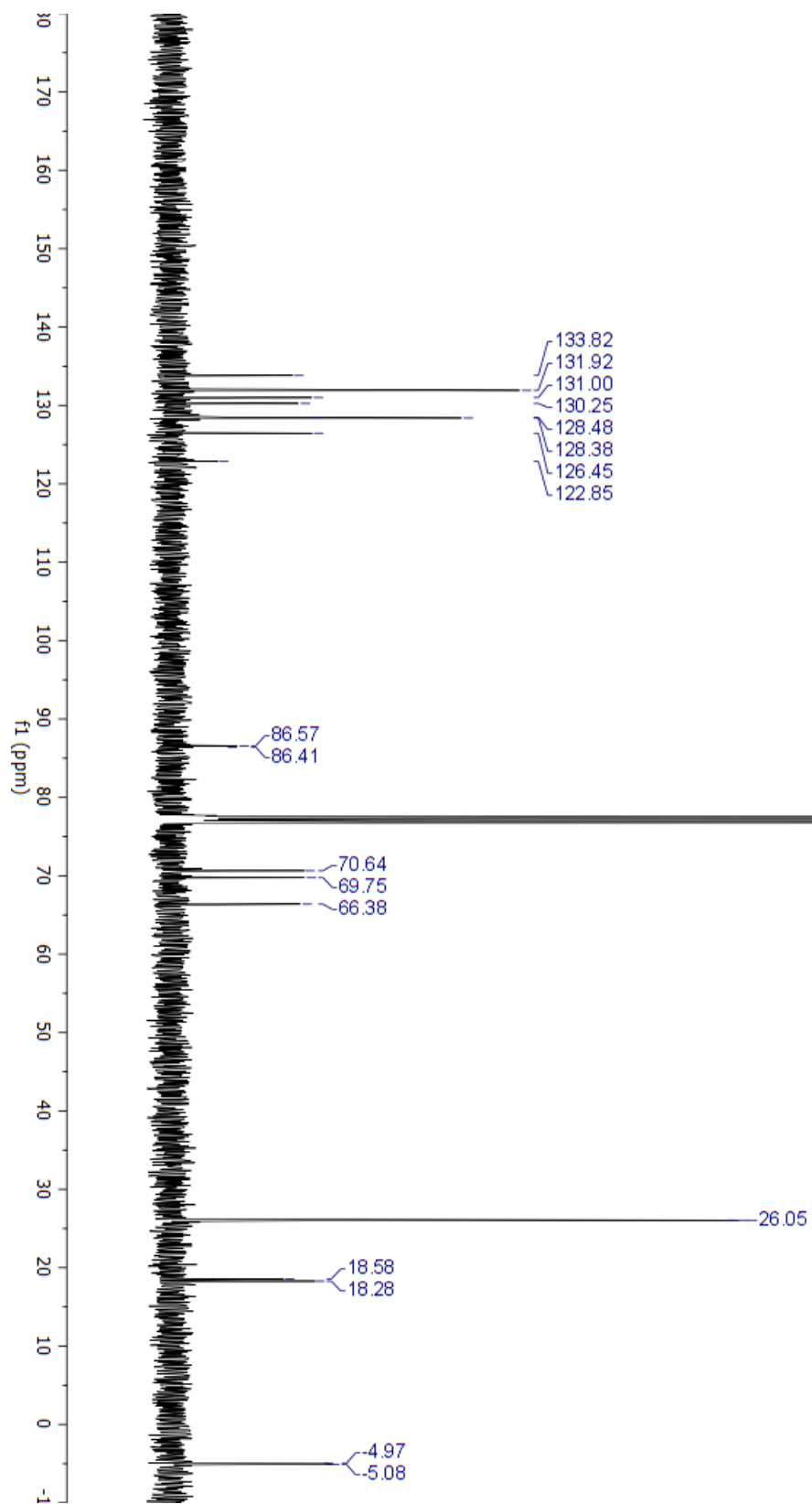
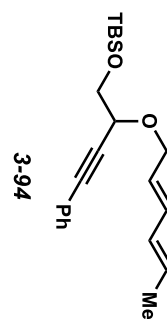
E:/NMR DATA/DECOOH/CMH-4-95-p-190716/11/pdata/1/1r



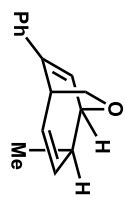
E:/NMR DATA/DECOOH/CMH-4-60-p-180525/10/pdata/1/1r



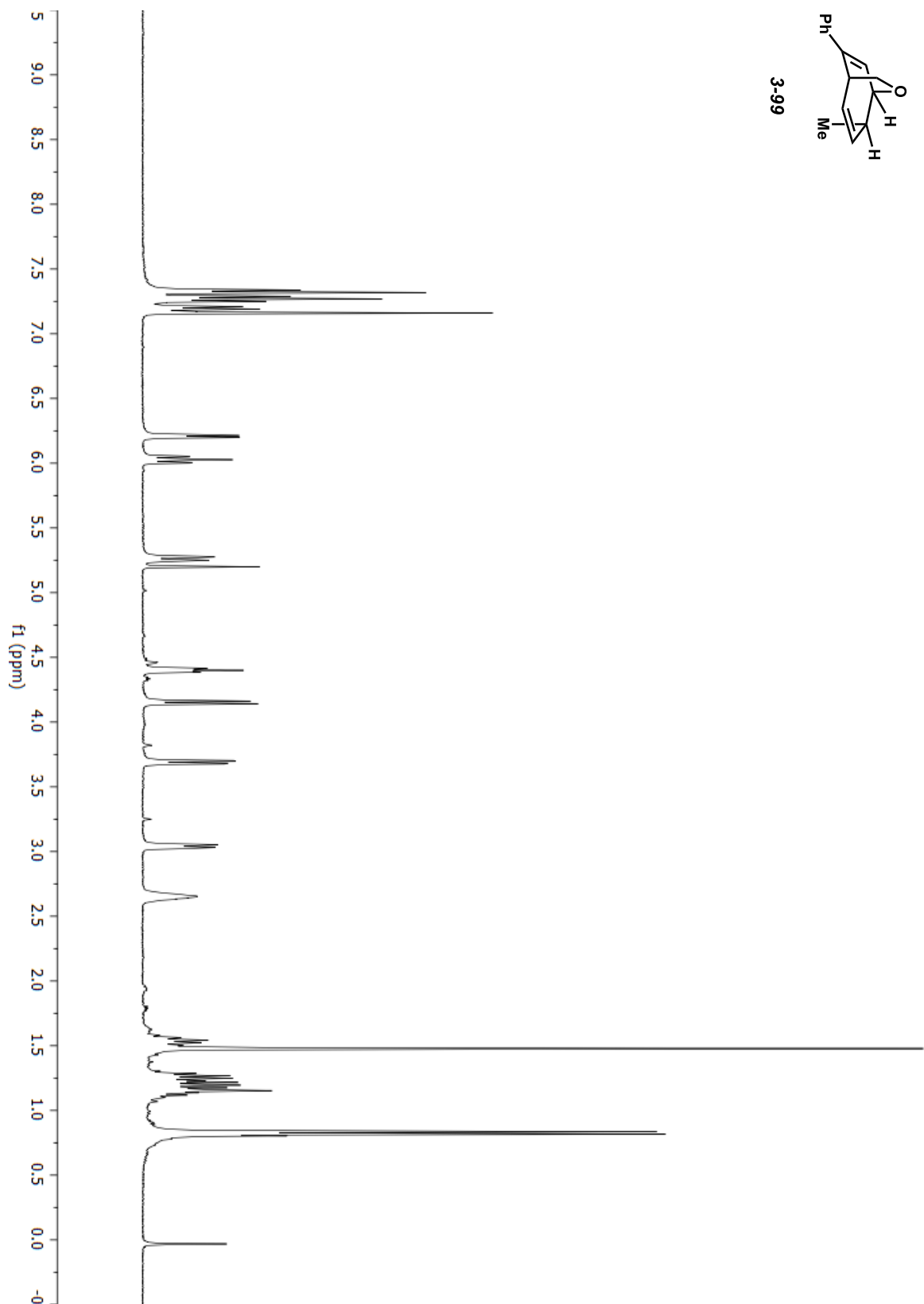
E:/NMR DATA/Chirality Xfer/CMH-4-60-4-190722/1/fid



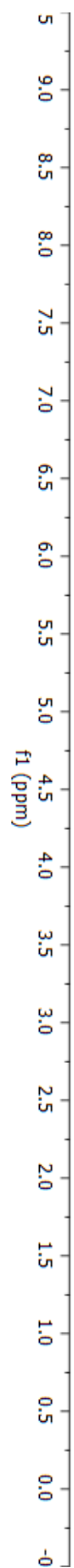
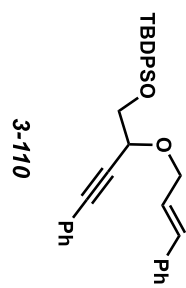
E:/NMR DATA/DECOOH/CMH-4-96-p-180726/10/pdata/1/1r



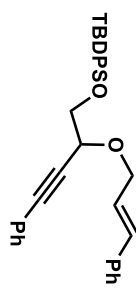
3-99



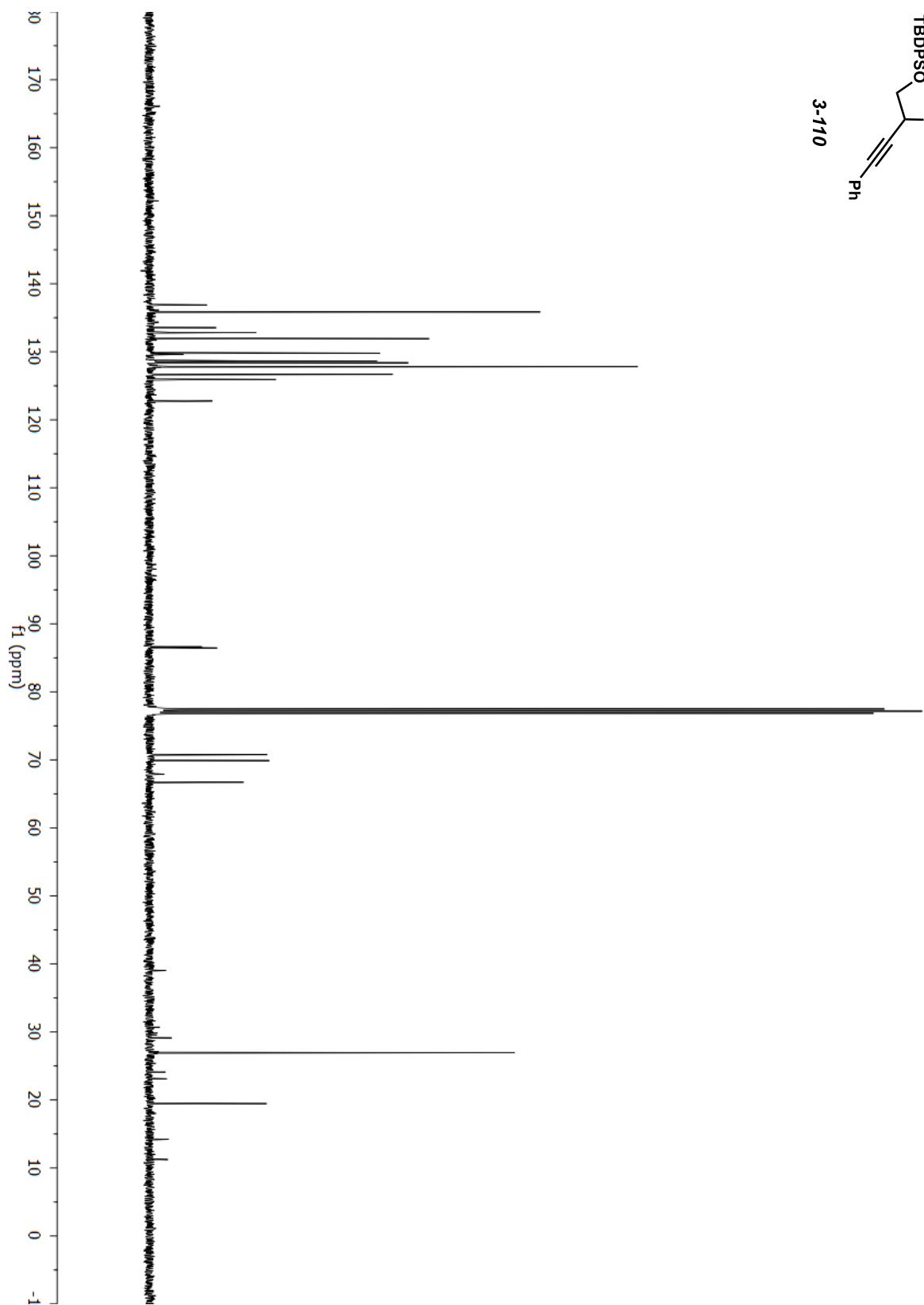
E:/NMR DATA/Chirality Xfer/CMH-5-73-p-181115/10/pdata/1/1r



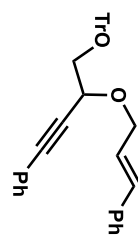
E:/NMR DATA/Chirality Xfer/CMH-6-49-2-p-190715/1/1/pdata/1/1r



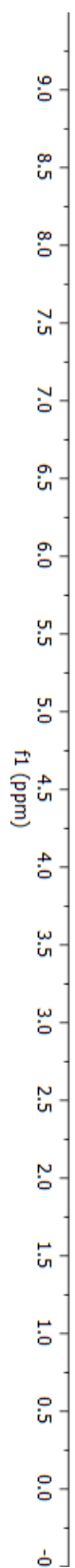
3-110



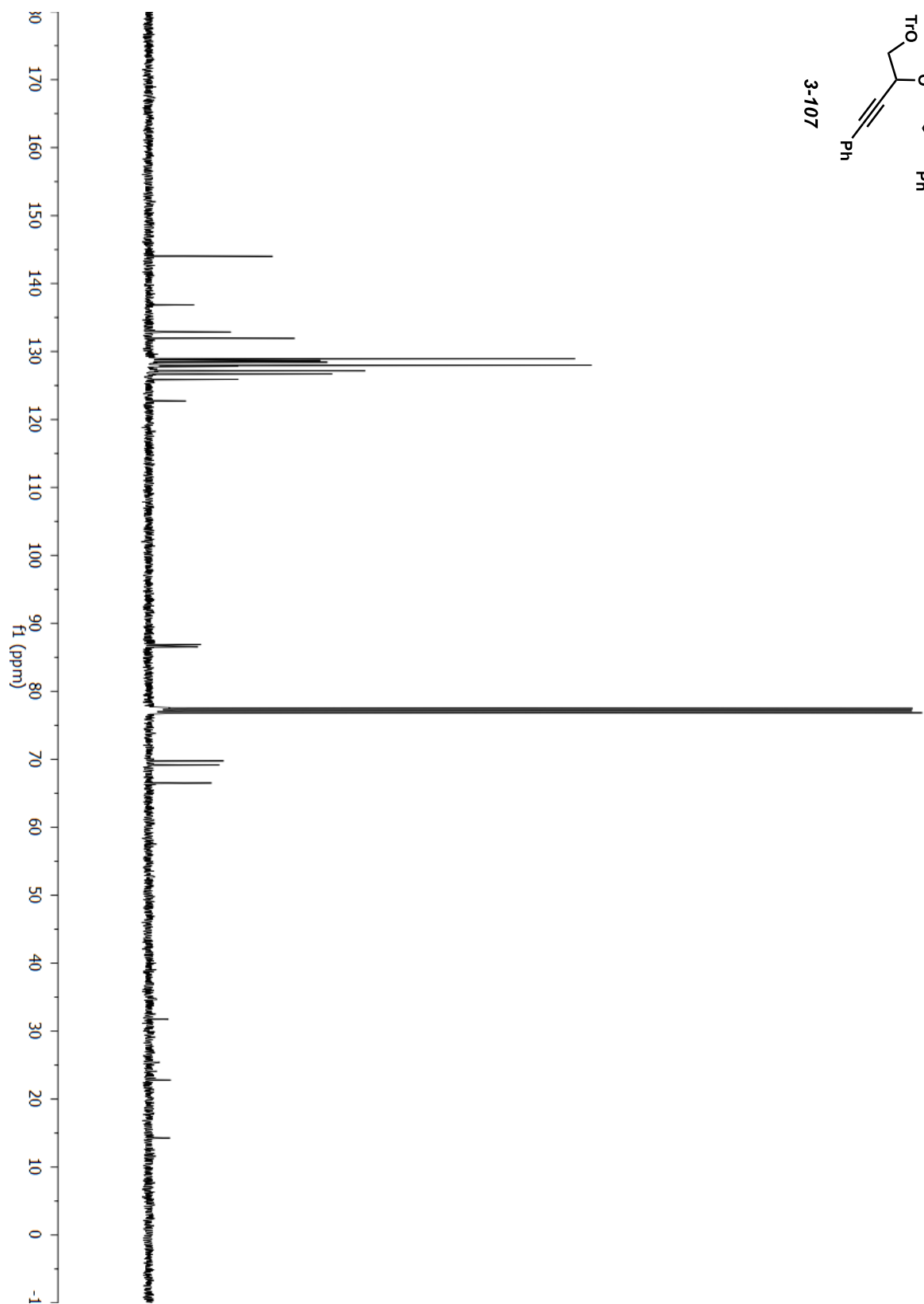
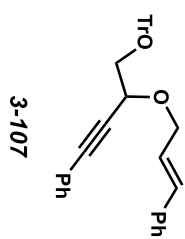
E:/NMR DATA/Chirality Xfer/CMH-5-84-p-181129/10/pdata/1/1r



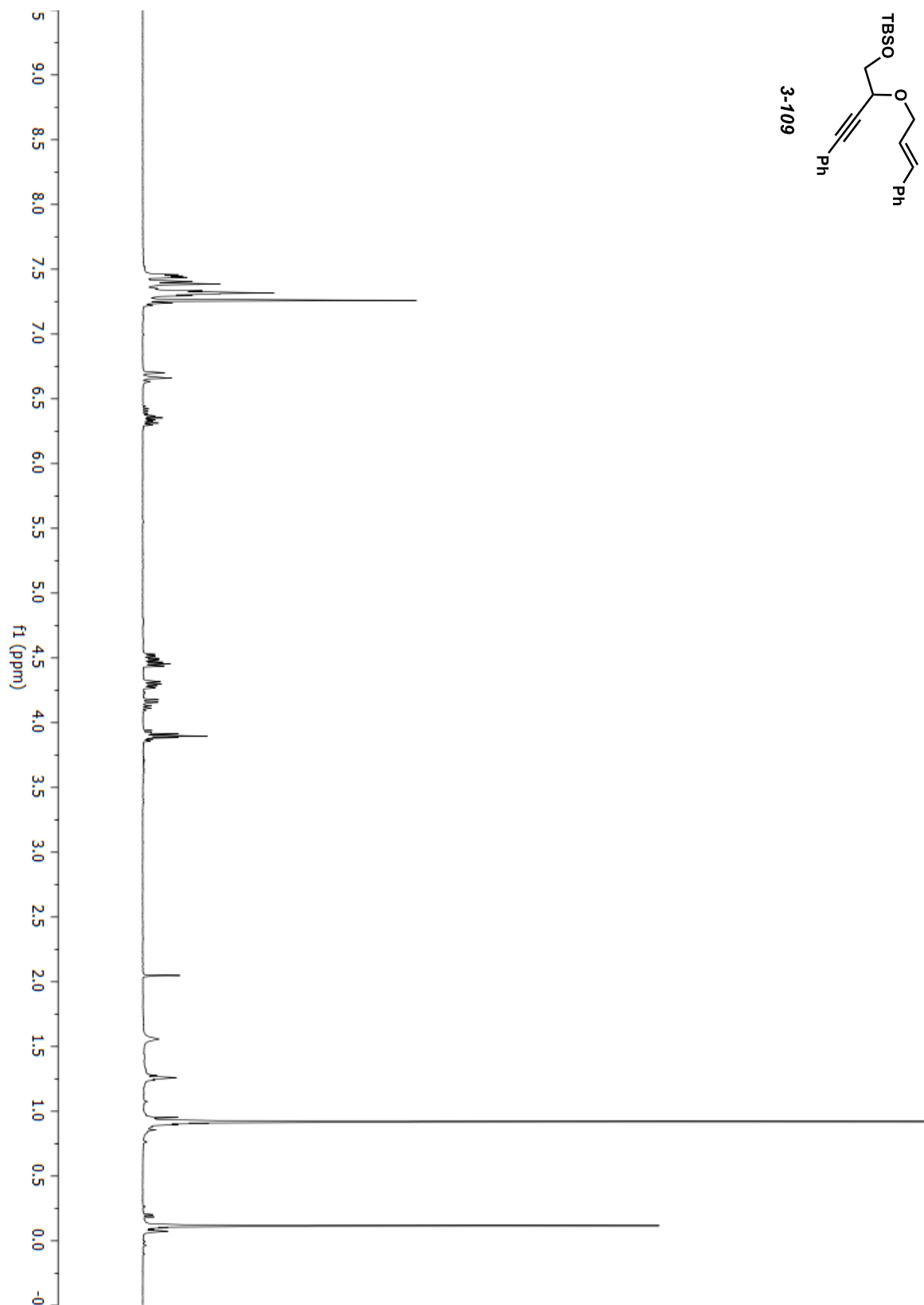
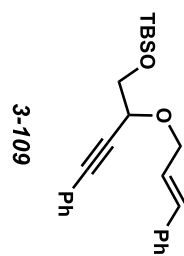
3-107



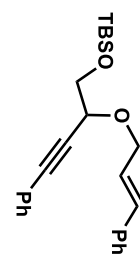
E:/NMR DATA/Chirality Xfer/CMH-6-50-p-190715/11/pdata/1/1r



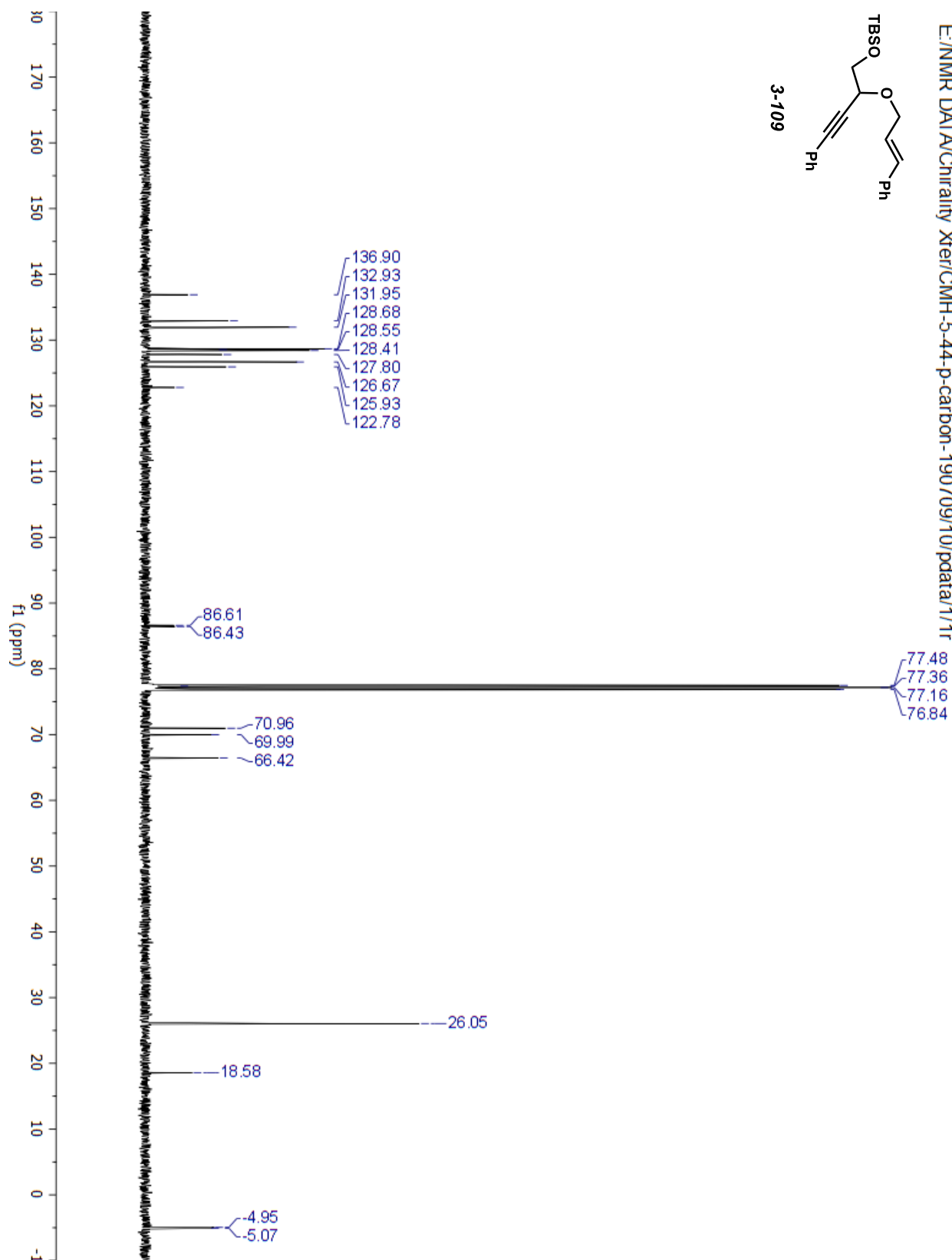
E:/NMR DATA/Chirality Xfer/CMH-5-85-C-181130/10/pdata/1/1r



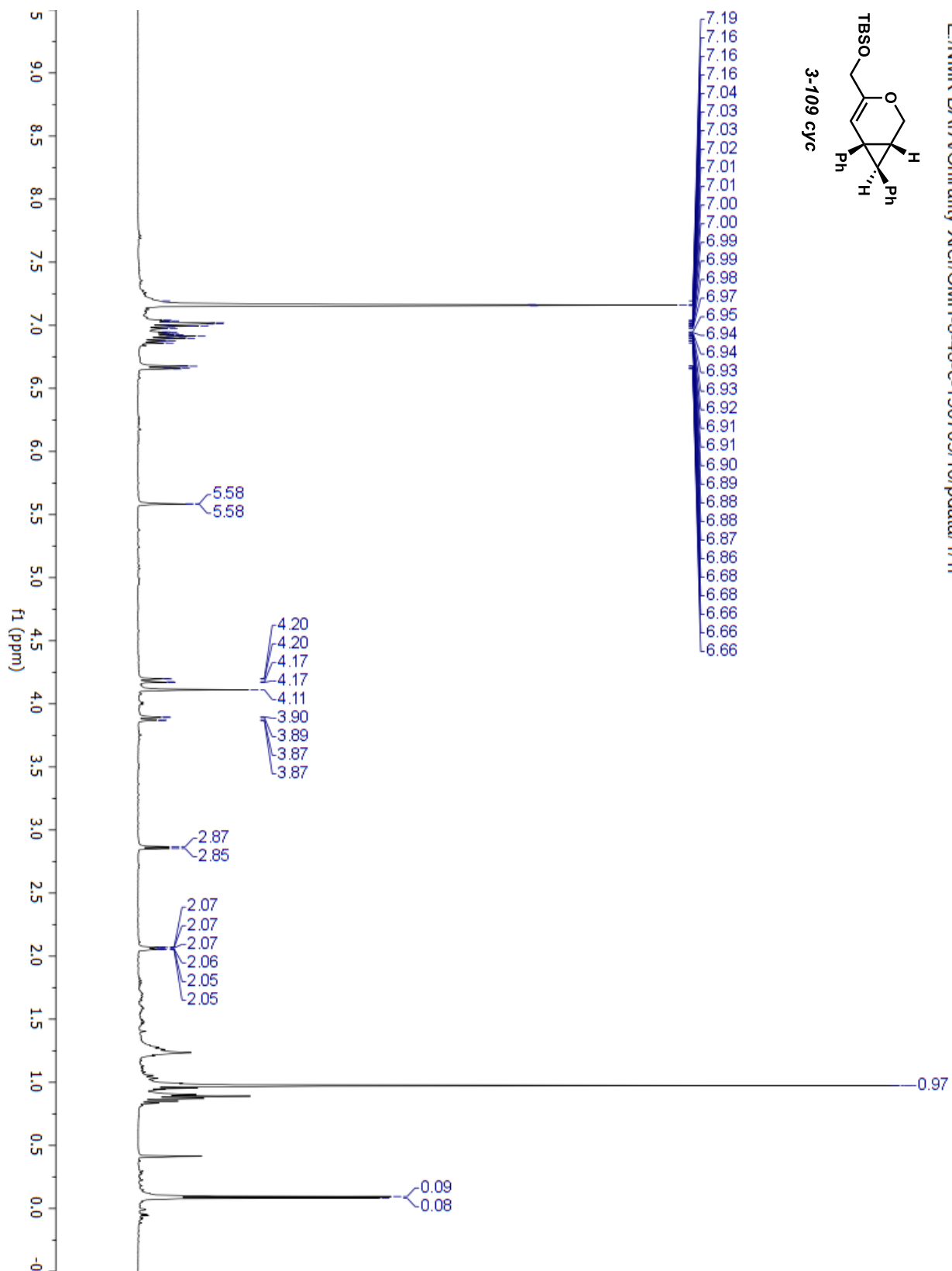
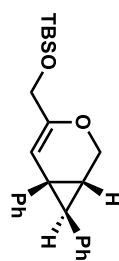
E:/NMR DATA/Chirality Xfer/CMH-5-44-p-carbon-190709/10/pdata/1/1f



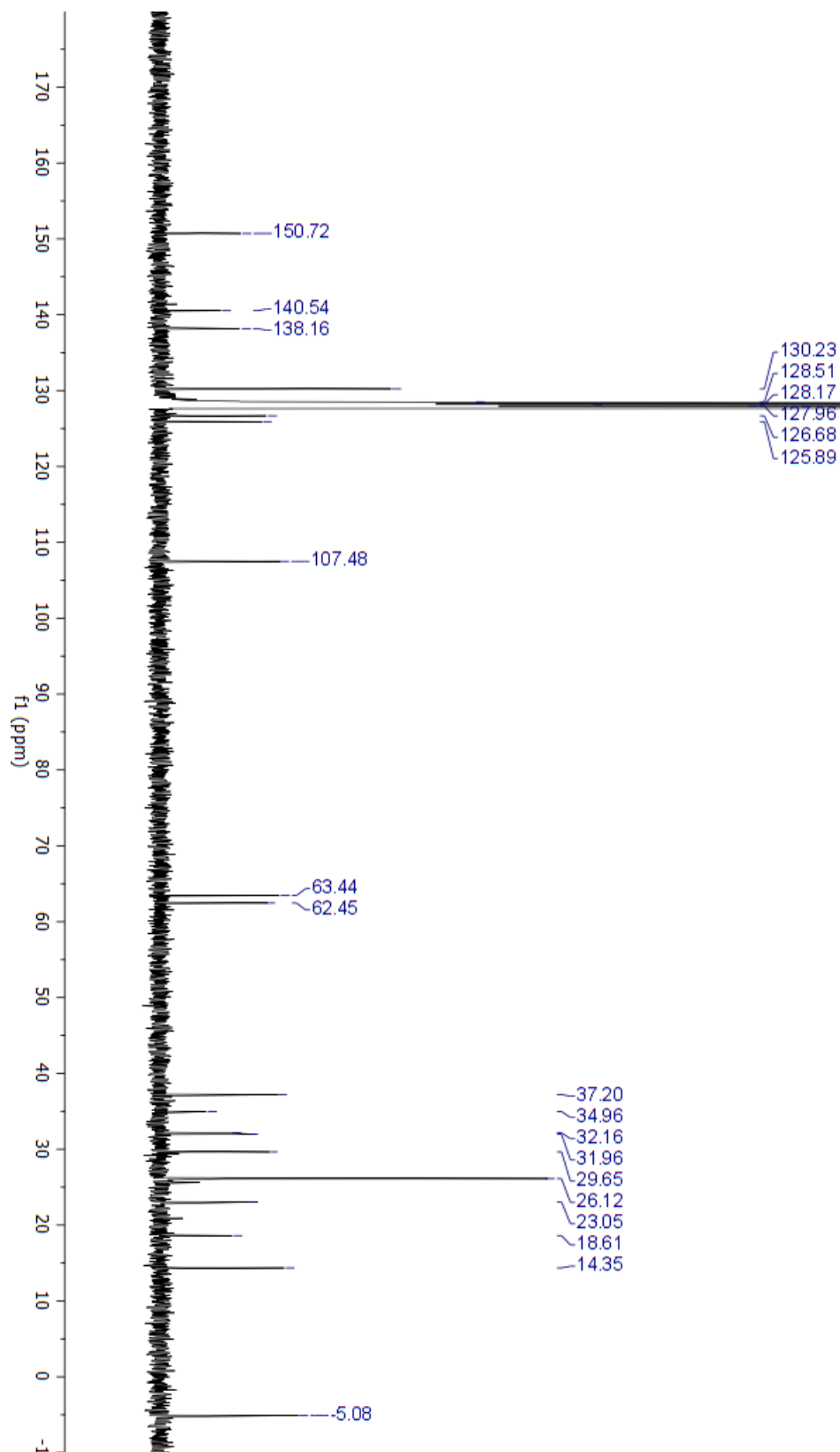
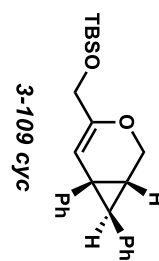
3-109



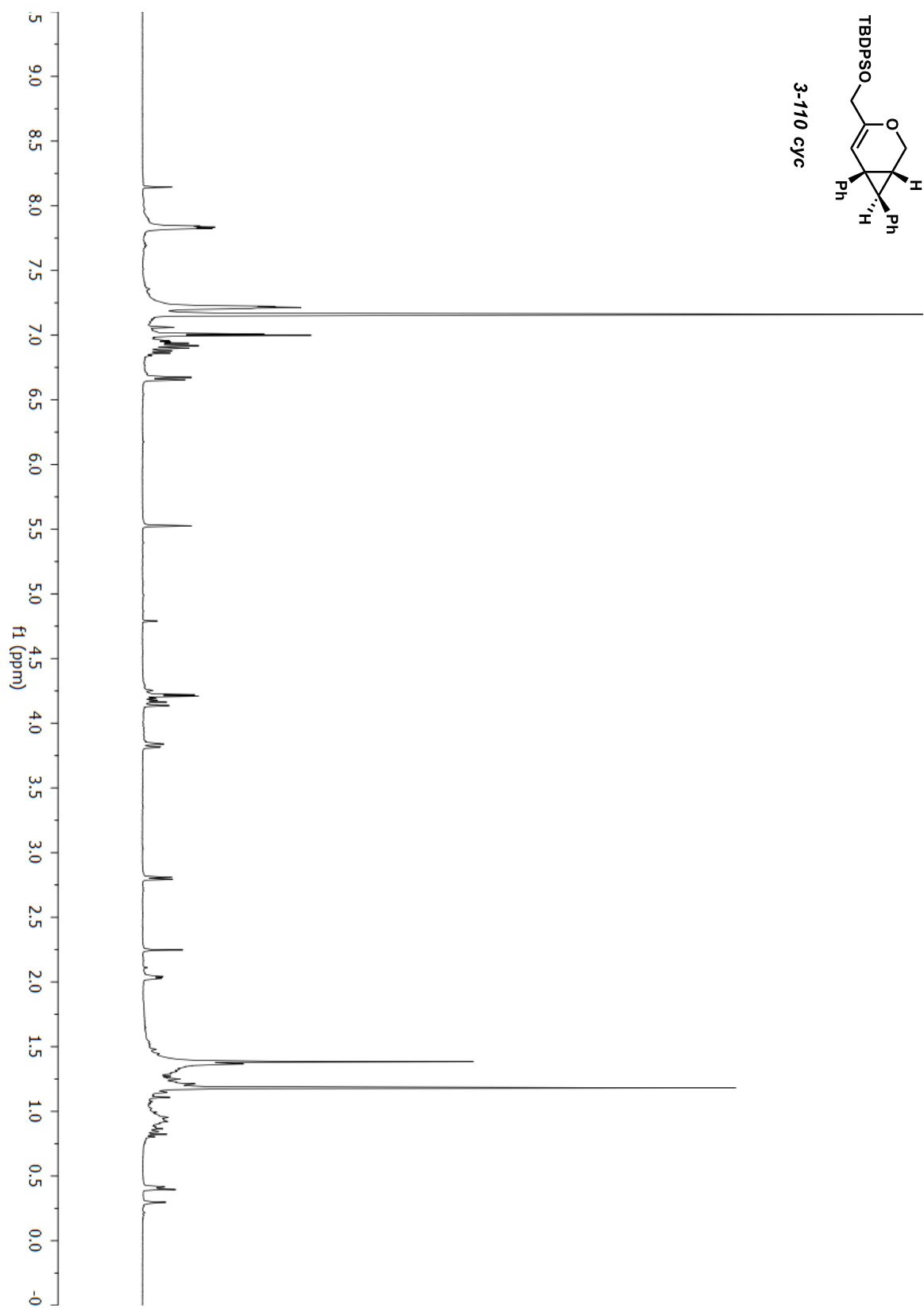
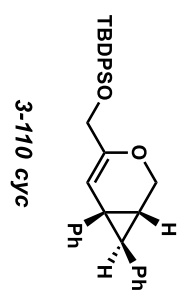
E:/NMR DATA/Chirality Xfer/CMH-5-45-C-190709/10/pdata/1/1r



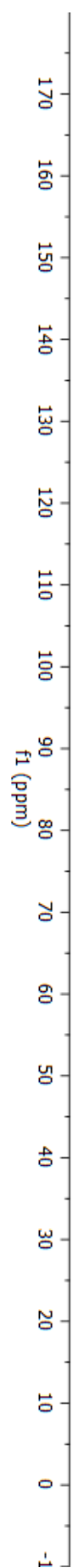
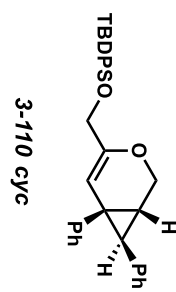
E:/NMR DATA/Chirality Xfer/CMH-5-4b-C-190709/11/pdata/1/1r



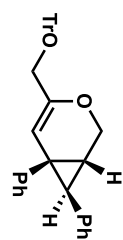
E:/NMR DATA/Chirality Xfer/CMH-6-49-cyc-190717/10/pdata/1/1r



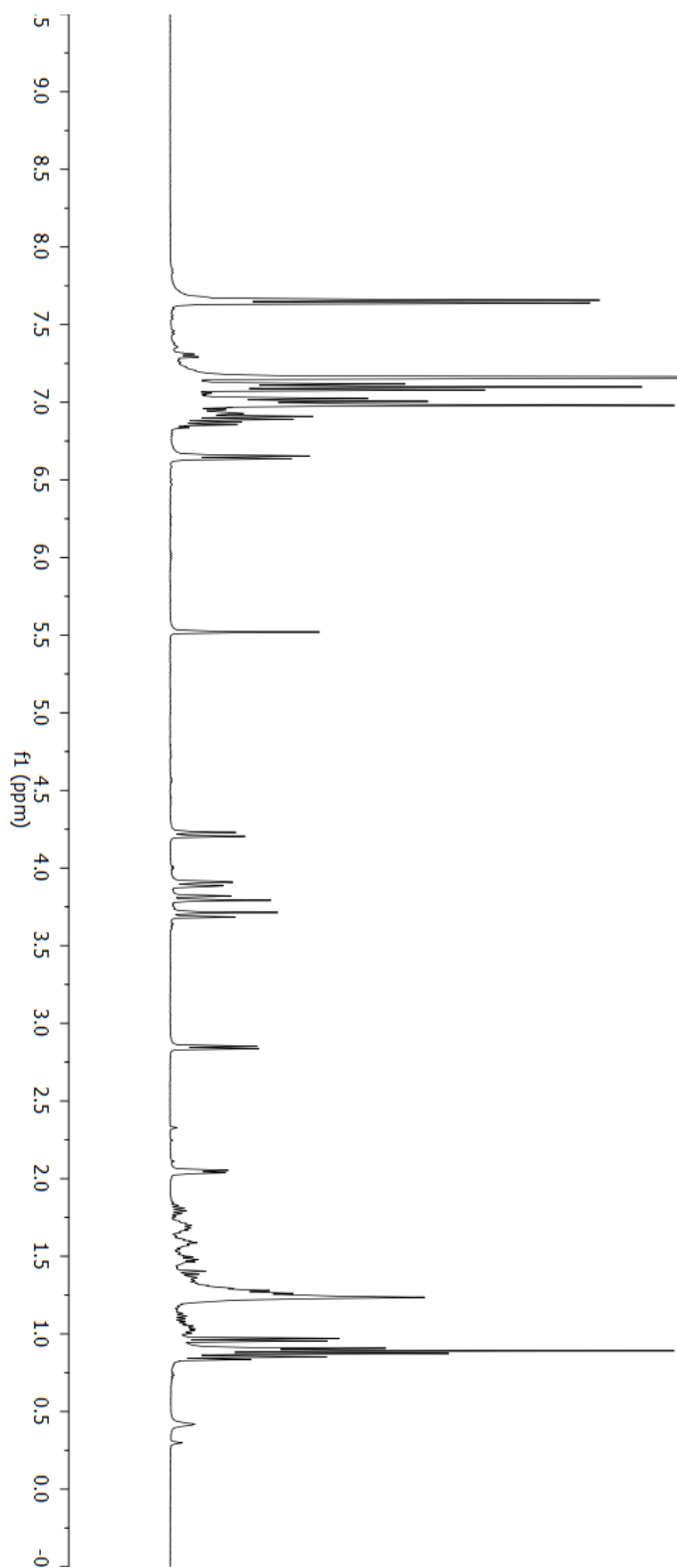
Z:/data/charrington/nmr/CMH-6-49cyc-190721/11/pdata/1/1r



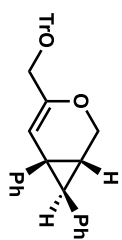
E:/NMR DATA/Chirality Xfer/CMH-6-50-cyc-c-190715/10/pdata/1/1r



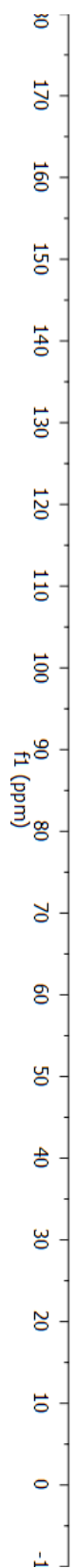
3-107 cyc



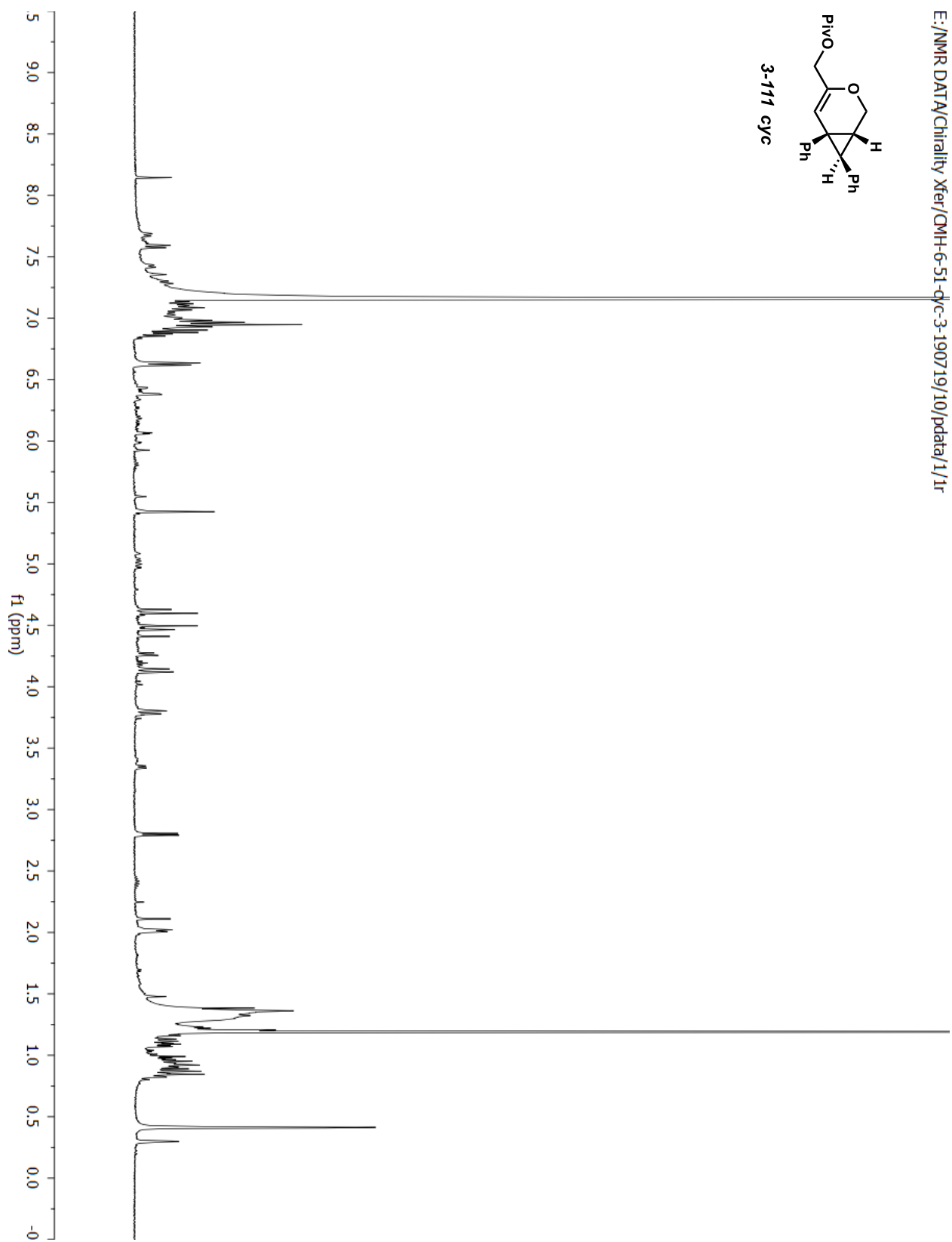
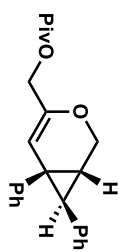
E:/NMR DATA/Chirality Xfer/GMH-6-50-cyc-c-190715/1/1/pdata/1/1r



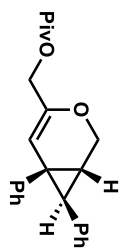
3-107 cyc



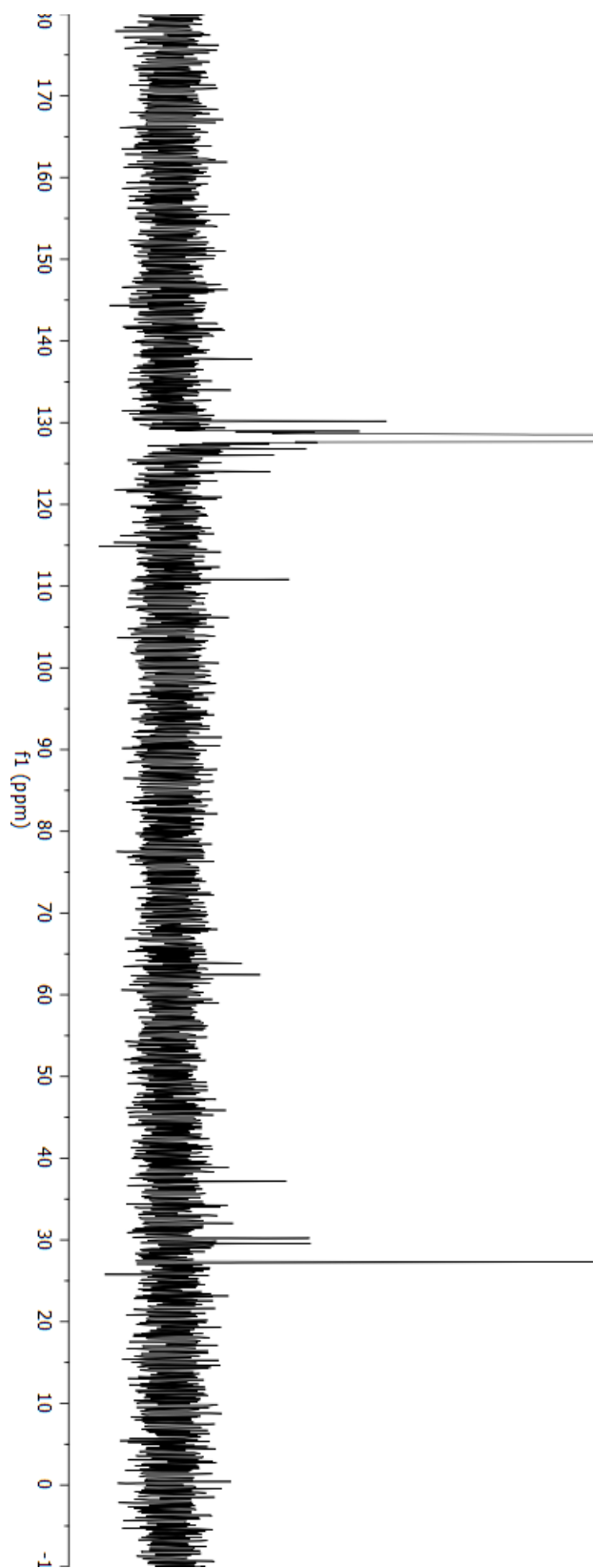
E:/NMR DATA/Chirality Xfer/CMH-6-51-q/c-3-190719/10/pdata/1/1r



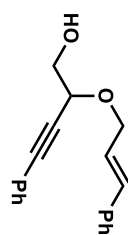
E:/NMR DATA/Chirality Xfer/CMH-6-51-cyc-3-190719/12/pdata/1/1r



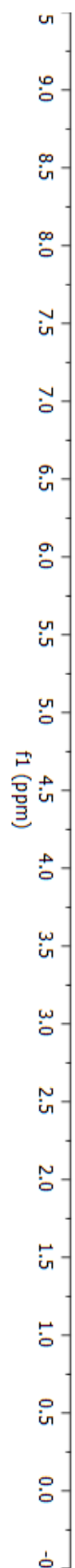
3-111 cyc



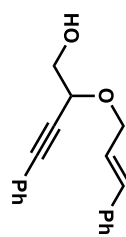
E:/NMR DATA/Chirality Xfer/CMH-5-87-p-181206/10/pdata/1/1r



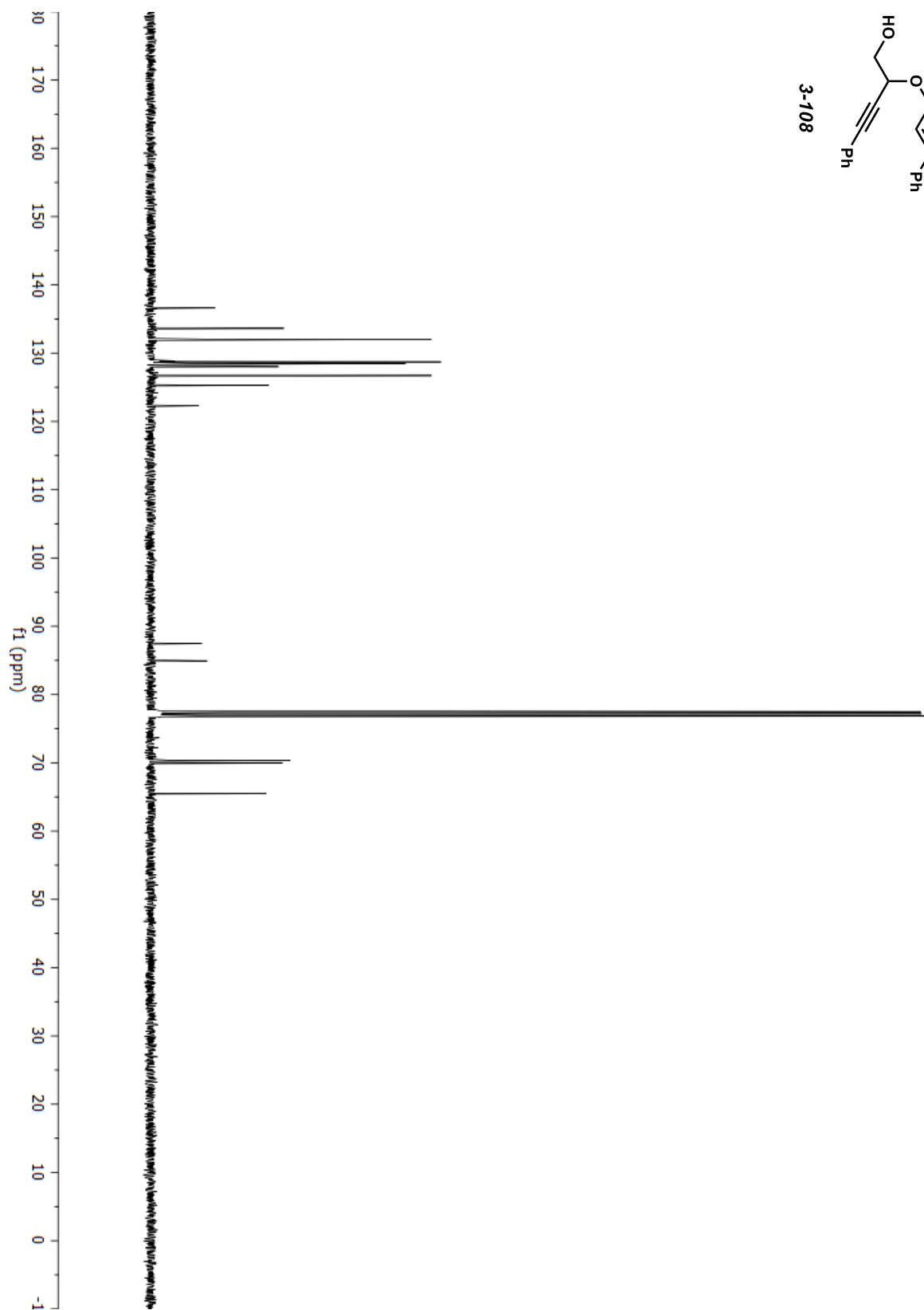
3-108



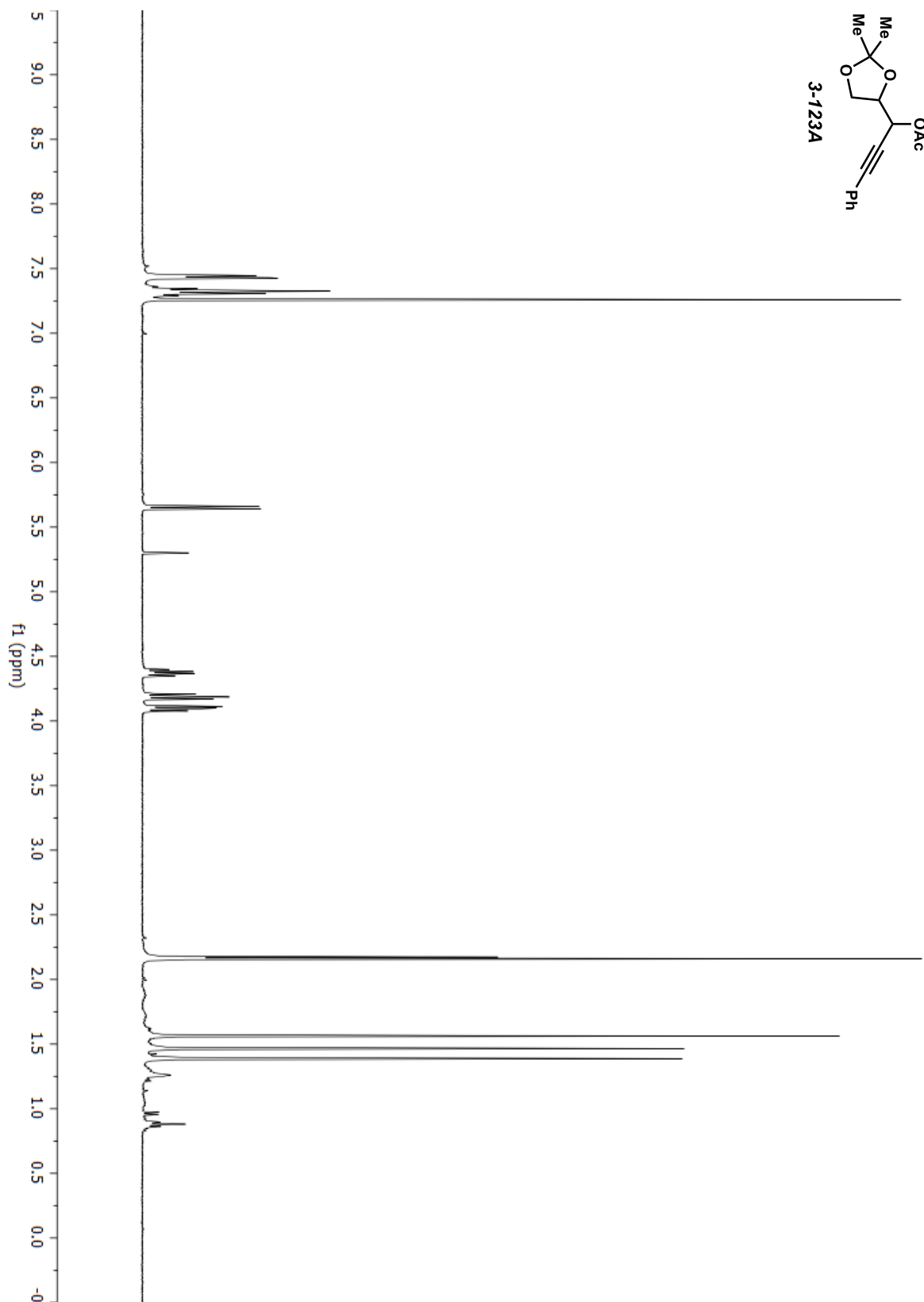
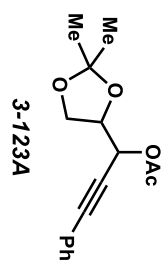
E:/NMR DATA/Chirality Xfer/CMH-5-87-p-181206/11/pdata/1/1r



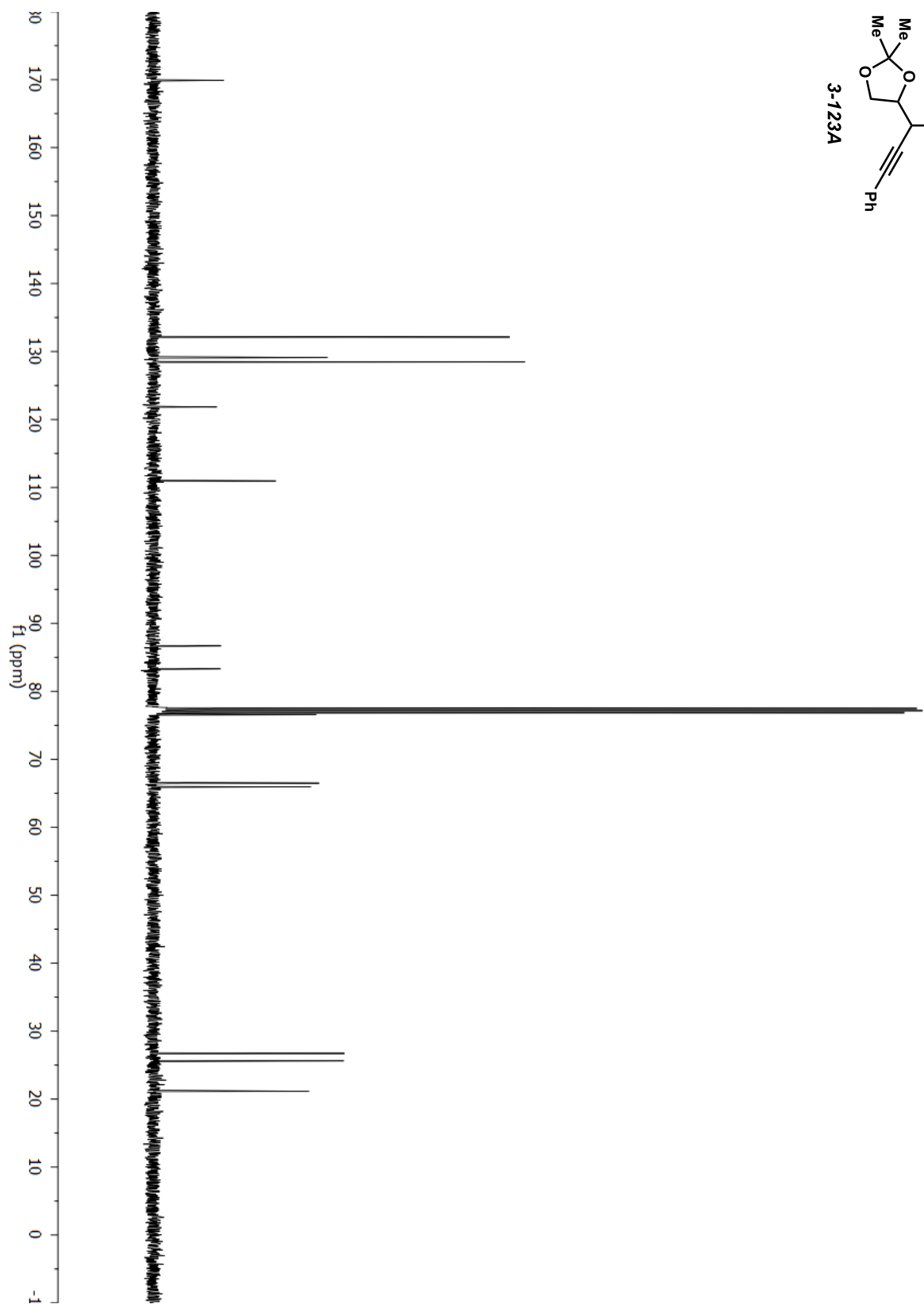
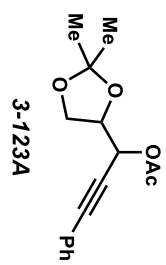
3-108



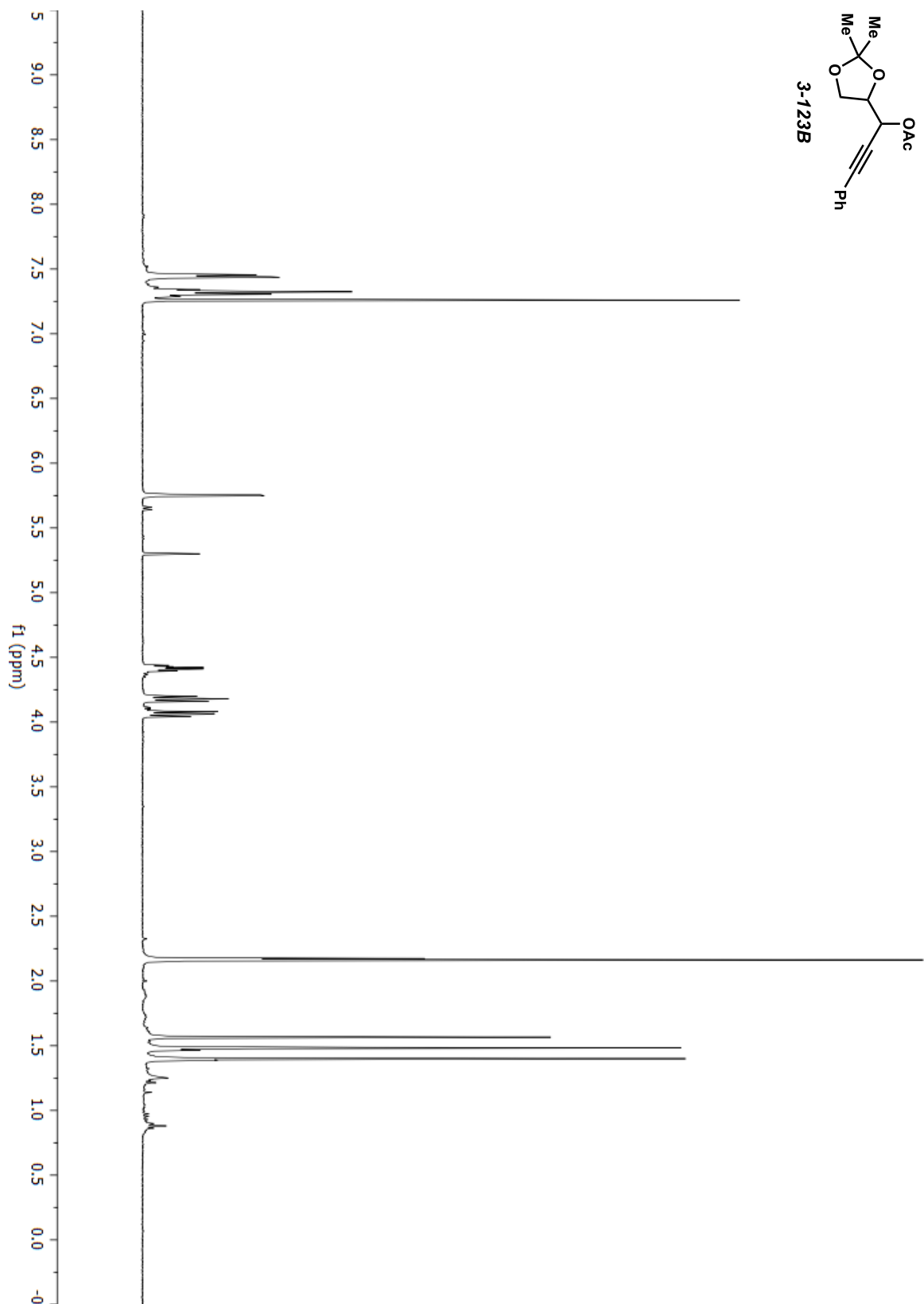
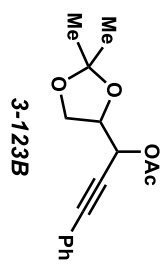
E:/NMR DATA/Chirality Xfer/CMH-6-22-p-top-190227/10/pdata/1/1r



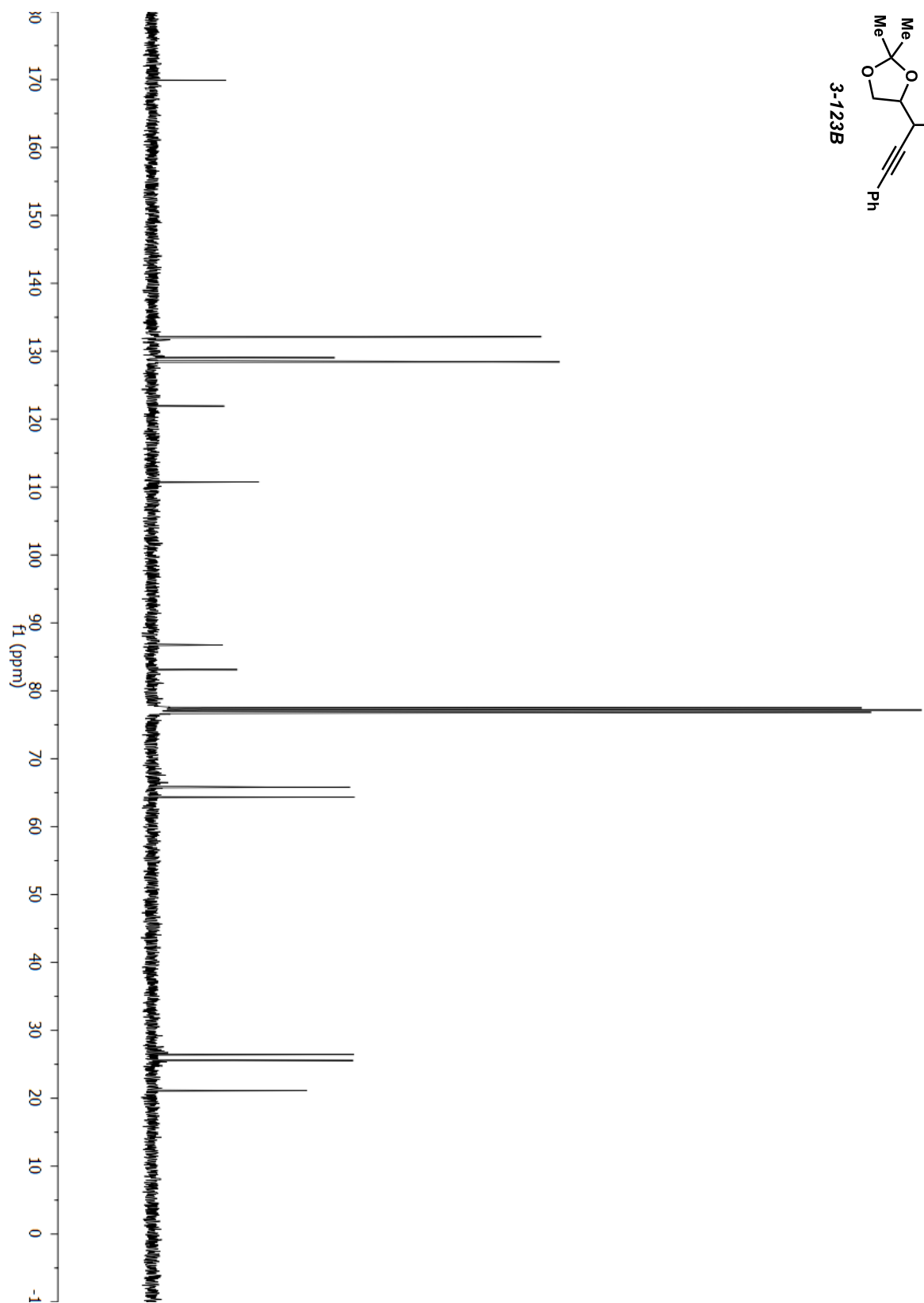
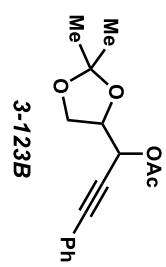
E:/NMR DATA/Chirality Xfer/CMH-6-OAc-A-190716/11/pdata/1/1r



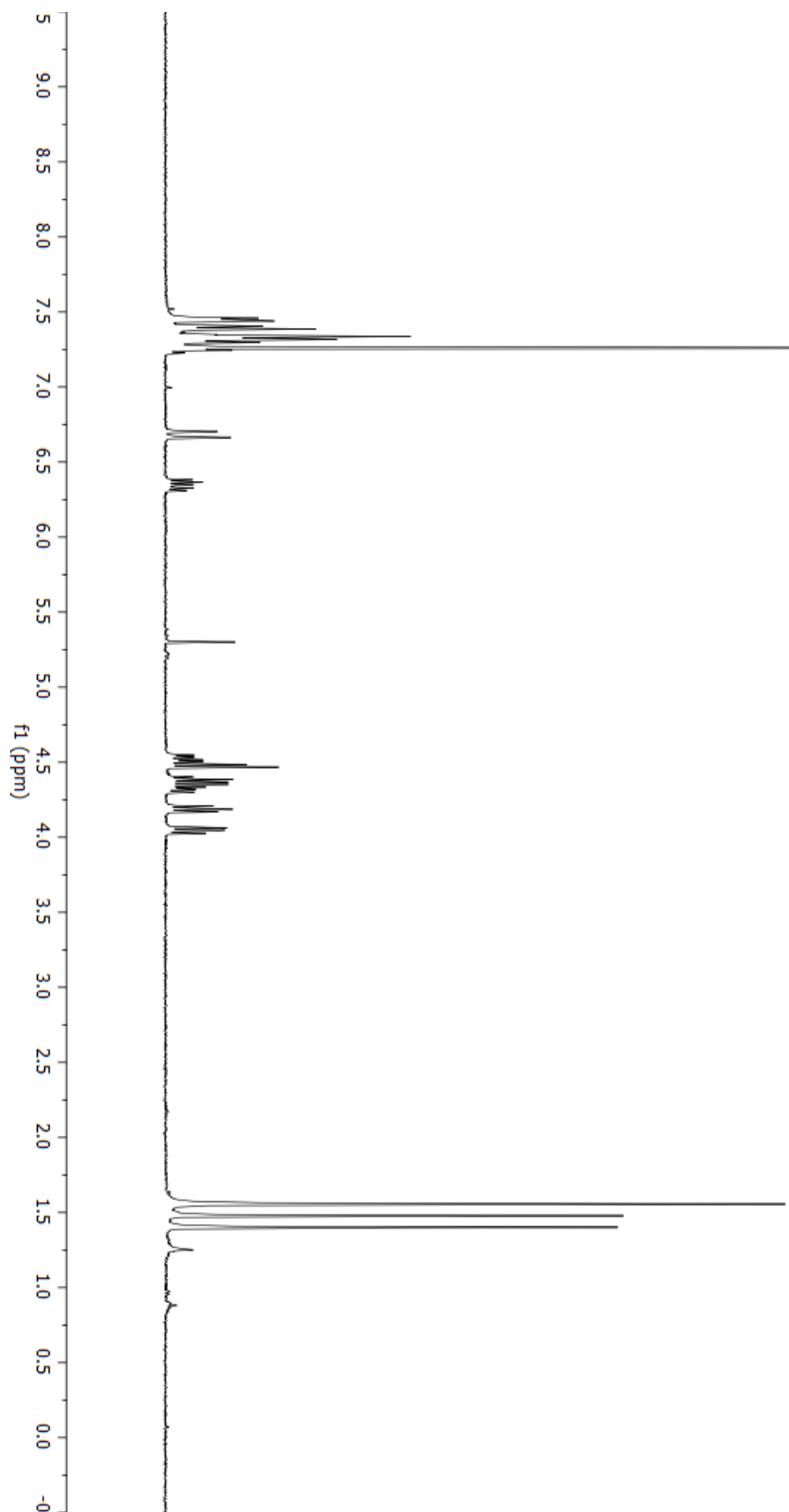
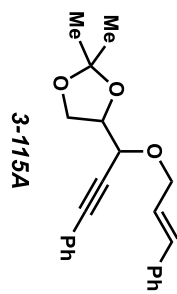
E:/NMR DATA/Chirality Xfer/CMH-6-22-p-bot-190227/10/pdata/1/1r



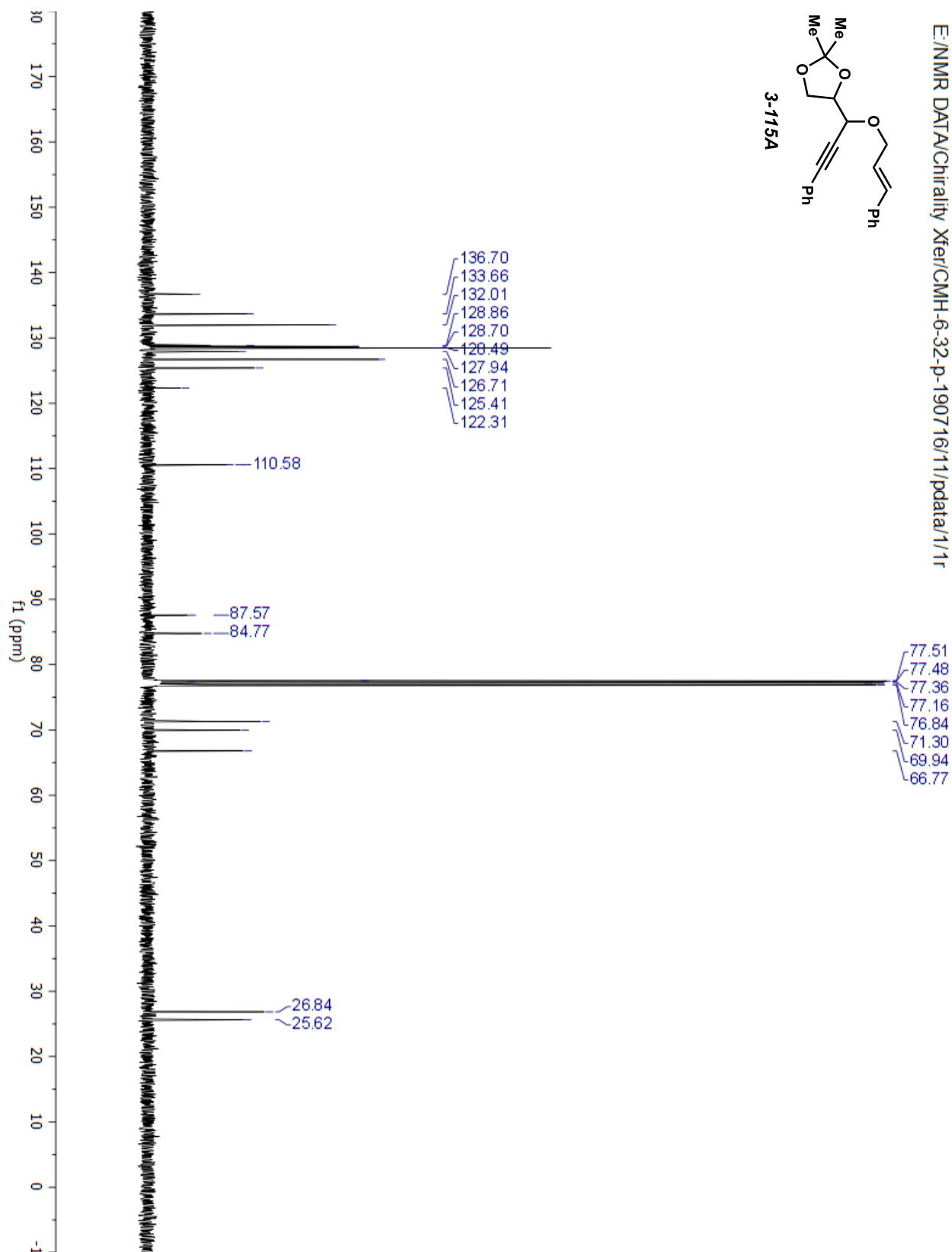
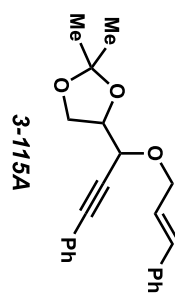
E:/NMR DATA/Chirality Xfer/CMH-6-OAc-B-190716/11/pdata/1/1r



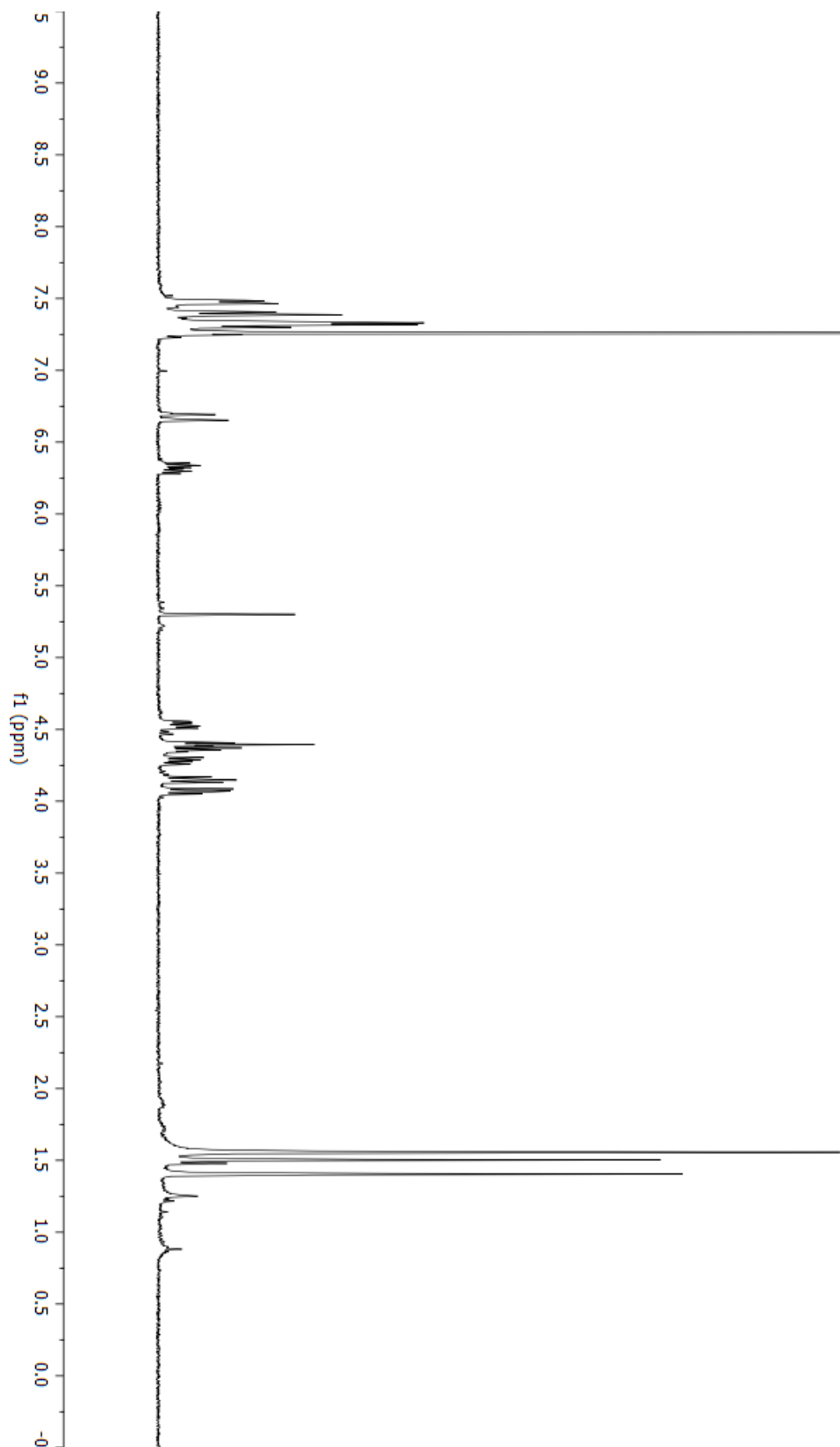
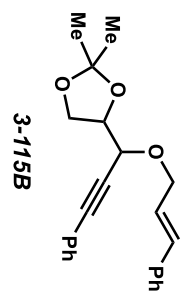
E:/NMR DATA/Chirality Xfer/CMH-6-25-p-190304/10/pdata/1/1r



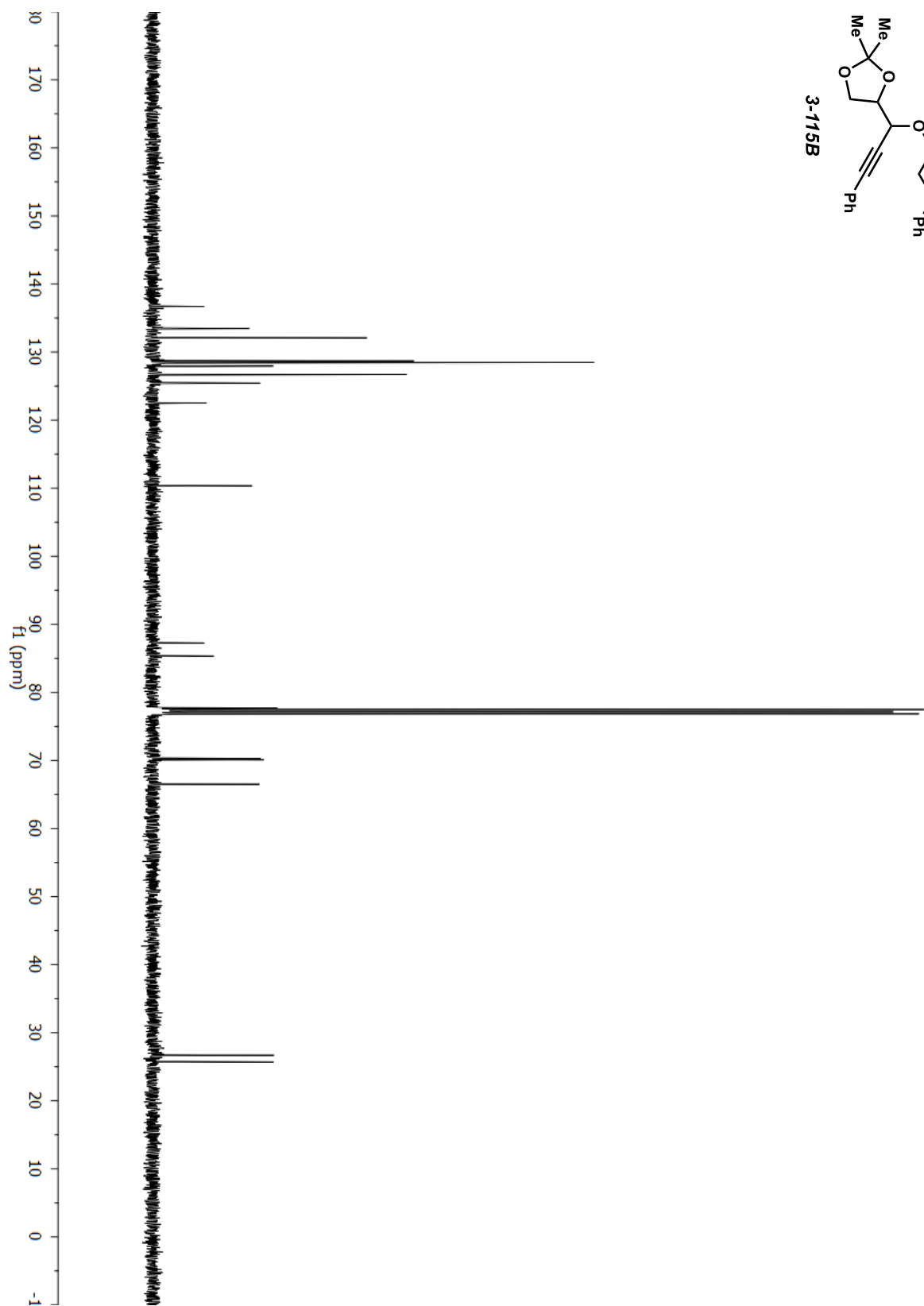
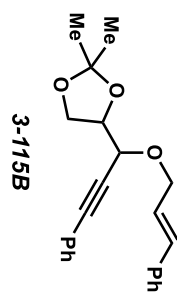
E:/NMR DATA/Chirality Xfer/CMH-6-32-p-190716/1/pdata/1/1r

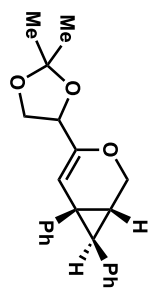


E:/NMR DATA/Chirality Xfer/CMH-6-26-p-190304/10/pdata/1/1r

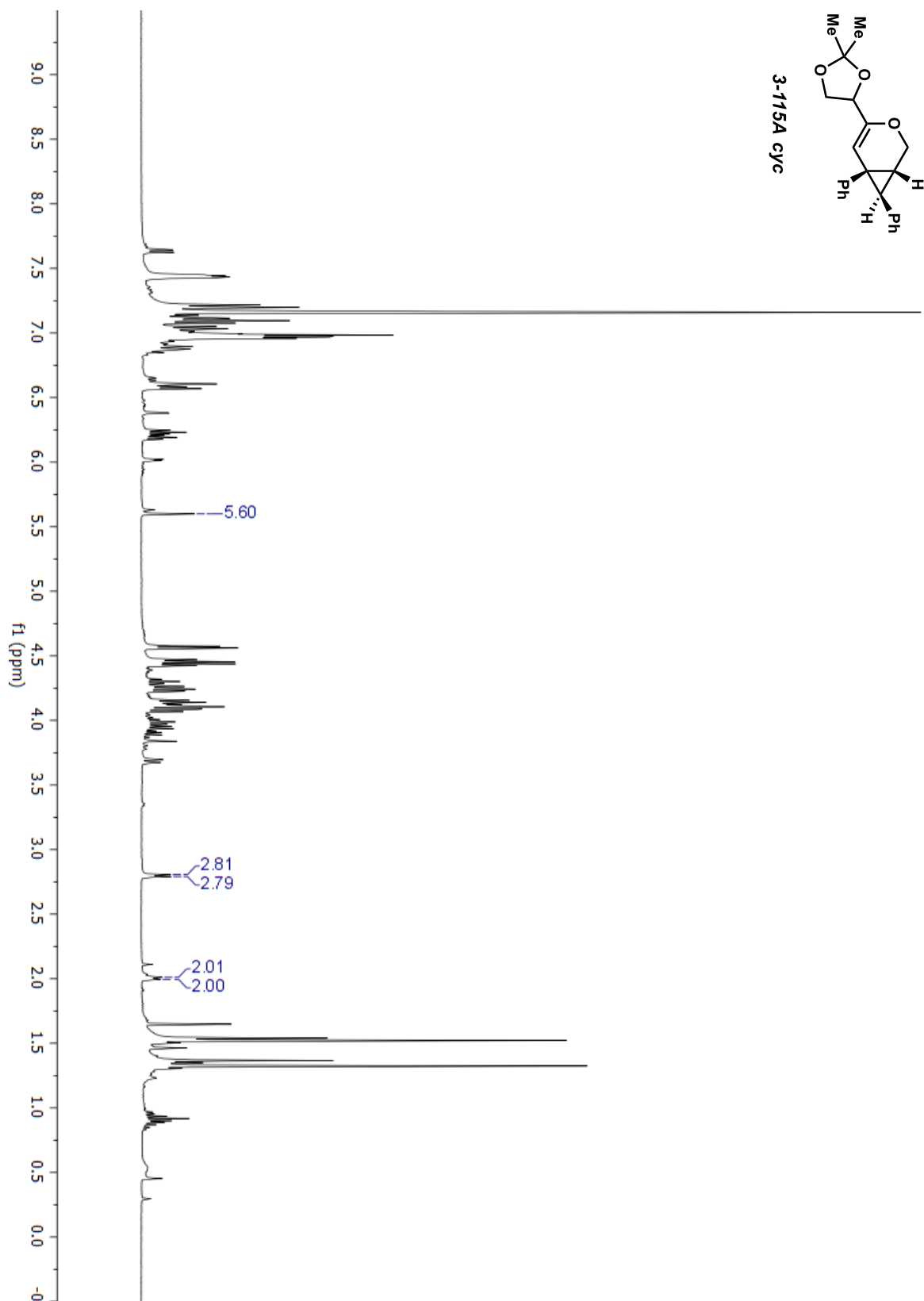


E:/NMR DATA/Chirality Xfer/CMH-6-33-p-190716/1/pdata/1/1r

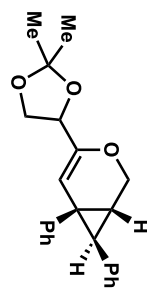




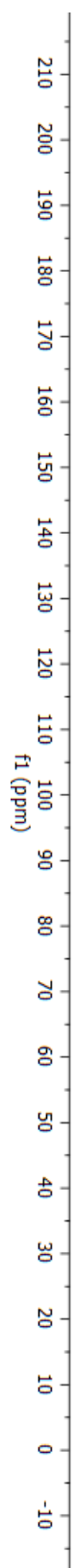
3-115A cyc



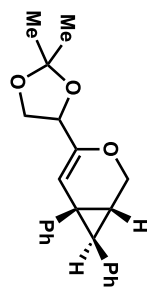
E:/NMR DATA/Chirality Xfer/CMH-6-acecyctOP-190721/11/pdata/1/1r



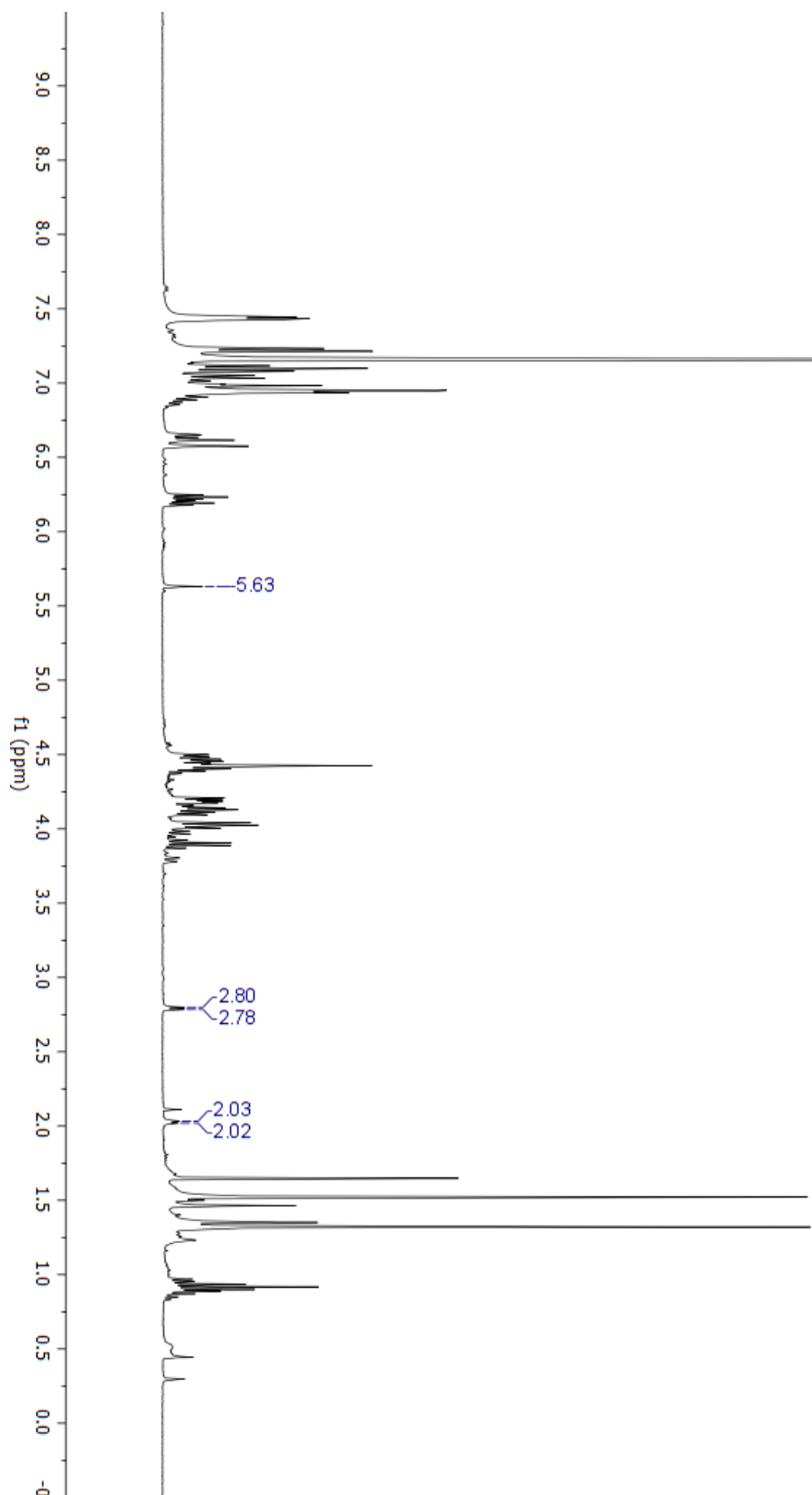
3-115A cyc



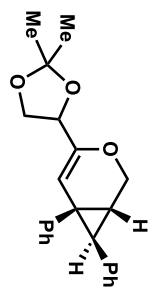
E:/NMR DATA/Chirality Xfer/CMH-6-acecyCBOT-190721/10/pdata/1/1r



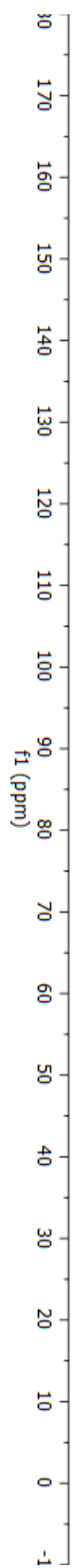
3-115B cyc



E:/NMR DATA/Chirality Xfer/CMH-6-acetycBOT-190721/1/1/pdata/1/1r



3-115B cyc



Chapter 3 References

-
- ¹ Struwe, L.; Albert, V. A.; Bremer, B. *Clandistics* **1994**, *10*, 175–206.
- ² Paris, A.; Schmidlin, S.; Mouret, S.; Hodaj, E.; Marijnen, P.; Boujedaini, N.; Polosan, M.; Cracowski, J. L. *Fundam. Clin. Pharmacol.* **2012**, *26*, 751–760.
- ³ Takayama, H.; Sakai, S. I. *Alkaloids, Vol. 49*, Academia Press, San Diego, **1997**, pp. 1–78.
- ⁴ Kitajima, M.; Nakamura, T.; Kogure, N.; Ogawa, M.; Mitsuno, Y.; Ono, K.; Yano, S.; Aimi, N.; Takayama, H. *J. Nat. Prod.* **2006**, *69*, 715–718.
- ⁵ Lin, H.; Danishefsky, S. J. *Angew. Chem. Int. Ed.* **2003**, *42*, 36–51.
- ⁶ Ghosh, A.; Carter, R. G. *Angew. Chem. Int. Ed.* **2019**, *58*, 681–694.
- ⁷ a) Hiemstra, H.; Rutjes, F. P. J. T.; Fieseler, R. M.; Beyersbergen van Henegouwen, W. G. *Angew. Chem., Int. Ed.* **1999**, *38*, 2214–2217. b) Beyersbergen van Henegouwen, W. G.; Fieseler, R. M.; Rutjes, F. P. J. T.; Hiemstra, H. *J. Org. Chem.* **2000**, *65*, 8317–8325.
- ⁸ Abelman, M. R.; Oh, T.; Overman, L. E. *J. Org. Chem.* **1987**, *52*, 4130–4133.
- ⁹ a) Shimokawa, J.; Harada, T.; Yokoshima, S.; Fukuyama, T. *J. Am. Chem. Soc.* **2011**, *133*, 17634–17637. b) Shimokawa, J.; Harada, T.; Yokoshima, S.; Fukuyama, T. *Pure Appl. Chem.* **2012**, *84*, 1643–1650.
- ¹⁰ a) Diethelm, S.; Carreira, E. M. *J. Am. Chem. Soc.* **2013**, *135*, 8500–8503. b) Diethelm, S.; Carreira, E. M. *J. Am. Chem. Soc.* **2015**, *137*, 6084–6096.
- ¹¹ Cordero, F. M.; Pisaneschi, F.; Goti, A.; Ollivier, J.; Salagn, J.; Brandi, A. *J. Am. Chem. Soc.* **2000**, *122*, 8075–8076.

-
- ¹² Newcomb, E. T.; Knutson, P. C.; Pedersen, B. A.; Ferreira, E. M. *J. Am. Chem. Soc.* **2016**, *138*, 108–111.
- ¹³ Ganesan, K.; Brown, H. C. *J. Org. Chem.* **1994**, *59*, 2336–2340.
- ¹⁴ Harada, T.; Shimokawa, J.; Fukuyama, T. *Org. Lett.* **2016**, *18*, 4622–4625.
- ¹⁵ Huang, Y. M.; Liu, Y.; Zheng, C. W.; Jin, Q.W.; Pan, L.; Pan, R. M.; Liu, J.; Zhao, G. *Chem. Eur. J.* **2016**, *22*, 18339–18342.
- ¹⁶ Wang, P.; Gao, Y.; Ma, D. *J. Am. Chem. Soc.* **2018**, *140*, 11608–11612.
- ¹⁷ Newcomb, E. T.; Ferreira, E. M. *Org. Lett.* **2013**, *15*, 1772–1775.
- ¹⁸ Barton, D. H. R.; Crich, D.; Motherwell, W. B. *J. Chem. Soc., Chem. Commun.* **1983**, 939–941.
- ¹⁹ Urabe, D.; Yamaguchi, H.; Inoue, M. *Org. Lett.* **2011**, *13*, 4778–4781.
- ²⁰ Tran, V. T.; Woerpel, K. A. *J. Org. Chem.* **2013**, *78*, 6609–6621.
- ²¹ Han, S.-J.; Stoltz, B. M. *Tetrahedron Lett.* **2016**, *57*, 2233–2235.
- ²² Banert, K.; Fendel, W.; Schlott, J. *Angew. Chem. Int. Ed.* **1998**, *37*, 3289–3292.
- ²³ Sorbyl bromide was synthesized from sorbitol using the procedure from: Vayer, M.; Fang, W.; Guillot, R.; Bezzenine-Lafollee, S.; Bour, C.; Gandon, V. *Org. Biomol. Chem.*, **2017**, *15*, 584–588.
- ²⁴ Kim, S.-Y.; Park, Y.; Chung, Y.-K. *Angew. Chem. Int. Ed.* **2010**, *122*, 425–428.
- ²⁵ Jogula, S.; Soorneedi, A. R.; Gaddam, J.; Chamakuri, S.; Deora, G. S.; Indarapu, R. K.; Ramgopal, M. K.; Dravida, S.; Arya, P. *Eur. J. Med. Chem.* **2017**, *135*, 110–116.
- ²⁶ Decuyper, L.; Piens, N.; Mincke, J.; Bomon, J.; De Schrijver, B.; Mollet, K.; De Winter, K.; Desmet, T.; D'hooghe, M. *RSC Adv.* **2016**, *6*, 54573–54579.
- ²⁷ Ohira Bestmann reagent was made according to the procedure from: Kalhor-Monfared, S.; Beauvineau, C.; Scherman, D.; Girard, C. *Eur. J. Med. Chem.*, **2016**, *122*, 436–441.

-
- ²⁸ Mames, A.; Stecko, S.; Mikolajczyk, P.; Soluch, M.; Furman, B.; Chmielewski, M. *J. Org. Chem.* **2010**, *75*, 7580–7587.
- ²⁹ Shen, W.; Wang, L. *J. Org. Chem.* **1999**, *64*, 8873–8879.
- ³⁰ Mukai, C.; Kim, J.-S.; Sonobe, H.; Hanaoka, M. *J. Org. Chem.* **1999**, *64*, 6822–6832.
- ³¹ Sirotkina, J.; Grigorjeva, L.; Jirgensons, A. *Eur. J. Org. Chem.* **2015**, *31*, 6900–6908.
- ³² Chittenden, G. J. F. *Recl. Trav. Chim. Pays-Bas* **1989**, *108*, 14–19.
- ³³ Fan, S.; He, C.-Y.; Zhang, X. *Tetrahedron* **2010**, *66*, 5218–5228.